UNIVERSITY OF CALIFORNIA
RIVERSIDE

The Genetics of Plant Meristem Development in Response to Alternate Bearing, WUSCHEL, and Cytokinin

A Dissertation submitted in partial satisfaction
of the requirements for the degree of

Doctor of Philosophy

in

Plant Biology

by

Aaron Edward DeVries

December 2015

Dissertation Committee:

- Dr. G. Venugopala Reddy, Chairperson
- Dr. Patricia S. Springer
- Dr. Morris M. Maduro

The Dissertation of Aaron Edward DeVries is approved:

Committee Chairperson

University of California, Riverside

Acknowledgments

The work presented in this document would not have been possible without the contributions and support from many others. First is for Dr. Harley M.S. Smith who readily accepted me into his lab and introduced me to the interesting world of field research. Much of the work in his lab also would not have been possible without the support of the Hofshi foundation, which generously donated trees for our experiments, and Mary Lou Arpaia, whose vast technical expertise helped precipitate many the ideas discussed in chapter 2. I am further indebted to Dr. G. Venu Reddy, who was kind enough to accept me into his lab when I had nowhere else to go, and who taught me the art of scientific pointillism. Special thanks go to Dr. Sean Cutler, who adjusted his schedule upon short notice to participate in my oral exam committee, along with Dr. Linda Walling, Dr. Morris Maduro, and Dr. Julia Bailey-Serres.

I must also thank the National Science Foundation for providing my IGERT funding, which considerably eased my financial burden for several years. I also owe my experiences in the Chemical Genomics program to Dr. Bailey-Serres (again), and thank Matthew Collins and Ronly Schlenk for their support while completing my IGERT requirements.

Within the department of Botany, I'd like to thank Diedra Kornfeld for helping me through registration issues in my first year, in addition to Dr. Edith Allen and the Department chair Mikeal Roose for arranging supplemental funding for my final year. Finally, there is Dr. Norman Ellstrand, who very patiently helped guide me through my first teaching experience. Among my lab mates, I owe thanks to Dr. Kaori Miyawaki for introducing me to my future work with cytokinin signaling, and whom also provided the *ahk2/3/4* triple mutant data in shown Figure 22. Likewise Mariano Perales, Steven Snipes, Kevin Rodriguez, and Ricardo Muir, who generously donated their seeds and provided many stimulating conversations. I am also indebted to Shruti Lal for providing her microarray data, which made the completion of chapter 1 possible. Though

I have not had the pleasure of meeting them personally, I must also thank Dr. Bruno Mueller in the Harvard Medical School for providing the pTCSn1:mGFP5-ER seed line. Finally, I am also indebted to Dr. Patricia Springer and Dr. Morris Maduro for serving on my dissertation committee.

ABSTRACT OF THE DISSERTATION

The Genetics of Plant Meristem Development in Response to Alternate Bearing, WUSCHEL, and Cytokinin

by

Aaron Edward DeVries

Doctor of Philosophy, Graduate Program in Plant Biology
University of California, Riverside, December 2015
Dr. Gonehal Venugopala Reddy, Chairperson

The ability of plants to produce new leaves and flowers depends largely on a small population of stem cells found at the apex of the stem, which is known as the Shoot Apical Meristem (SAM). The activity of the SAM can be influenced by the development of immature fruit, often causing a biennial pattern in yield called Alternate Bearing (AB). In order to understand how the SAM responds to the fruit at a genetic level, the expression profile of inflorescence meristems from *Arabidopsis thaliana* were studied under high fruit load conditions. The pattern of responses was found to resemble carbohydrate starvation, supporting the competition hypothesis. Several additional discussions are provided to revise old concepts, offer suggestions for improvement, and describe how genetic tools could be best applied to alternate bearing research.

On a more basic level, the SAM is maintained by the WUSCHEL-CLAVATA feedback loop, where WUS is thought to directly activate CLV3 expression. The nature of the CLV3 regulome was studied by combining phylogenetic footprinting with large promoter deletions. This found that the 5' CLV3 promoter is less than 70bp long, and is likely to be regulated in part by an auxin

response element. In addition, three large cis-regulatory modules were found in the 3' enhancer, two of which were found in a naturally occurring transposon. The role of transposition in the evolution of the WUS-CLV3 feedback loop is discussed. Finally, the role of cytokinin hormones on WUS regulation was investigated by adjusting native cytokinin levels with receptor mutants and genetic constructs, in order to observe changes in WUS, CLV3 and cytokinin fluorescent reporters. The results found that cytokinin had little or no effect on the transcription, nuclear transport, or protein degradation of either gene, while auxin responses rapidly reduced WUS protein levels. Surprisingly, the complete absence of cytokinin responses in the central zone was found to be critical for meristem maintenance, and the response-free zone existed independently of WUS-CLV3 feedback loop.

Table of contents:

Figures

Section 1 overview

Chapter 1

Section 2 overview

Chapter 2

Chapter 3

Tables

Chapter 1

Chapter 2

Appendices

Chapter 1

Preface:

In the course of my graduate career I have had the great opportunity to study plant development under two different advisors, providing a broader research experience than would otherwise be possible. Thus my work first began under the supervision of Dr. Harley Smith, who was then starting a research program with alternate bearing Avocado trees (*Persea americana*), while my second advisor was Dr. G. Venu. Reddy, who studied the organization of the Shoot Apical Meristem (SAM) in *Arabidopsis thaliana*, with special emphasis on the role of a gene called WUSCHEL (WUS). However, because there is little, if any overlap in the work performed between these two labs, I have chosen to divide this dissertation into two independent sub-sections. Each section begins with a separate introduction to help the reader become acquainted with common topics in each field of study, and then breaks into chapters to discuss the narrower topics that formed the basis of my research.

Section 1 covers my work with Dr. Smith, which was originally intended to show how plant development in *Arabidopsis thaliana* was functionally homologous to similar developmental patterns that occur in Avocado trees. By doing so, it would become possible to study many aspects of alternate bearing behavior in a more convenient model organism, while also quickly incorporating the vast genetic resources that are available for *Arabidopsis* into this slow-growing tree. Unfortunately, our progress towards that goal was cut short when Dr. Smith relocated to Australia, and I was unable to follow. As a result much the comparative work with Avocados could not be performed as expected, and large portions of my work with *Arabidopsis* are incomplete. Fortunately, it was possible to salvage a microarray study of fruit load in *Arabidopsis thaliana* meristems, and this is presented in Chapter 1. The results of the arrays, plus related evidence, suggest that strong fruit loads are perceived as carbohydrate starvation within the SAM.

Section 2 in contrast, examines a much narrower field of study concerning the genetics of meristem maintenance, which has often synonymous with the WUS-CLAVATA3 (CLV3) feedback loop. Both genes are studied from slightly different perspectives, which are presented in separate chapters. For example, Chapter 3 describes the identification of CLV3 cis-regulatory elements, in order to clarify the regulatory structure of this gene. Among the more interesting findings was an unusually complex enhancer element in the 3' UTR, and that CLV3 is likely to be sensitive to auxin hormone responses. Chapter 4 in turn, explores how the plant hormone cytokinin controls the distribution of WUS proteins and *vice versa*. The results instead found that cytokinin did not directly influence WUS, and unexpectedly, a novel cytokinin-free zone was found to be critical part of SAM structure. The role of auxin is also revisited, and likely has a direct role in controlling WUS protein stability.

Section 1:

What is Alternate Bearing?

In the simplest possible terms, Alternate Bearing is a two year cycle of fruit production that occurs in perennial plants, and is best known from fruit-bearing trees like apples and avocados. In one year, the plants will produce many fruits, while in the second year, they produce very few. This biennial pattern then often repeats itself in the following years creating a repetitive cycle, revealing itself as a saw-toothed line when fruit yields are plotted over many years (Figure 1.0). The fluctuation in yield is usually quite moderate and only rarely reaches the extreme values of 0% and 100%, but even minor variations can readily be detected in commercially grown orchard trees. The phenomenon is not limited to trees though, as similar biennial cycles have also been documented to occur in perennial herbs [1], monocots [2, 3], and forest trees [4-6], which suggest that alternate bearing is a fairly common, if seldom seen plant behavior.

From an economic standpoint though, the presence of alternate bearing in commercial orchards is considered to be undesirable for many reason. Not only do alternating trees tend to produce less fruit on average than regular-bearing varieties [7], the resulting fruit often display characteristic variation in size and appearance that reduces their market value [8]. For example, large crops tend to produce small and poor quality fruits, while small crops can occasionally produce large and abnormally swollen fruit. Many fruits are sorted into sizes according to their intended market, where this variation makes it more difficult for the farmer to produce sufficient numbers of each [9]. Harvest costs are largely the same whether the crop is large or small, and large crops often incur extra processing and storage fees when they can't be sold immediately. In addition, alternate bearing trees are prone to synchronization, during which all of the trees in the orchard fluctuate in lock-step with each other. Frequently attributed to a late flower-destroying frost [10-12] or other temperature anomalies [13], such synchronization can occur over a wide range of

scales, ranging from isolated trees, to whole orchards, and even entire geographic areas [13, 14]. Fruit production in synchronized areas tends to saturate the market with low-quality fruit in one year, and provide little or no fruit in the second, thus limiting the potential profit in both years of the cycle. Although there are horticultural techniques available to force the trees to become regular bearing again, these introduce additional expenses in the form of time, labor, and materials. Thus the combined effects of yield, quality, irregular production, and additional expenses can easily make alternate bearing crops uneconomical to produce, despite any other attractive qualities they might have.

Alternate bearing is also perhaps one of the oldest known plant behaviors, as written descriptions of it can be found going back over several millennia. Most often these references are simple observations of trees that flower in one year but not the next [15, 16], or as one early account of cider production in England elegantly described it, the trees would ". . . provide a full and complete blessing every second year" [17]. Other written accounts offer advice on how to get sterile trees back into production [15, 18, 19], though it is not always clear if these early authors were aware of the full two-year cycle. Nevertheless, the prescribed regimes of girdling, branch twisting, and pruning are well-matched to its existence nonetheless: by removing a lot of branches or inflicting specific types of damage, this advice would stimulate the trees to produce a dense crop of new branches, which go on to bear fruit in the following year. Other accounts instead try to explain the biennial pattern by speculating that the trees require a period of "rest" before [20] or after a large crop [21, 22]. Alternatively, the cycle has been suggested to be the result of rainfall [23], variation in cross-pollination efficiency [24], and/or total the flower numbers [25]. Not everyone was inclined to such speculation though, as Japanese farmers reportedly accepted the cycle as nature's way, without trying to intervene at all [26].

Despite the long history of this tree behavior, there have been relatively few attempts to learn how or why the plants produced the cycle. Even when descriptions of such experiments have survived, they tend to be hearsay accounts published by 3rd parties, making it difficult to determine what exactly transpired. For example, one horticultural manual from the 1800's recognized that an unequal growth trade-off between the fruits and branches was a significant symptom of alternate bearing trees, and recommended that farmers artificially restore that balance by cutting off excess vegetative growth [15]. In another example twenty five years later, a reporter for a popular horticultural magazine visited a nearby orchard and held a walking interview with the owner. In the process, we learn that the proprietor had performed an experiment some years earlier, in which he had removed all the flowers from a single tree one season, and found an abundance of fruit in the next [27].

In contrast, academic interest in alternate bearing was essentially non-existent until the late 1800's, when the subject apparently received a major boost from the establishment of state-sponsored agricultural experiment stations. This was apparently a global trend, as England adopted a private research station that began as early as 1843, Japan obtained one by official decree in 1871, and United States began building its research stations following the Hatch Act in 1887. By the turn of the century, these and other experiment stations had begun to produce a large number of agricultural publications, quickly establishing the foundation of crop science as we know it today. Research in the alternate bearing field lagged behind somewhat, perhaps by the need to establish experimental orchards, but began to produce a burst of new research starting around 1900. Thus began a roughly 30 year period of clever experimental designs and careful scholarship, ultimately producing the tools and basic concepts of alternate bearing research. Beginning with the development of chemical sprays in the 1940's, the focus of this research began to shift away from basic inquiries and instead frequently focused on practical farming

issues. Over the next few decades, this work made slow but steady progress towards understanding the physiological mechanism that propagates the cycle, while also identifying a broad array of species with similar physiological symptoms. The past few decades were also an extremely productive time for alternate bearing research, as this student estimates that the field has accumulated more than 1200 papers that mention the cycle by name, as well as another 3-4000 papers in closely related subjects, with less obvious key words.

In contrast, work to incorporate modern genetic tools is a much more recent phenomenon, beginning with just a handful of papers in the early 2000's [28-30], then escalating rapidly by the end of the decade [31-35]. Generally such genetic work has attempted to observe when and where key developmental genes respond to the cycle, because it is not yet possible to make an entirely predictive model of alternate bearing, based on known developmental pathways from other species. Such knowledge is however, is expected to help farmers precisely control the behavior in popular tree crops, either through selective breeding , transgenic modification, or predictive mathematical models. A genetic understanding may even provide a way to clarify current ideas about the ecology and evolution of the cycle, while also identifying key developmental differences that separate annual and perennial species. Thus genetics is quite likely to usher in an exciting era of alternate bearing research.

The basic anatomical model

In many cases alternate bearing is described largely in terms of fruit production, but close observations have shown that the actual phenotype is much more complicated. Similar two-year cycles have also been found in leaf area [36, 37], flower numbers [38, 39], branch lengths [10, 40], and trunk diameter [10, 41], just to name a few (more than 40 different measures have been described). Several physiological parameters have also been found to change in phase with the cycle, including mineral nutrients [42-46] and carbohydrates [36, 47-50], which tend to

accumulate in the fastest growing organ, and are depleted in slower growing organs. Plant hormones have also been correlated with specific parts of the cycle, and are important regulators of floral induction [51, 52], dormancy [53, 54], fruit ripening [55-57], and abscission [58-60]. Collectively, these findings outline an inverse relationship between fruit and vegetative growth that is broadly applicable to all species: When fruits are abundant, the vegetative growth is reduced. Conversely, when fruit are rare, the vegetative growth is abundant. This pattern is commonly known as a growth trade-off. Such trade-offs have been known to plant specialists for almost two centuries [15, 61], and there are numerous documented examples where the fruits are negatively correlated with growth elsewhere in the plant [10, 62-67], and occasionally with tissue death, especially of the meristem region [68-72].

The existence of a growth trade-off however, does not immediately explain how this contributes to a biennial cycle. Most temperate trees shed their fruits in the fall, and there is usually nothing left to affect growth at the start of the second season. With the exception of more tropical trees like Avocados, this suggests the plants actually retain a "memory" of the fruit load from the previous season, a hypothesis that immediately raises questions about how that information is stored and transmitted over time. While the idea that plants may retain that memory in terms of their gene expression patterns has never been tested, the available evidence instead suggests that this information is recorded in the plant's physical anatomy. For example, most trees produce flowers from their axillary buds a few months to a year after the buds are first produced. The number of such buds is proportional to the vegetative growth in the previous season [67], and since vegetative growth is often coeval with immature fruit, it is easy to see how a growth trade-off might be recorded directly by the number of axillary buds. In addition, immature flowers and inflorescences typically begin growing while still inside the buds many months before they burst open [73], so the growth trade-off has the potential to affect the size of the inflorescence (and the

number of flowers) at a very early stage in their development. Any initial differences in size incurred in this way are then likely magnified in the second season, when both inflorescence and vegetative growth resumes at an accelerated rate. Together the combination of inflorescence size and number can substantially change the number of flowers in subsequent season, and thus have an indirect control over number of subsequent fruits.

In fact, when branch lengths and flower numbers are mapped to a generic branch structure, it is possible to derive a reasonably descriptive model of alternate bearing anatomy, summarized in Figure 1.0. In the "ON" year, the presence of a large number of fruit is thought to cause the reduction in vegetative branch length and leaf numbers, providing fewer axillary buds for the return bloom in the next season. In the following "OFF" year, the axillary buds produce fewer flowers and fruit, allowing the vegetative longer branches to grow longer and bear more leaves. The cycle then repeats itself when the axillary buds produce a large number of flowers in the 3rd season, creating yet another "ON" year. Once started, this mechanism is thought to be sufficient to propagate the biennial cycle indefinitely, barring intervention by the environment or anthropological factors. The variation in branch length is also permanently recorded in the plant anatomy, and with a few caveats, several years worth of cycles can be seen simply by noting the distance between successive sets of bud scars, or the remnants of old cones or inflorescences [74].

The simplicity of this model is perhaps its greatest selling point, as it can readily incorporate information from several other areas of research. Following the discovery of plant hormones for example, it was soon found that gibberellic acid was an important regulator of flower numbers in many species, either as an activator or a repressor [75-77], and has its strongest effect during the period of floral induction [78, 79]. The response to auxin apparently changes over the course of the season, as mid-season auxin treatments can increase fruit abscission rates [80], while applications to immature inflorescences and mature fruit tend to prevent abscission [60, 81-83].

Ethylene seems to have a dual function, enhancing the number of flowers in some cases [9, 84], while stimulating abscission of young fruits in others [80, 85-87]. The role of abscisic acid is not quite as clear, but the concentration of this hormone is known to fluctuate with the cycle in citrus trees [88-90], yet it was not correlated with abscission of immature pistachios nuts [91]. In addition to the hormones, the distribution of starches [47, 92], soluble carbohydrates [93, 94] and even inorganic mineral content [46, 95, 96] can be mapped to anatomically different phases of the cycle.

The result is a comprehensive physiological model of alternate bearing, which can be used to make reliably accurate predictions for both practical and theoretical applications. The basic physiological model is also surprisingly compatible with more recent concepts of plant development. For example, most vegetative branches do not grow continuously, but are instead produce in regular bursts commonly known as a "flush". Also variously known as a "growth unit" [97] "iterative growth" or even polycyclic growth [98], a flush typically occurs once per year in temperate climates, but tropical trees can produce as many as 3-4 flushes per year [99]. Each flush is composed of at least two discrete phases of growth, known as the juvenile and adult phases. Confusingly, these two terms are also used to describe growth patterns related to the age of the plant in years, so for the sake of clarity it is necessary to borrow a slightly different terminology and refer to the variation along a single branch as "seasonal heterophylly" [100]. The first leaves of the flush are distinguished from the later leaves by subtle-to-significant differences in trichome density, color, size, and leaf morphology, and typically, the first leaves are also abscised while still immature. Typically a flush is thought to begin and end with SAM dormancy, and as a result, alternate bearing anatomy can easily be outlined as the sum of two consecutive flushes, attached end to end.

The flowers in contrast, are born on a completely different type of flush, usually called an inflorescence. These are typically produced from dormant axillary buds, though some plants also use the SAM as well. All such buds have the option of producing vegetative or reproductive structures, and the deciding factor is determined by a combination of information derived from the external and internal environments. Once the correct combination for each species is recognized though, the buds are said to be "induced", irrevocably committing them to a reproductive fate [101]. The resulting Inflorescence Meristem (IM) then produces the branches, bracts and flowers of the mature inflorescence. While the flowers are an obvious indication of reproductive growth, the inflorescence branches may also be distinguished from vegetative branches by their unique patterns in color, diameter, and trichomes. In addition, the inflorescence is also a determinate structure that senesces at maturity. The resulting abscission zone or boundary with dead tissue then provides a clear indication of which tissues were reproductive and which were vegetative (personal observation). Recognition of this pattern of senescence thus suggests that many trees do not produce one large inflorescence, but instead produce many smaller ones.

Fruit drop

Another phenomenon that has frequently been correlated with alternate bearing is the abscission of immature fruit. Descriptively called a "fruit drop", the abscission of immature fruit often appears to occur in three distinct cycles over a single season, typically numbered 1-3. The first drop occurs when old flowers are shed just after pollination. Where this has been studied in tomatoes, the first drop appears to be the result of abscisic acid buildup in unpollinated ovaries, which is normally reversed by fertilization [102]. The second drop (a.k.a. the "June" drop) occurs a few weeks later when apparently healthy immature fruits are shed, much to the consternation of the farmer who was expecting a bountiful crop up until this point. Internally

though, the abscised second drop fruits often have dead or dying ovules, which is potentially the result of inter-fruit competition [103, 104]. The exact cause for this behavior is not completely understood, but it appears to reflect the competition for nutrients between the individual fruits, carried out though a complex array of hormone pathways [105, 106] and involves different responses by different tissues in the fruit anatomy [107]. Finally, the 3rd drop occurs at the end of

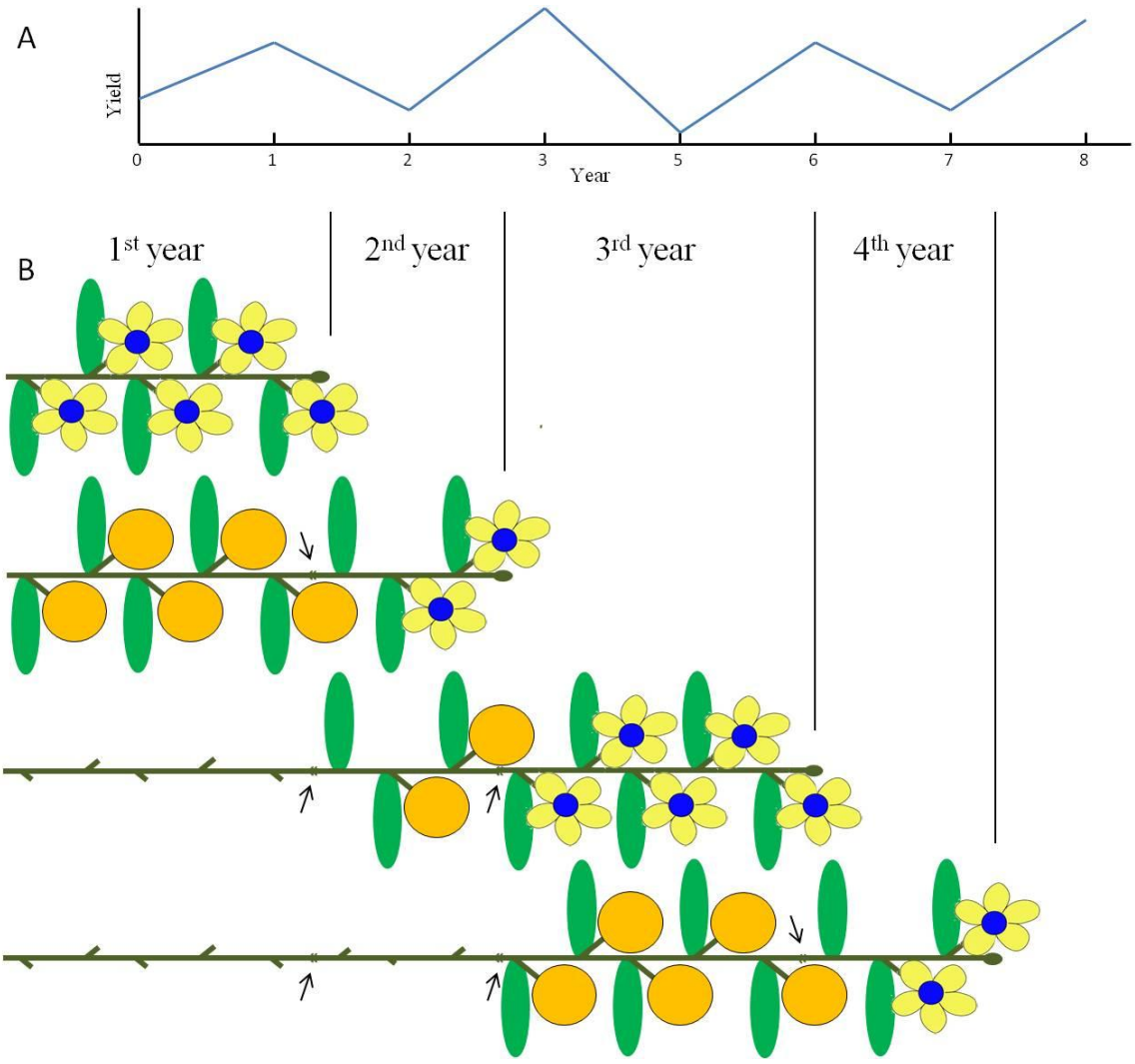

Figure 1.0. **The alternate bearing cycle.** (**A**) A generic saw-toothed graph produced when alternate bearing yields are plotted as a function of year. (**B**) The growth of a single branch is depicted over four progressively older time points, starting with an "ON" year (top), and ending with an "OFF year (bottom). Two cycles are shown. Green ovals= leaves, Orange circles = fruit. Arrows depict location of bud scars, while the tick marks on the naked stems of older branches indicate leaf scars.

the season when the fruits become mature, and is often associated with ethylene induced ripening [55, 56].

Of the three drops, the 2nd seems to have the most significant influence on the alternate bearing cycle. Current evidence suggests that this process is regulated by the seeds, as seeded fruits tend to be retained and grow larger, while the seedless fruits are smaller and are frequently abscised [108-110]. The abscission caused by Pistachio fruits appears to be even more severe, as this species is known to cause entire immature inflorescences to abscise [111], even before the fruits are present. Such intra-fruit competition is known as correlative inhibition, which at least in some species, has been linked to auxin-based apical dominance mechanism [112, 113]. Although there has been relatively little research to investigate why the 2nd drop occurs at all, it has been suggested to be a self-pruning mechanism, allowing the plant to control the final number of progeny [114].

Why does the cycle happen?

One key feature of the alternate bearing model as described above is that it is necessary for the fruits to negatively influence growth somewhere else in the plant. However, the model itself does not explain how this is accomplished, how the presence of the fruit is transmitted between organs, or even how particular plant tissues respond to that signal. To help fill this void, three different ideas have been proposed over the years, known as the competition, inhibitor, and fruit dominance hypothesis. Each is discussed below.

The competition hypothesis

In most plants, the distribution of carbohydrate and other nutrients is commonly thought to rely on the bulk flow of phloem sap between source and sink tissues. Within this framework, the competition hypothesis predicts that the ratio of sink strengths directly determines the ratio of nutrients that are provided to each organ, regardless of the overall supply. Thus when the fruits

are present, the vegetative portion of the plant may receive so few nutrients that it suffers from nutrient starvation, forcing the branch to slow down or stop growing all together. Interestingly such effects have actually been observed in living plants, as the excessive consumption of nutrients by the fruit; or even large branches [115], can lead to visible signs of nutrient deficiency, stress, and even the death of large portions of the plant [72, 116]. This hypothesis might also explain why fertilizer treatments have been repeatedly found to partially alleviate alternate bearing symptoms [11, 117-119], and why the removal of excess fruit tends to increase the size of the remaining fruits [120]. The result of girdling a branch can also be explained as a temporarily increase the relative amount of carbohydrates in isolated branches [89, 121-123], as this practice blocks sugar export to other parts of the tree. Alternatively, it is also possible to exacerbate the competition by removing leaves, which are usually the primary source of carbohydrates. In fact, organ removal is commonly used experimental tool, both for leaves [36, 77, 124-126], and fruits [38, 43, 127-129].

Identification of limiting nutrients can be difficult though, because the limiting one appears to change with the seasons, and there are variations caused by differences between species, soils, cultivation practices, and even the vascular anatomy of the plant in question. In most cases, carbohydrates and nitrogen are by far the most important nutrients relevant to alternate bearing, which together are often referred to as the C/N ratio [49, 130-132]. In rare cases though, the cycle can be affected by micronutrient deficiencies [46].

The Inhibitor Hypothesis

This hypothesis is based on the idea that the plant produces a signaling compound that is able to block growth elsewhere in the plant, even in the face of adequate nutrition. Exactly how this works on a biochemical level is not well understood, in part because this idea actually seems to encompass more than one phenomenon. Many early accounts use the term “inhibited” to

describe situations where the plant grew *less* than expected, suggesting that the definition has changed over time. With the benefit of hindsight, it is possible to recognize that some reports actually describe plant behaviors that would later be known as dormancy and apical dominance [133, 134]. More recently, there have also been many reports showing that plants sprayed with the gibberellic acid can prevent flower formation [68, 135-137], implying the endogenous levels of this hormone could play a similar role in the alternate bearing cycle. Whatever the identity of the inhibitor might be, current evidence suggests that it has a local effect, with a range of a few centimeters [128, 138, 139].

The source of the inhibitor has been speculated to reside in the leaves [140], though it has been suggested to be produced by the fruits themselves [138, 139]. Remarkably, attempts to extract such a substance from apple leaves identified a common glycoside known as phloridzin, which displays growth inhibitory effects in *Avena* coleoptile tests [141, 142]. The mechanism of inhibition was later revealed by the breakdown products of phloridzin, one of which is phloretic acid, a known auxin response inhibitor [143]. Thus at least within the spur-shoot of apple trees, the inhibitory hypothesis has a plausible mechanism that resembles apical dominance, though phloridzin has received scant attention in other species.

The role of plant hormones however, has received much more attention, and many of them have roles both promoting and inhibiting growth. Exogenous sprays of gibberellic acid or its inhibitor, paclobutrazol, are known to regulate flower numbers in many species [52, 83, 144, 145]. The seeds are also known to be significant sources of auxin [146-148], and gibberellic acid [149]. Interestingly, radio-labeled tracer experiments have repeatedly shown that hormones and sugars can move out of the immature fruit and into the subtending branch. However the reported values suggest that less than 1% of the radioactivity leaves the fruit and enters the SAM or nearby leaves [150, 151], making it unclear if this is movement is enough to have a physiological effect. So far

as this student is aware, only a single report has attempted to identify radio-labeled substances *after* they were secreted, which found both sucrose and malic acid [152]. The export of common metabolites from a major sink tissue is an unexpected finding, but it might be related to the effects of transpiration, as it has been shown that *Pisum sativum* fruits can temporarily supply water to the rest of the plant late at night [153]. It would thus be of some interest to repeat this experiment in fruit-bearing trees, where the large size of apples, oranges, or avocados might exacerbate such an effect.

Rather than being a pure chemical though, there is evidence to suggest the inhibitor might be a protein that affects the floral induction pathway. Many plants for example, have been found to produce a short-range signal in their leaves, which in *Perilla* is capable of inducing flower production in nearby axillary buds [154]. Known as the "florigen" [155], this substance was eventually traced many years later to FLOWERING LOCUS T (FT), a protein that is produced by the vasculature in the leaves and stems of *A. thaliana* [156]. Once produced, FT has been shown to travel through the phloem to the SAM, where it helps trigger the process of floral induction [157]. Induction in turn, is known to involve an array of other proteins, such as FLOWERING LOCUS D (FD), SUPPRESSOR OF THE OVEREXPRESSION OF CONSTANS1 (SOC1), SHORT VEGETATIVE PHASE (SVP), and AGAMOUS-LIKE24 (AGL24), which help establish inflorescence meristem identity, and later the expression of LEAFY, which initiates individual flowers. Thus rather than directly inhibiting flower production, it is possible that the inhibitory model might function by blocking the activity of one or more of these genes. Interestingly a known inhibitor of FT function, TERMINAL FLOWER 1 (TFL1), is expressed in the seeds of orange trees (*Citrus unshiu*) [158]. If CuTFL1proteins are sufficiently non-cell autonomous, this also holds the potential to propagate the alternate bearing cycle by inhibiting floral induction in nearby buds. A similar paralog in apples,MdTFL1, is expressed in apical buds

before the reproductive transition, and is known to extend the period of vegetative growth when expressed in *A. thaliana* [159]

The Fruit Dominance Hypothesis

Another way in which the fruits are thought to suppress growth is by taking advantage of a mechanism that already exists in most plants: apical dominance. As commonly understood, growth of axillary buds along the sides of the stem is suppressed due to the rootward transport of auxins produced by the apical meristem. When the SAM is removed, the lateral buds sprout in basipetal sequence reflecting the depletion of the auxin flow. A similar suppression of growth also occurs in the inflorescence, as the first formed fruit suppress the growth later formed fruits in tomato trusses [110], which is also known as king fruit dominance. The term correlative inhibition has also been used to describe dominance between fruits in the same inflorescence [112]. As a result, it is not hard to imagine how this auxin-based mechanism might be used to suppress the growth of the SAM and other vegetative structures, where it is known as fruit dominance [101]. This idea has some support, as plants with parthenocarpic fruits have higher fruit set rates than seeded ones [160], and removal of the SAM improves seed set in peas [161]. One prediction of the fruit dominance model suggests that the flow of auxin between the fruit and apical bud would be reversed [101], and this reversal has actually been observed following the injection of radio-labeled auxin into various plant organs [162].

The mechanics of dominance however, are still poorly understood. Studies in both *A. thaliana*, and in the *P. sativum* models have identified the importance of the auxin transporter PIN1 [163], and a potential root-derived chemical inhibitor of dominance. This root-derived substance was later identified as strigolactone [164, 165], a molecule whose biosynthesis and perception is at least partially regulated by MORE AXILLARY MERISTEM (MAX) genes [166-168], and also by several CARATENOID CLEAVAGE DIOXYGENASES (CCD) genes [169, 170].

Interestingly, strigolactone molecules also bear a passing structural resemblance to phloridzen, suggesting that the latter may be a functional analog of this plant hormone. Much more recently, sugar distribution was found to be a significant part of establishing dominance [171], suggesting that all three hypothesis may be needed for a full explanation of growth trade-off.

CHAPTER1 Expression profiling of fruit load in *A. thaliana* inflorescence meristems

In alternate bearing theory, there are three competing hypothesis that attempt to explain how the fruit negatively influence vegetative growth. The competition hypothesis suggests that the demand between two sink tissues determines the flow of nutrients to each organ, the inhibitor hypothesis suggests that either the leaves or the fruits suppress flower development even when nutrient supplies are adequate, while the dominance hypothesis suggests that the fruits reverse the apical dominance mechanism, suppressing the apical meristem and subsequent vegetative growth. Although the competition hypothesis is favored by the growth trade-off observed in many alternate bearing species, there been few attempts to determine which of the mechanisms predominates in actual growing tissues. One way of doing this would be to observe the expression profile of actively growing meristems subjected to a heavy fruit load, as each of the hypothesis could be expected to produce a unique signature of up and down regulated genes. For example, a recent genetic study of alternate bearing apple trees was able to demonstrate several genes related to auxin and gibberellin hormone pathways were located in alternate bearing quantitative trait loci (QTL) [33]. The presence of auxin genes could be used to support the fruit dominance hypothesis, while gibberellin and floral induction genes might indicate the presence of an inhibitor pathway. An impressive set of microarray data from alternate bearing mandarin scions [35] found that several glucan and trehalose sugar-related genes were activated during the ON year. The authors further argued that the FT paralogs CiFT1 and CiFT3 were involved in suppressing vegetative growth, but recommended more work to validate this idea.

One aspect not captured by either study is the degree of fruit load, which varies continuously over the annual production cycle and may even produce a concentration gradient in the case of the inhibitor theory. However, even if reported in terms of the alternate bearing index or fruit

biomass, the use of averaging and biological replicates would obscure the signal before dosage sensitive responses could be extracted from the data.

In order to avoid this issue, the present study examined the effects of fruit load in *A. thaliana*. Although an annual species, this plant produces many more fruits than alternate bearing trees, and has the potential to exacerbate the fruit load experienced by the inflorescence meristem. To identify how the fruit load changes expression patterns, surgically dissected IM apices were collected after producing more than 30 fruits, and were profiled with ATH1 microarrays. This analysis found relatively few differentially expressed genes, though the overall pattern was consistent with carbohydrate starvation and clearly supports the competition model. No evidence of flower inhibition was found, and instead flower promoting genes were strongly up regulated, which is inconsistent with the inhibitor hypothesis. The fruit dominance model was only weakly supported by the present data, though this may be related to an atypical dominance mechanism in *A.thaliana*. Further analysis of IM growth patterns supported the existence of a determinate growth pattern, which displayed both fruit load dependent and independent effects. The arrest of IM activity was correlated to rosette leaf senescence, and eventually terminated through a localized senescence mechanism.

Microarray Results

In order to observe how fruit load affects meristem activity, a microarray experiment was performed to correlate gene expression patterns with the three alternate bearing hypothesis. However, because microarrays only measure the relative concentration s between different transcripts, this procedure cannot directly identify the cause of the observed levels. The input from mRNA biosynthesis is differentially regulated than the catabolism processes that reduce the

overall transcript pool, and both forms of regulation are in turn affected by changes in any of the multitude proteins that control them. In order to obtain this regulatory information, it would normally be appropriate to perform additional microarray experiments in the presence of chemical inhibitors to block key enzymatic steps, and to validate the actual expression levels in a subset of genes with RT-PCR or qPCR methods. Unfortunately, due to the circumstances of Dr. Smith's departure, none of this work was performed as expected. Consequently, the data presented below is best interpreted as a preliminary analysis, providing a number of hypothesis that might be investigated in future studies.

To begin, meristem tissues were surgically dissected from *A. thaliana* 1° inflorescences using plants grown in both long day (16/8) conditions (2 biological replicates), and from plants grown in continuous light (3 biological replicates). Total RNA was extracted from each replicate, and then hybridized to five individual Affymetrix GeneChip ATH1 microarrays (22750 unique probe sets). An initial analysis revealed less than 100 differences between the two photoperiod treatments, and no clear patterns were found in any cellular functions, gene families, or metabolic pathways. In the absence of any significant differences between the two photoperiods, the data sets were combined, providing a total of five biological replicates for the high fruit load treatment.

Unfortunately, due to the abrupt end of my work in this lab, control tissues from de-fruited plants (low fruit load) could not be collected as expected. Instead, a previously published microarray data set [172] was chosen to replace the missing controls, providing 3 biological replicates. From the combined 5 x 3 array analysis, 15,473 genes were detected at least once, and 7337 were detected in all eight arrays. This list was further filtered to remove genes that had Bayesian probability scores below 1.5, and filtered to remove genes than had an adjusted p-values greater than 0.05. To focus on those that were most significantly affected by fruit load, only genes with

logFC values above +2 or below-2 were selected for further analysis, providing a list of just 512 genes.

Initial examination of functional annotations however, revealed a large number of genes known to be exclusively expressed in the pollen, most of which had elevated transcript levels in the high fruit load treatment. Curiously, this pollen signal was shared with a previous meristem profiling experiment [173], where it seemed equally anomalous This prompted a re-evaluation of the tissue collection procedure used in the present study, which revealed a highly probable route of pollen contamination that had previously been overlooked. This finding strongly suggests that the pollen-specific genes detected in both studies are false positives. To remove this source of bias, the expression pattern of all 512 genes was scored using the eFP browser [174]. This found 66 genes that were exclusively expressed in the pollen, and another 33 that were specific to green embryos, and are also likely products of contamination. In contrast, 17 genes were expressed largely in immature flower buds, but unlike the pollen signal, these were often had severely reduced transcript levels. Instead of contamination, the reduction of flower bud specific transcriptsmost likely reflects a tissue collection bias The tissue for the control arrays (low fruit load) removed flower buds around the SAM older than stage 6, while the present study removed flower buds older than about stage 3 (see methods). All 117 atypical genes (Appendix 2) were subtracted from the total, leaving a final list of 389 differentially expressed genes (Appendix 1). Of these genes, 103 (26.5%) had reduced transcript levels, and 286 (73.5%) had increased transcript levels. Mapping of functional annotations within this data set revealed no clear trends, but instead found a widespread pattern where most functional pathways were represented by at least one or two genes. Although coverage is sparse, in many cases it was possible to estimate the direction of metabolic flux and the larger impacts on cell physiology. These are summarized below:

Cell wall and plasmamembrane integrity

When compared to SAM tissue collected under low fruit load conditions, the high fruit load treatment correlated with reduced transcript levels for several cell wall components, including the glycoproteins *PRP2, PRP4,* and the putative leucine-rich protein At4g18670. The existing glycoproteins may also be degraded, as the xyloglucan hydrolase *TCH4* transcripts were elevated. These observations also parallel the findings for lipids, where several biosynthetic genes had reduced transcript levels (At1g43800 and, *ADS1, NMT1, GPAT6,* and *GPAT8*), whereas one lipid catabolism gene showed an increased transcript level (At1g68620). The reduction of two potassium channel transcripts, *KUP7* and *KEA2,* might also suggest that the plasma membrane and chloroplast envelope have a reduced capacity to maintain normal charge separation.

Dessication stress response

For the high fruit load treatment the meristem tissue was collected near the time of apical arrest, after which the meristem tissues often became visibly dehydrated. To see if the early symptoms of dehydration were already present when the tissue was collected, the data was compared to young meristems in the absence of fruit load. This revealed a reduction in the transcripts of *CER1,* a gene involved in wax biosynthesis, suggesting a loss of the waxy cuticle. Desiccation stress responses are indicated by the elevated transcript level of the abscisic acid biosynthesis gene *NCED3*. Several other abscisic acid responsive genes had elevated transcripts, including *HVA22J, TSPO, HB5,* and so did genes known to be up regulated by drought stress, such as *HIS1-3, ERD14,* and *RD20*.

Senescence

Many senescence-related genes also had comparatively high transcript levels under high fruit load conditions, including *SAG12,* At5g65040, At1g22160, though *PUB44* transcripts were reduced. The high level of transcripts found for the AP2-like transcription factor At5g51190 might suggest

that the ethylene response pathways are involved with senescence, though no other genes in this pathway were detected. However, ethylene perception by *ETR1/2* is known to require a copper ion co-factor [175], so it is at least noteworthy that several copper-related genes show elevated transcripts, including two copper binding proteins (*MT1A*, *MT1C)*, two copper chaperones At5g17450, At3g56240, and the putative copper-amine oxidase At1g62810.

Programmed cell death

Most intriguingly, the high transcript levels of *METACASPASE3* (*MC3*) suggests the existence of a programmed cell death (PCD) response in the apical tissues. Although the exact role of *MC3* is not well understood in plants, in animal models PCD is typically activated following the rupture of the mitochondria, flooding the cytoplasm with free radicals that then triggers a proteolytic cascade regulated by CASPASE enzymes. Depending on the tissue type and the nature of the stimulus, the destruction of the cell can follow one of three recognized patterns: necrosis, where the cell is rapidly destroyed by physical damage to its membranes, apotosis, where the cell breaks apart into small fragments that are eventually cleaned up by macrophages in the bloodstream, and autolysis, were significant portions of the cytoplasm and nuclei are enclosed in lytic vesicles and digested. Apotosis is further correlated with DNA laddering produced by the fragmentation of nucleosomes, while necrosis and autolysis tend to produce high molecular weight smears.
In plant tissues, the mitochondria have been found to play a similar role in autolysis pathways [176], and this is supported by the present study, which found that two carbonic anhydrase transcripts, *BCA3* and *BCA6*, were elevated under high fruit load treatment. The proteins produced by these two genes are localized to thechloroplasts and mitochondria, and this pattern suggests an increase in the concentration of dissolved bicarbonate ion. However, no other free-radical responses were detected in the current data, so the significance of this observation is unclear.

In order to discriminate between the three modes of cell death, multiple attempts to observe the characteristic DNA laddering of apotosis were performed. Surprisingly, this found traces of DNA laddering in actively growing meristems, but not in older quiescent meristems, which instead produced high molecular weight smears (Figure 1.4). The necrotic mechanism might be indicated by the previous predictions for a weak cell wall, and by the presence of senescent pathways, though it is unlikely in the absence of any obvious sources of physical damage. Autophagy in contrast, is supported by the high transcript levels of AUTOPHAGY 8H (ATG8H), which may also have a role in ubiquitin-related protein degradation.

Protein recycling

An examination of ubiquitin related pathways in turn, reveals that most components related to proteosome-mediated decay have elevated transcript levels under high fruit load treatments, including three F-BOX proteins, two RING domain zinc fingers, and two E2 ligases *UBC17,UBC29*. The de-ubiquitinating protein product of *UBP14* might also be down-regulated, as its transcripts were reduced, potentially removing this brake on protein recycling pathways. In addition, at least eleven peptidases enzymes were detected, eight of which had higher transcript levels under high fruit load, including: *GAMMA-VPE, MC3, SCPL48, At2g39850, SBT5, SAG12, SCPL36, SCPL38,* while three of which were found to have reduced transcript levels: *At5g42620, SCPL35, DegP7*.

Protein catabolism and nitrogen release

Under high fruit load conditions three catabolism genes were found to have higher transcript levels, which suggests that nitrogen is released as a part of protein catabolism. One is At4g33150, which is involved in lysine and α-ketoglutarate hydrolysis, and the other is At5g18860, involved in nucleoside hydrolysis. The third gene, the methionine gamma-lyase At1g64660, more specifically suggests that nitrogen is released as ammonia. This is at odds

however, with the increased transcript levels of the glutamine synthetase *GLN1-4* and the nitrate importer *NRT1.2*, both of which suggest nitrogen shortages. The elevated transcripts of *AGL44* is more difficult to interpret, because although *AGL44* is annotated as a nitrate responsive gene, this gene does not always respond to nitrogen starvation [177, 178].

Carbohydrate mobilization

Compared to the absence of fruit load, meristems treated with high fruit load appear to convert their starch reserves into sucrose and exported the sugar out of the SAM. This is supported by the increased transcript levels of two putative Trehalose 6-Phosphate Phosphase genes (*TPPG, TPPH*) which suggests that less starch biosynthesis occurs, and this correlates well to the increased transcript levels of the starch degrading enzyme *AMY1*. Although there are no detected genes for glycolysis or the TCA cycle, the simultaneous increased transcription of the sugar importers *SUC2* (sucrose) and *ATPLT5* (short oligosaccharides) suggests that the meristem cells are experiencing a carbohydrate shortage.

Signaling

Calcium signaling pathways are over-represented in the data set, comprising 48% of all detected signaling components, most of which show increased transcript levels under high fruit load conditions. Those with annotated functions (*PBP1, TCH2, CML38, RD20*) suggest a role in wound, phosphate starvation and/or desiccation responses. These functions are also shared with the *WNK4* kinase, which strongly implies that these signaling components have role in the senescent pathways described above. Others like *FZL* and *ELIP2* are known to be involved with chloroplast development. Mutants of *FZL* are known to produce irregular grana structure [179], while the over expression of *ELIP2* reduces chlorophyll content [180]. These findings mirror the reduction of *FZL* transcripts and the increase of *ELIP2* transcripts detected in the present study, and suggests that chloroplast function has been compromised.

Two component of the cytokinin hormone pathway (*AHP1, ARR9*) were also found to have increased transcript levels, though no other cytokinin responsive genes were detected, nor were any genes involved with cell cycle regulation. The presence of the A-type *ARR9* suggests suppression of cytokinin signaling. Finally there is *STRUBBELIG (SUB*), a serine/threonine kinase known for its positive regulation of trichome differentiation. It is also known to be involved in meristem activity and integument development, but in this study, *SUB* transcript levels were strongly reduced. Given that older flower buds have better developed trichomes than younger flower buds, this finding may be related to the tissue collection bias discussed above

Auxin Signalling

Auxin hormone signaling is likely down-regulated in response to fruit load, indicated by the increase in IAA7-repressor transcripts, and the decrease in ARF2-activator transcripts. This also agrees with the increase in MAX1 transcript levels, which is thought to inhibit apical dominance mechanisms. Curiously, three Small AUxin Responsive (SAUR) genes also had elevated transcripts. Although their function is not well understood, the annotations of related SAUR's suggest that they may be part of a stress response pathway.

Development

The fruit load treatment also increased the transcripts of MADs box development transcription factors such as *SOC1, AGL71,* and especially *FT,* all of which are known for promoting flower development. This short list may also include the MADS box gene *AGL44,* though the functions of this gene in flower development or nitrogen starvation responses are not well understood. Several homeobox transcription factors also had higher transcript levels, including the clearly abscisic acid responsive *BLH1, ATHB7, ATHB12*, and a few that were more broadly expressed, such as *ATHB2* and *ATHB8.* In contrast, *ATHB40* was found to be partially expressed in the anthers [174], which again is suggestive of pollen contamination. Only *HDG12* had reduced

transcript levels, perhaps because its role in flower differentiation would not be needed in arrested apices that are no longer producing flowers.

Chromatin structure

Most chromatin binding proteins had reduced transcript levels under high fruit load, such as *FAS1, ATX1, DMT7,* and *BRAHMA.* Mutants in *FAS1* are known to reduce heterochromatin [181], so the reduction of *FAS1* here might lead to an increase of euchromatin. This is also supported by the reduced transcript levels of the histone methyltransferase *ATX1*and the DNA methyltransferases (*DMT7*), which would likely increase the amount of euchromatin simply by shifting the balance toward acetylated histones, and by making it harder to maintain silenced DNA though cell division. However the reduction of the chromatin remodeling factor *BRAHMA* suggests that transcription rates in general might be reduced, despite the possible increase in exposed DNA. There is also evidence of DNA damage, as two nucleases (*BFN1* and At3g56170) had elevated transcript levels, while a loss of double-strand break repair is suggested by the reduction of *HDG12* transcripts.

Characterization of Meristem Activity

Preliminary analysis of the microarray data indicated a strong senescent response, which was unexpected given that several steps had been taken in order to avoid senescent tissue. Reasoning that the tissue collection procedure had relied on an inadequate predictor of senescence, an attempt was made to identify better markers for future use. This was done by measuring leaf and bud growth rates every two days over entire lifespan of the plant, then searching for strong correlations that occurred at least 3-4 days before the symptoms of senescence became visible. Under the long day conditions, Col-0 plants were found to have a population of immature flower buds (stages 3-11, see [182]) that varied over time, reaching a maximum at the first flower and then declining briefly before leveling off at about 10 buds (Figure 1.1). Open flowers meanwhile,

occurred at an overall linear rate of 1.37 flowers/day, which is somewhat slower than the 2.6 flowers per day linear rate reported for L*er* plants grown in continuous light [183]. However, when the total number of flowers+buds was used to calculate growth rates over shorter time intervals, the bud production rate was not found to be precisely linear, but instead consisted of two acceleration trends, one rapidly increasing the number of flower buds, and the other decreasing. towards zero (Figure 1.2). The declining trend began before significant numbers of senescent leaves were observed, and continued unperturbed even after most leaves had been lost In comparison, rosette leaf initiation rates (Figure 1.3) revealed a nearly constant production rate at about 1.1 leaves per day, which is about the same as the initial rate of flower bud production. Meristem growth stopped between 26-28 days after induction, indicated by the simultaneous plateau in both immature green bud numbers and total flower numbers (Figure 1.1). In many

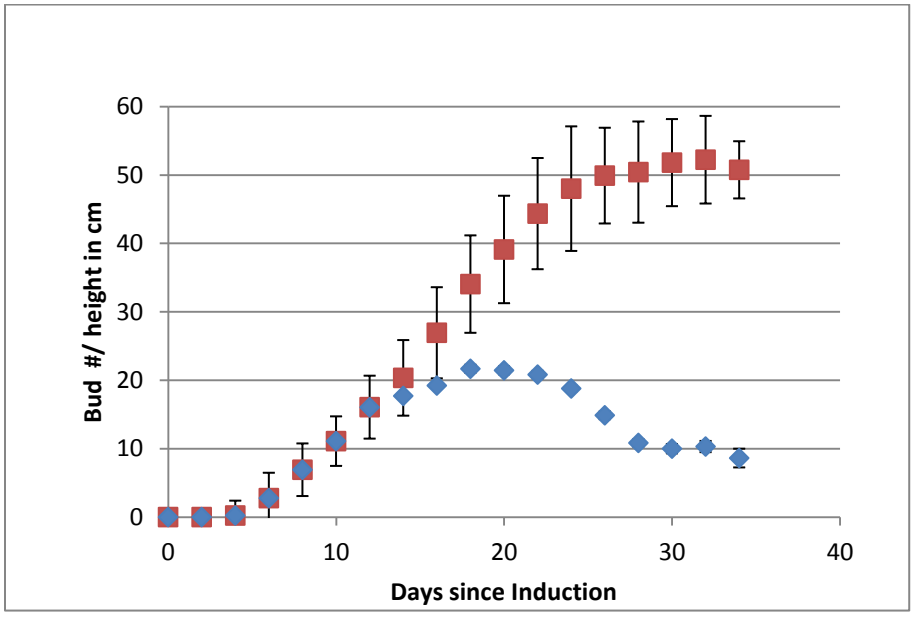

Figure 1.1. Flower bud numbers over time. Data has been aligned relative to the estimated time of induction, see methods. Red= total number of flower buds produced. Blue= number of immature buds between stages 4-11). Error bars are calculated as mean±SEM, n=50.

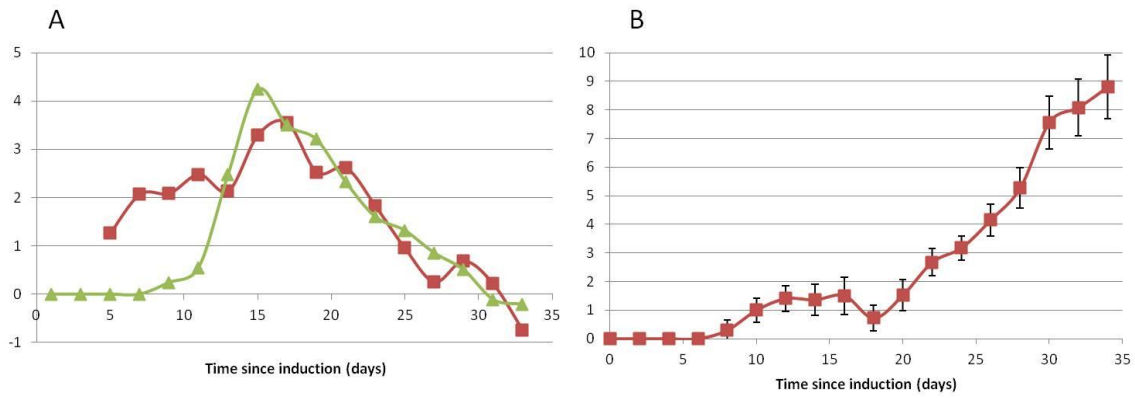

Figure 1.2. Rate of flower bud production over time. Data has been aligned relative to the estimated time of induction.. **(A)** Anlagen productivity Red= flower bud production rate (buds/day). Green = stem length growth rate (cm/day). **(B)** Total number of senescent leaves. Error bars are calculated as mean±SEM, n=36.

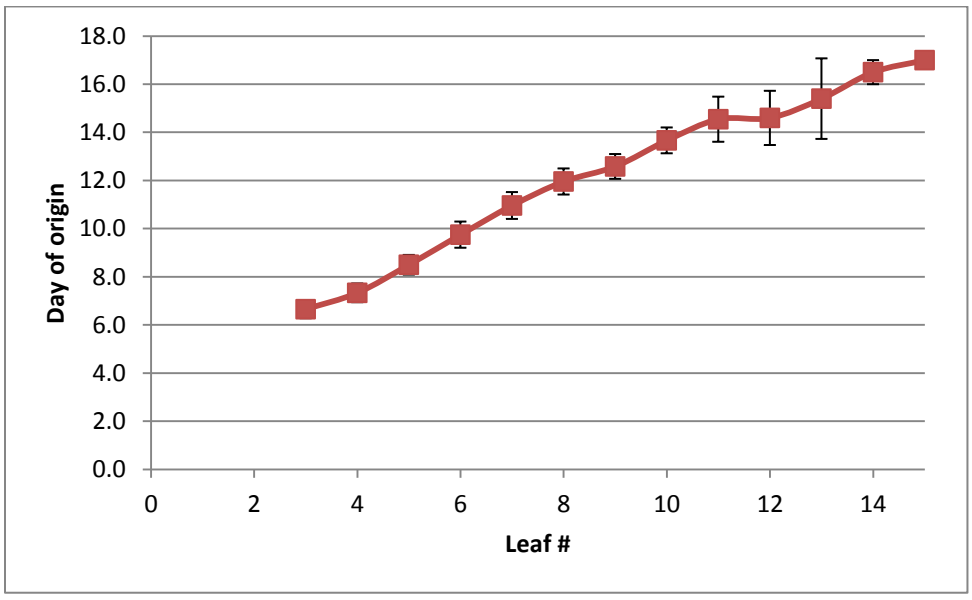

Figure 1.3. Rate of rosette leaf initiation. Day of origin is calculated from the first measurable leaf length. Leaves 3-10 are rosettes leaves, while 11-15 are cauline. Error bars are calculated as mean±SEM, n=12.

cases the buds around the arrested meristem remained green for several days, during which time they can be induced to resume growth by removing the fruits or following the senescence of the old fruits [184]. Flowers produced during the transition to this quiescent phase were often small, infertile, and had petals that did not exceed the sepals. The visible symptoms of senescence eventually appeared as an abrupt color change, proceeding from pale green, yellow, dark red in less than 48 hours, and eventually became brown as the tissue dried out. Senescence affected multiple tissues within the apical region simultaneously, including the SAM, 1-2 mm of the subtending stem, and all attached flower buds within that region, while tissues immediately below remained green (Figure 1.4). No abscission layer was detected. One possible trigger for such apical senescence may come from the leaves, which showed an increasing trend of senescence prior to meristem arrest (Figure 1.5). To study the possibility that apical senescence might be triggered by mobile signal produced by senescent leaves, a further experiment was performed that removed leaf tips from adult-phase leaves before they began to display senescent-related color changes. Removal was timed to coincide with the maximum leaf length growth rate, well before senescence could occur. The results however, show that this actually had the opposite effect,

Figure 1.4. **Terminal Meristem Phenotypes**. A-C = Col-0 wild-type, D = *soc1/ful* mutant. **(A)** Actively growing meristem. **(B)** Quiescent meristem. **(C)** Senescent meristem. **(D)** *soc1/ful* double mutant terminal meristem. **(E)** DNA fragmentation in actively growing L*er* SAM (lane 1) and senescent meristems (lane 2). DNA ladder is indicated in base pair units.

as meristem arrest occurred on average 4.6 buds, or about 1.8 days sooner in leaf-tipped plants than it did in the controls (Figure 1.5).

Alternatively, the fruits might be the source of a growth inhibitor, as predicted by the alternate bearing inhibitor hypothesis. To eliminate this possibility, the flowers were removed on a daily basis in order to observe changes in meristem activity and the time of growth arrest. Because previous results had shown that the rate of immature bud production and total stem height were closely correlated during the flowering period (r^2=0.95), internode lengths were measured as a proxy for meristem activity in *A. thaliana*. The resulting data revealed that both the controls and de-fruited plants displayed a similar declining trend of meristem activity (Figure 1.6) that eventually reached zero growth (meristem arrest). However, de-fruited plants clearly offset the time of meristem arrest through an extended period of almost linear bud production rates. This linear trend began a day before the control meristems slowed to zero growth, and lasted for

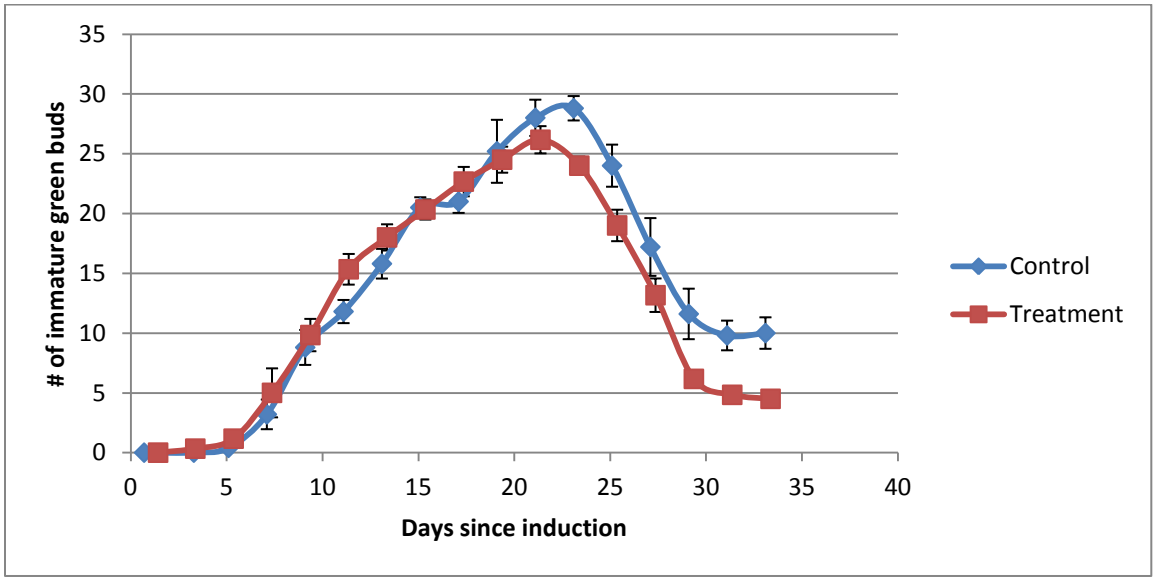

Figure 1.5. Leaf tip removal affects SAM growth. Leaf tips were removed during their period of maximum growth to eliminate possible senescence-produced SAM inhibitors. Data is aligned with the estimated day of floral induction. Error bars are calculated as mean±SEM, n=12.

almost a week (30 buds) before resuming the declining trend that the control plants had already completed.

To verify the effects of fruit load in Avocados, SAM tissue was collected from branches with and without subtending fruit, four months after anthesis. To test the dominance and inhibitor hypothesis, the expression profile of four genes were measured with qPCR, yet this analysis found no significant patterns related to the presence of the fruit (Figure 1.7).

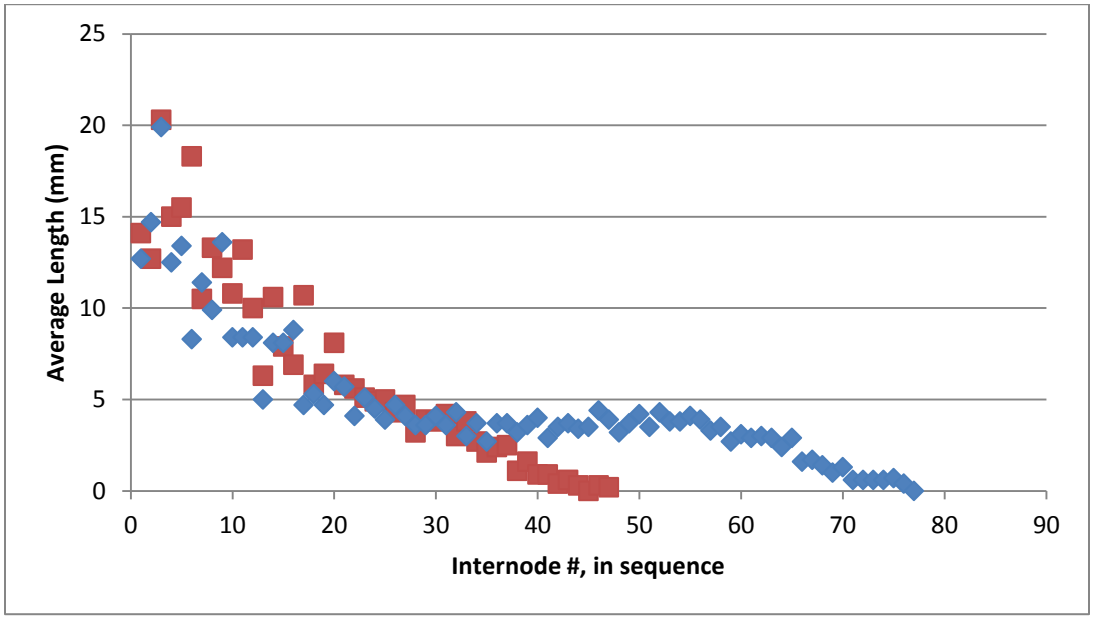

Figure 1.6. Fruit removal affects meristem growth rates. Growth rates are inferred from internode lengths in *A thaliana*, measured after whole plant senescence. Internodes are shown in consecutive order. Red= untrimmed control, Blue= continually de-fruited plants, n=10

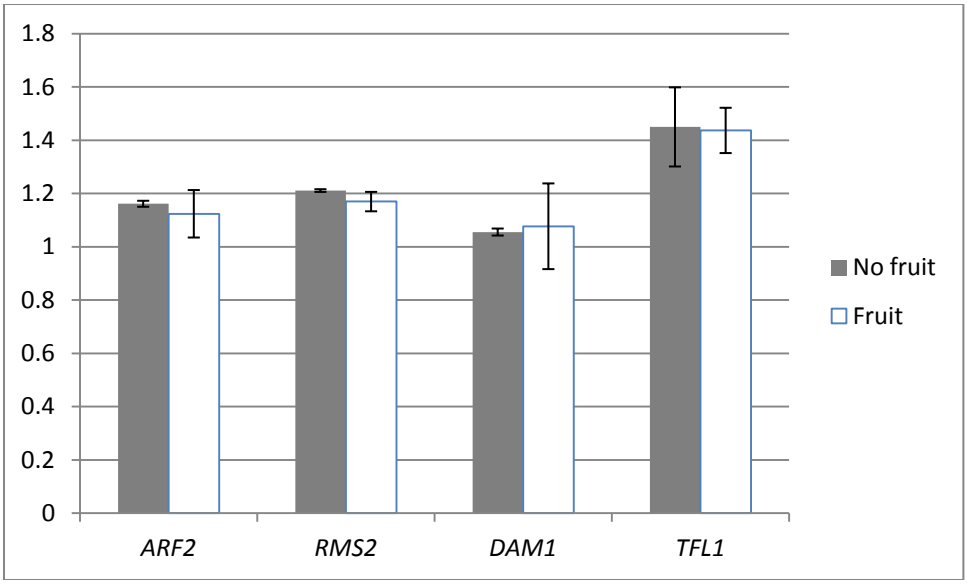

Figure 1.7. Expression of dominance and flower-related genes in Avocado meristems. Avocado genes were identified by sequence similarity to *Arabidopsis* genes, and measured with qPCR. Dominance related genes include *AUXIN RESPONSE FACTOR2 (ARF2*) and *RAMOSUS2 (RMS2)*. Flower related genes include *DORMANCY ASSOCIATED MADS-BOX1 (DAM1)* and *TERMINAL FLOWER1 (TFL1)*. Tissue collected 21-June from branches with and without attached fruit. Results are shown relative to PaActin =100%. Error bars show 95% confidence intervals, n=3.

Discussion

Competition model

In the carbohydrate competition model, the fruits are thought to consume the majority of available nutrients, leaving little if any for the rest of the plant. The remaining parts must either reduce their growth in direct proportion to the limiting nutrient, or trigger starvation responses in order to survive short-term depletions. In most plants, the two most commonly encountered nutrient depletions involve carbohydrates and nitrogen, both of which have well-characterized response patterns that also show a significant degree of overlap. Under carbohydrate starvation conditions, for example, the plant tissues typically suppress respiration and growth while consuming their starch reserves [28, 185]. Eventually both proteins and lipids are degraded

[186], releasing free amino acids and nitrogen in the form of ammonia [187, 188]. Some nitrogen is recovered in glutamine or asparagine biosynthesis [188], while the rest either diffuses into the media or is consumed by the nearest available sink tissue [186]. Under prolonged conditions, large portions of the cytoplasm are consumed by autophagy [176], in which even organelles are degraded in lytic vacuoles containing cysteine/serine proteases [189, 190]. These vacuoles eventually coalesce until the cell consists of little but the nucleus and a large vacuole [189], which is followed by cell death under extreme cases.

This pattern of responses is also strongly reflected in the present study. Starch breakdown is predicted both by trehalose signaling and direct digestion by *AMY1*. Protein breakdown is supported by the increase in proteosome enzymes and two amino acid catabolism genes. Although an increase in asparagines biosynthesis was not detected, the methionine gamma-lyase enzyme (At1g64660) is known to release ammonia, and two nitrate transporters were upregulated, perhaps reflecting a decrease in free nitrates. Autophagy is consistent with the up-regulation of an array of cystein/serine proteases, the near-lack of DNA laddering, and the presence of MC3. Carbohydrate starvation has also been reported to reduce osmolarity and membrane permeability [191], which parallels the observation of a weak plasmembrane, and the up-regulation of desiccation responses found by the present study.

Nitrogen starvation in contrast, is associated with the suppression of most chloroplast and photosynthesis related enzymes, loss of starch reserves, and the increase in uptake transporters and various storage compounds, including asparagine [188], glutamine, and various organic acids, while reducing losses that occur through degradation[177, 178]. Prolonged shortages typically result in anthocyanin production. Autophagy also seems to be an important part of nitrogen recycling in senescent leaves [187], though this may not have been detected in published studies that rely on short term starvation experiments.

In the present data, the symptoms of nitrogen starvation are equivocal. Two photosystem subunits were reduced (*PSBH, PSAA*), which is broadly consisted with the degradation of the chloroplasts predicted by *FZL* and *ELIP2*. Autophagy signals do occur in the data, but the collected tissues were not obviously senescent, suggesting that autophagy may be more closely related to carbohydrate starvation. The increase of *PAP1* is consistent with the biosynthesis of flavonols and other red pigments under nitrogen stress, though the much stronger increases in *GL3, PAP2*, and *MYB12* reported by [192] were not detected in the present study. The nitrate importer NRT1.2 was increased, but this conflicts with the earlier interpretation of amino acid catabolism in the present data. Thus the IM does not appear to be synthesizing storage proteins as predicted by nitrogen starvation studies. In consideration that the growth conditions used in this study included supplemental nitrogen fertilizer, the existence of a nitrogen shortage is unlikely. Instead, the relatively weak nitrogen starvation signal found here is potentially a consequence of the much more significant carbohydrate starvation response.

Inhibitor model

Among the candidate induction genes that might be inhibited by high fruit loads, the results found that none of the floral induction pathways were reduced. Instead the expression of *FT* was strongly increased (LogFC = +5.95), as were several downstream targets including *SOC1*, *AGL71*, and perhaps also *AGL44*. One possible explanation for this pattern might be found in the expression pattern of *FT*, which based on microarray data [174] is also produced by the ovaries and immature fruits, in addition to the leaf and stem vasculature [156]. The failure to remove all immature flower buds during tissue collection might then bias the results in favor of these induction genes. In avocado trees, the *TFL1* and *DAM1* paralogs showed no significant response to fruit load (Figure 1.7). The biosynthetic enzymes that produce phloridzen are currently unknown, so the presence of this compound cannot be evaluated with the present data.

Fruit dominance model

The fruit dominance hypothesis also does not seem to be strongly supported by the present study, as all detected parts of the auxin response pathway were suppressed by high fruit load conditions. However, *Arabidopsis* is among the minority of species that do not have strong apical dominance responses [193], which could imply that this finding is an artifact. The failure to abscise immature fruits like many alternate bearing trees, for example, may indicate the lack of a functional fruit dominance system. However, the observation that isolated nodes of *Arabidopsis* can suppress axillary bud growth following auxin treatment [194], and that the lower portion of *Arabidopsis* branches initiate growth in a basipetal pattern [195], suggest that the dominance mechanism has not been lost, but is instead suppressed. A likely candidate for this suppression is the plant hormone strigolactone [196], which is able to suppress branching in the shoot when expressed in the roots [197, 198]. In *A. thaliana*, the widespread expression of the strigolactone biosynthesis gene *MAX1* in the vasculature [199, 200] is consistent with the broad suppression of dominance pathways in the species.

Given that strigolactones appear to inhibit bud growth by blocking their ability to export auxin [201], this system has interesting parallels with the 2nd fruit drop, king fruit dominance, and even the number of flowers produced by axillary inflorescences. Immature fruits are already known to export auxin, suggesting that the plant may control their numbers by secreting root or shoot derived strigolactone into the inflorescence. The up regulation of strigolactone production under starvation conditions [202-204] is certainly consistent with the increase in *MAX1* expression levels found in the present microarray data. Such a role may explain the different alternate bearing amplitudes that were found when avocado trees were grafted to different rootstocks [205]. Expression of ARF2 and RMS2 paralogs in Avocado trees however, did not reveal a significant response to fruit load (Figure 1.7).

Trehalose

Another potential candidate for fruit inhibition might also include the trehalose signaling pathway. Although the precise role of this signaling sugar is not well understood, biosynthesis mutant are lethal [206, 207], and high concentrations of trehalose-6-phosphate do seem to be correlated with starch biosynthesis [208, 209]. Accumulating evidence however, suggests that trehalose may have a central role in controlling the broad details of cellular metabolism. Several TPP genes are upregulated in response to nitrate treatments [177, 178, 210], and also by carbohydrate starvation [211, 212]. This mirrors the findings of the two trehalose phosphate phosphatases (TPP) that were identified in this study, and in a recent profiling experiments with alternate bearing trees [35, 213]. Trehalose has also been shown to inhibit the kinase activity AKIN10/11 [214], which has broad effects throughout the cell [215], and may explain how trehalose can regulate pathways such as cell size [216] and stress tolerance [217]. Intriguingly, the vegetative-adult phase change has also been implicated to be a product of carbohydrate supply, which also involves trehalose signaling [218].

Senescence

Although the data supports the existence of a massive senescence response, much of this signal disappears when the symptoms of carbohydrate starvation are considered. This is consistent with observations of the tissue during collection, which was often still green and displayed no external symptoms of senescence. The only remaining sign of biologic stress is the slight increase of AtRLP54 expression levels.

Meristem arrest

The inflorescence meristem of *Arabidopsis* is a determinate growth, known to stop functioning after producing a predictable number of flowers in the L*er* ecotypes [183]. Under the growth conditions used by this study for the Col-0 ecotypes, the time of meristem arrest was slightly

more variable, but otherwise displayed a nearly identical pattern. Growth arrested meristems however, do not immediately terminate their activities, but instead exists in a quiescent state for several days, during which they can resume growth when the subtending fruits are removed [183, 184]. The present data suggests that this behavior is driven to a large extent by the re-allocation of carbohydrate resources. Interpreted in this way, the quiescent state is comparable to the survival phase exhibited by excised maize root tips, where growth could be resumed by adding supplemental sugar to the media. [191].

However, starvation isn't sufficient to explain all of the behaviors of the inflorescence meristem. In contrast to previous report of a linear rate of anthesis [183], a closer examination of meristem activities revealed a number of subtle trends. When measured in terms of anlagen/day, the vegetative meristem is found to have a nearly constant rate of production that does not change with the juvenile/adult phase transition, which occurred between leaves 6-8 (Figure 1.3). After induction, the inflorescence meristem revealed a rapid rise in flower buds/day, a period of time that corresponds to an enlarged SAM diameter, and an increase in gibberellic acid biosynthesis [219]. As anlagen production requires a finite surface area in order to develop, the increase rate of bud production may be related to the larger diameter of the meristem during this time. The steady decline in the distance between meristems as previously observed [220], may simply reflect the decreasing size of the central area. Such an effect may be widespread among angiosperms, as bud rates increased following induction in chrysanthemums [221] and *Chenopodium amaranticolor* [222], *Protea spp*. [223], while increased meristem sizes following induction have been found in apple [224], strawberry [225], chrysanthemums [221], and *Protea spp*.[223].

At about the time the first flower reaches anthesis, the inflorescence meristem then begins a long steady decline in activity. This begins well before the rosette leaves begin to senesce, and

continues unperturbed well after most leaves are gone (Figure 1.2). A similar declining pattern was also found in continually de-fruited plants (Figure 1.6). Both of these patterns are poorly correlated with the supply of carbohydrates, which suggests that this growth pattern is actually the product of a different developmental program. One clue about the nature of the other developmental mechanism might come from an age-related response of the meristem maintenance gene *WUSCHEL*, which was reduced over time in the *clv3-2* background [226]. This may reflect a broader phenomenon, as the IM tissues compared in the present study were of considerably different ages. The failure to detect more than 8000 genes in the present study could thus be a result of an age-related decline in transcriptional activity, rather than the result of fruit-load effects.

Additional evidence of a non-carbohydrate limited developmental mechanism comes from the analysis of de-fruited plants, which displayed a peculiar pattern of prolonged activity that began at almost just before WT plants began to reach meristem arrest (Figure 1.6). This also corresponds to a time when the majority of leaves have already senesced, implying that the trigger for meristem arrest is at least partially independent of carbohydrate supply. This can also be seen in the *soc1/ful* double mutant, which maintains large numbers of leaves throughout its lifespan [227], and thus has an abundant carbohydrate supply. However, under continuous light, it was found that the *soc1/ful* IM began to break down after producing approximately 60 lateral organs (data not shown: averaging 12 leaves, 41 flowers), a figure that is remarkably similar to the maximum number obtained with de-fruited Col-0 plants (Figure 1.6), and with male sterile plants in the L*er* background [183]. Thus it would appear that maximum lifespan of an IM is genetically determined, though carbohydrate supplies probably trigger arrest at a predictable point long before the maximum is reached. However, it remains unclear why that predictable point occurs at approximately 40 flowers, as leaf senescence patterns would favor an earlier time point.

Interestingly, calculations based on the diameter of the *Arabidopsis* meristem at induction (~120μm) combined with the reported 10% decrease between spacing of successive flower primorida [220] and the minimum size of meristem cells (~6 μm) suggest that the IM is capable of producing about 20 flowers before the size of the meristem drops below a single cell diameter. Although this is only half of the actual number of buds that are produced on most plants, this estimate is a close match for the number of flowers produced after the start of the declining trend, 15 days after induction. This suggests that meristem maintenance pathways may be turned off as early as the first open flower, while subsequent flower bud production merely consumes the remaining stem cells.

Apical senescence

Once an inflorescence meristem has reached a quiescent phase, it will eventually be permanently inactivated by one of two different mechanisms. In the L*er* ecotype, it was reported that certain meristems eventually produced a number of carpel-like bracts before being entirely lost [183]. A similar pattern is observed in the *soc1/ful* mutant [227], which often produces carpel-like bracts over an extended period of time, and even rosette-like whorls of small leaves in place of the flowers. These anomalous carpel-like structures have also been reported for other *Brassica spp*. [66], suggesting the existence of a single mechanism derived from a common ancestor. In this case however, even carbohydrate starvation can be ruled out, as *soc1/ful* double mutants retain large numbers of green leaves throughout the time of growth arrest (personal observation). The mixing of different developmental programs (leaves/ovules/flowers) in these terminal structures further implies that the meristem gradually loses its ability to define organ identities.

Another potential route of meristem termination is the targeted senescence of the apical tissues. This is perhaps not unique to *Arabidopsis*, as it has also been observed in vegetative apices of a broad array of angiosperm species, including blueberries [58], elms [69], willows [228], mulberry

[229], peas [68], kiwifruit [230], lilac [70], *Brownea ariza* [231], maple trees [232], *Tilia chordata* [233], *Theobroma cacao* [234] and alternate bearing pistachios [235]. The localized nature of the senescent pattern suggests that only a small group of cells actually perceive the triggering event. Combined with the observation that multiple nearby tissues senescence simultaneously, even when they are not in direct contact with each other, this also strongly suggests the involvement of the ethylene hormone.

The most likely hypothesis to explain this pattern is an ethylene "burst", similar to the pattern of ethylene production that occurs in climacteric fruit. Provided ethylene biosynthesis was of short duration, this would be sufficient to explain the simultaneous senescence of the meristem and adjacent flower buds and the limited range of the senescent signal. Intriguingly, the ethylene biosynthesis gene *ACS5* does appear to be upregulated in the apices of old inflorescence meristems [236], which correlates well the up-regulation of copper-related genes found in the present study, which may result in enhanced ethylene perception. The weakening of the cell wall predicted suggested by xyloglucan hydrolase *TCH4*, the starch degradation and even the expression of *PAP2* to produce red pigments in the present study also closely parallel the process of fruit ripening in other species, which involve an increase in pectinesterases, an increase in free sugars and the synthesis of anthocyanin pigments.

Methods

Immature bud counts

To estimate meristem activity in terms of the rate of new anlagen production, Col-0 plants were grown in long-day conditions (16/8). The number of immature flower buds between about stage 4 and stage 11 were counted every other day on the 1° meristem, along with the number of

mature flowers and fruits. Stem height was measured by placing one end of a 2.5 cm wide ruler on top of the rosette as the stem began to bolt, recording the position of the flat apical region, not the highest flower bud. The flower buds were visualized with 10x magnification, allowing minimally invasive and repeated counts of the same plant. The time of floral induction was calculated using the formula: T= A-(F/R)-D-E, where T= plant age at induction, A=chronological age of plant, F= the total number of open flower/fruit present when first recorded, R= the rate of floral anthesis (empirically determined from the data), D= 13.25 days to complete flower bud development [182], E= the 2 day delay reported by [183].

Leaf tip removal

Leaf lengths were measured every two days until they began to senesce. This was then used to plot the average growth rates, identifying their length at the time of their maximum growth rate. Growth rates during their first six days were accurately predicted by the empirically determined formula: Leaf length = $1.05t^2$, where length is in millimeters and "t" is measured in days. This was used to calculate the age of the leaf at the time of its first measureable length, then subtracted from the chronological plant age to obtain the time of leaf initiation. Leaf tip removal was timed to occur just after maximum leaf growth, on a leaf by leaf basis. Roughly 1/3 of the total leaf area was removed, using two cuts to remove a diamond-shaped section, reflecting the pattern of senescence. Stem heights, buds and fruits numbers were measured every other day until meristem arrest became visible.

Internode lengths

All fruits were removed daily from plants grown in long days (16/8h) until the meristems reached arrest and the plant began to senesce. The distance from the basal rosette to every fruit node was measured in millimeters, pulling the stem straight where necessary. Internode lengths were then averaged and plotted by position.

Microarray

Meristem collection for microarray analysis used Col-0 plants grown in both long day conditions and in continuous light. In order to maximize fruit load, but to avoid collecting senescent tissues, all plants were harvested simultaneously when a single meristem anywhere in the flat was found to be arrested, under the expectation that the rest would become senescent within 48 hours as previously established [183]. Meristem tissue collection proceeded in a stepwise manner, first by harvesting 3-5 cm sections of *Arabidopsis* branch tips, followed by micro-dissection of the SAM in batches of 10-15 meristems. These included all 1°, 2°, 3° and higher order branch meristems, as available. All flowers and fruits older than stage 2-3 [182] were surgically removed from each section using a dissecting microscope, first removing mature flower buds and fruits, then by collecting a volume of SAM tissue of equal height and width, measuring roughly $0.2mm^3$. The same blade and cutting surface were used for all cuts. The SAM tissue was flash-frozen in liquid N_2 within 30 seconds of dissection. A total of about 1500 meristems (50 mg) were pooled for each biological replicate, for a total of five replicates. RNA was extracted from the plant tissue by grinding the tissue under liquid nitrogen with Triazol reagent, then extracted with a Qaigen RNA easy kit. The RNA was submitted to UCR core facility http://genomics.ucr.edu for hybridization to ATH1 affymetrix microarrays.

The collection of control tissues was previously described by [172], pg 68). To summarize, the meristems were collected from bolting shoots just after the first flower reached anthesis, using Col-0 plants grown in long days (16/8). Each replicate contained 100-120 wild-type meristems collected at the end of the day, removing all flowers older than stage 6. RNA extraction and hybridization were as a described above.

Data analysis

The .CEL files were processed by statistical software R and Bioconductor packges (http://www.r-project.org). Expression data was normalized with RMA (Robust Multichip Average) method using default settings of the R function. Analysis of differentially expressed genes (DEGs) was performed with the LIMMA package using the RMA normalized expression values. Empirical Bayes was used to assess differential gene expression, to adjust p-value for multiple testing and to determine false discovery rate. Cells missing data from one or more of the replicates were removed from the analysis. Cellular functions for the remaining differentially expressed genes were observed using MAPman software (version 3.5.1R2) [237, 238] to provide annotations and metabolic detail, with TAIR 10 annotations.

qPCR

Avocado meristem tissue samples were harvested 21-June 2011 at Farm ACW in Fallbrook, California (33.38°, -117.25°), from 'Hass" avocado trees grafted onto Duke 7 rootstock. Tissue was stored on dry ice in the field, and transferred to -80°C within 4 hours. RNA was extracted using Epicentre MasterPure™ Plant RNA Purification kit. First strand cDNA was synthesized with SuperScript-II reverse transcriptase (Invitrogen) and stored at -20°C. Homologous Avocado genes were identified by using *Arabidopsis thaliana* protein to perform tblastn searches of Avocado meristem EST libraries, developed by the Ancestral Angiosperm Genome Project http://ancangio.uga.edu/. All reactions were run using Bio-Rad MyCycler™ Thermal Cycler, programmed to: 94°C 2:00, (94°C 0:30, 54°C 0:30, 72°C 0:45) x40, 94°C 0:30, 54°C 0:30, 72°C 7:00. Bio-Rad MyiQ™ Single-Color Real-Time PCR Detection software was used to calculate amplification thresholds as described [239].

DNA laddering

Apical meristems plus surrounding immature flower buds were collected from 50 primary racemes in the *Ler* ecotype. Actively growing green SAM's were collected after producing approximately 20 previous fruits, and senescent meristems were collected when red pigments became visible after meristem arrest. DNA was extracted with a mini-prep kit (Fermentas), digested with RNase H for 60 minutes, and calibrated to 5 μg DNA per lane

Table 1.1 Primers used for qPCR. Sequences were designed using *Persea americana* genomic DNA, found by BLAST searching the avocado genome with *A.thaliana* (ARF2, TFL1, ACTIN*),* *Prunus persica* (DAM1) and *Pisum sativum* (RMS2) genes.

Gene ID	Primer
ARF2	Forward: 5'-CTTTCTGAGCAGTGTCTGACTC-3' Reverse: 5'-CGTCTGAGTTCATTGTGCCGTT-3'
Actin	Forward: 5'-GCTATGCACTTCCACATGCTA-3' Reverse: 5'-CGGGCAGCTCATAGCTCTTTT-3'
DAM1	Forward: 5'-GCAAGGAGGGGGAGAATGGCG-3' Reverse: 5'-CTCATCTGCCTGAGAAGTTGG
RMS2	Forward: 5'-ATGGCTCCCGCAGAGAGGCG-3' Reverse: 5'-GTCAGCAATCAGGTGCAAAC-3'
TFL1	Forward: 5'-TCACCTCCTTGAATCTCAACCC-3' Reverse: 5'-TTATCCCACACCTTCAGCTTCC-3'

Works cited

1. Crone, E. and P. Lesica, *Pollen and water limitation in Astragalus scaphoides, a plant that flowers in alternate years.* Oecologia, 2006. **150**(1): p. 40-49.

2. Pillay, A.E., et al., *Boron and the alternate-bearing phenomenon in the date palm (Phoenix dactylifera).* Journal of Arid Environments, 2005. **62**(2): p. 199-207.

3. Kelly, D. and J.J. Sullivan, *Quantifying the Benefits of Mast Seeding on Predator Satiation and Wind Pollination in Chionochloa pallens (Poaceae).* Oikos, 1997. **78**(1): p. 143-150.

4. Hilton, G.M. and J.R. Packham, *Variation in the masting of common beech (Fagus sylvatica L.) in northern Europe over two centuries (1800-2001).* Forestry, 2003. **76**(3): p. 319-328.

5. Masaka, K. and S. Maguchi, *Modelling the Masting Behaviour of Betula platyphylla var. japonica using the Resource Budget Model.* Annals of Botany, 2001. **88**(6): p. 1049-1055.

6. Hilton, G.M. and J.R. Packham, *A sixteen-year record of regional and temporal variation in the fruiting of beech (Fagus sylvatica L.) in England (1980-;1995).* Forestry, 1997. **70**(1): p. 7-16.

7. Jonkers, H., *Biennial bearing in apple and pear: A literature survey.* Scientia Horticulturae, 1979. **11**(4): p. 303-317.

8. Singh, L.B., *Studies in biennial bearing II. A review of the literature.* Journal of Horticultural Science, 1948. **24**(1): p. 45-65.

9. Monselise, S.P. and E.E. Goldschmidt, *Alternate bearing in fruit trees*, in *Horticultural Reviews*, J. Janick, Editor. 1982, AVI Publishing Company, Inc.: Westport, Connecticut. p. 128 - 173.

10. Chandler, W.H., *Fruit Thinning and Alternate Bearing*, in *Fruit Growing*. 1925, Houghton Mifflen Co.: Boston. p. 219-231.

11. Beattie, J.M., *The effect of differential nitrogen fertilization on some of the physical and chemical factors affecting the quality of Baldwin apples.* Proceedings of the American Society for Horticultural Science, 1954. **63**: p. 1-9.

12. Ågren, J., *Between-Year Variation in Flowering and Fruit Set in Frost-Prone and Frost-Sheltered Populations of Dioecious Rubus chamaemorus.* Oecologia, 1988. **76**(2): p. 175-183.

13. Schauber, E.M., et al., *Masting by Eighteen New Zealand Plant Species: The Role of Temperature as a Synchronizing Cue.* Ecology, 2002. **83**(5): p. 1214-1225.

14. Williams, M.W. and L.J. Edgerton, *Biennial bearing of apple trees,* in *Proceedings XIX International Horticultural Congress. Warsaw*. 1974. p. 343-352.

15. Thatcher, J., *The American orchardist*. 1822, Boston: J. W. Ingraham. 226.

16. Knight, T.A., *Physiological and horticultural papers*. 1841, London: Longman, Orme, Brown, Greene and Longmans.

17. Beale, J., *Herefordshire orchards a pattern for all England*. 1656, London: Printed by Roger Daniel.

18. Forsythe, W., *A treatise on the culture and management of fruit trees. An Introduction and notes by William Cobbett*. 1802, Philadelphia: J. Morgan. 259.

19. La Quintinie, J.d., *Instructions pour les jardins fruitiers et potagers Pt. 2*. 1746.

20. Hartig, R., *Anatomie und Physiologie der Pflanzen*. 1891, Berlin.

21. Downing, A.J., *Fruits and Fruit Trees of America*. 1864, New York: John Wiley.

22. Gurney, C.W., *Northwestern Pomology*. 1894, Concord, Nebraska: Gurney, C.W.

23. Balmer, A.J., *Pruning Orchard Trees.* Washington Agricultural Experiment Station Bulletin, 1896. **25**.

24. Waugh, F.A., *The pollination of the plum.* Vermont Agricultural Experiment Station Bulletin, 1896. **53**: p. 47-64.

25. Chandler, W.H., *Pruning Apple Trees with Some Notes on their General Care*, in *Missouri State Board of Horticulture Report*, M.S.B.o. Horticulture, Editor. 1905. p. 200-218.

26. Ikeda, T., *Training and Pruning of Fruit Trees in Japan.* Journal of the Royal Horticultural Society, 1910. **36**: p. 581-586.

27. Anonymous, *Article II. Notes on Gardens and Nurseries*. Magazine of Horticulture, ed. C.M. Hovey. Vol. 13. 1847, Boston: Hovey & Co., Merchant's Row. 564.

28. Li, C., D. Weiss, and E. Goldschmidt, *Effects of carbohydrate starvation on gene expression in citrus root.* Planta, 2003. **217**(1): p. 11-20.

29. Garcia, M.R., M.J. Asins, and E.A. Carbonell, *QTL analysis of yield and seed number in Citrus.* Theoretical and Applied Genetics, 2000. **101**(3): p. 487-493.

30. Ziosi, V., et al., *Peach (Prunus persica L.) fruit growth and ripening: transcript levels and activity of polyamine biosynthetic enzymes in the mesocarp.* Journal of Plant Physiology, 2003. **160**(9): p. 1109-1115.

31. Pichler, F., et al., *Relative developmental, environmental, and tree-to-tree variability in buds from field-grown apple trees.* Tree Genetics & Genomes, 2007. **3**(4): p. 329-339.

32. Ipek, A., et al., *SSR analysis demonstrates that olive production in the southern Marmara region in Turkey uses a single genotype.* Genetics and Molecular Research, 2009. **8**(4): p. 1264-1272.

33. Guitton, B., et al., *Genetic control of biennial bearing in apple.* Journal of Experimental Botany, 2011. **err261v1**.

34. Zhang, J.-Z., et al., *Transcriptome profile analysis of flowering molecular processes of early flowering trifoliate orange mutant and the wild-type [Poncirus trifoliata (L.) Raf.] by massively parallel signature sequencing.* BMC Genomics, 2011. **12**: p. 63.

35. Shalom, L. and e. al., *Alternate bearing in citrus: changes in the expression of flowering control genes and in global gene expression in on- versus off-crop trees.* PLoS ONE, 2012. **7**: p. e46930.

36. Harvey, E.M. and A.E. Murneek, *The relation of carbohydrate and nitrogen of apple spurs.* Oregon Agricultural College Experiment Station Bulletin, 1921. **176**: p. 5-47.

37. Haller, M.H. and J.R. Magness, *Relation of leaf area and position to quality of fruit and to bud differentiation in apples*, in *Technical Bulletin 338*, USDA, Editor. 1933: Washington D.C. p. 1-35.

38. Harley, C.P., M.P. Masure, and J.R. Magness, *Fruit thinning and biennial bearing on Yellow Newtonian apples.* Proceedings of the American Society for Horticultural Science, 1933. **30**: p. 330-331.

39. Huet, J., *Étude des effets des feuilles et des fruits sur l'induction florale des brachyblastes du poirier.* Physiologia Végetale, 1972. **10**(3): p. 529-545.

40. Mecartney, J.L., *Relation of spur growth to blossom and fruit production in the Wagener Apple.* Proceedings of the American Society for Horticultural Science, 1925. **22**: p. 126-133.

41. Singh, L.B., *Studies in biennial bearing III. Growth studies in "On" and "Off" year trees.* Journal of Horticultural Science, 1948. **24**(1): p. 123-148.

42. Compton, C., *Phosphorus in alternate-bearing sugar prunes.* Proceedings of the American Society for Horticultural Science, 1933. **30**: p. 151-3.

43. Bowman, F.T., *The influence of early times of fruit removal on the growth and composition of alternate-bearing sugar prune trees with special reference to blossom bud formation.* Journal of Pomology and Horticultural Science, 1941. **19**: p. 34-77.

44. Fullmer, F.S., *Variations in the phosphorus and potassium content of the foliage from Fuerte avocado groves.* Yearbook of the California Avocado Society, 1945: p. 93-100.

45. Bielinska, M. and L. Włodek, *Contents of phosphorus, potassium and calcium in leaves and shoots of biennial bearing apple trees.* Prace Instytutu Sadownictwa w Skierniewicach, 1958. **3**: p. 5--29.

46. Fawzi, A.F.A., et al., *Navel orange alternate bearing in relation to micronutrient nutrition in Ismailiya.* Egyptian Journal of Botany, 1986. **26**(1-3): p. 73-80.

47. Davis, L.D., *Some carbohydrate and nitrogen constituents of alternate bearing sugar prunes associated with fruit bud formation.* Hilgardia, 1931. **5**: p. 119-54.

48. Wiggans, C.C., *Some factors favoring or opposing fruitfulness in apple*, in *Agricultural Experiment Station*. 1918, University of Missouri: Columbia. p. 60.

49. Fahmy, I.R., *Changes in carbohydrate and nitrogen content of Souri olive leaves in relation to alternate bearing.* Proceedings of the American Society for Horticultural Science, 1958. **72**: p. 252-256.

50. Harley, C.P., et al., *Investigations on the cause and control of biennial bearing in apple trees*, USDA, Editor. 1942: Washington D.C. p. 1-58.

51. Ljønes, B., *Biennial bearing in apples*, in *Meldinger fra Norges Landbrukshøgskole*. 1951. p. 36.

52. Thompson, P.A. and C.G. Guttridge, *Effects of gibberellic acid on the initiation of flowers and runners in the strawberry.* Nature, 1959. **184**: p. B.A. 72-73.

53. Domanski, R. and T.T. Kozlowski, *Variations in kinetin-like activity in buds of Betula and Populus during release from dormancy.* Canadian Journal of Botany, 1968. **46**(4): p. 397-403.

54. Hartmann, W., *Bud dormancy and abscisic acid (abscisin II, dormin).* Biologische Rundschau, 1970. **8**(3): p. 154-8.

55. Dal Cin, V., et al., *Fruit load and elevation affect ethylene biosynthesis and action in apple fruit (Malus domestica L. Borkh) during development, maturation and ripening.* Plant, Cell & Environment, 2007. **30**(11): p. 1480-1485.

56. Davenport, T.L., *Ethylene production in avocado flowers and fruit: its role in senescence and abscission.* Proceedings of the Plant Growth Regulation Society of America, 1983. **10th**: p. 213-15.

57. McGasson, *Ethylene and fruit ripening.* HortScience, 1985. **20**(1): p. 51-53.

58. Barker, W.G. and W.B. Collins, *Growth and Development of the Lowbush Blueberry: Apical Abortion.* Canadian Journal of Botany, 1963. **41**(9): p. 1319-1324.

59. Cornforth, J.W., et al., *Identification of the Yellow Lupin Growth Inhibitor as (+)-Abscisin II ((+)-Dormin).* Nature, 1966. **211**(5050): p. 742-743.

60. Edgerton, L.J., *Control of abscission of apples with emphasis on thinning and pre-harvest drop*, in *Acta Horticulturae*, S.J. Wellensiek, Editor. 1973: Wageningen. p. 333-352.

61. Warder, J., *American Pomology*. 1867, New York: Orange Judd Co.

62. Drobyshev, I., et al., *Masting behaviour and dendrochronology of European beech (Fagus sylvatica L.) in southern Sweden.* Forest Ecology and Management, 2010. **259**(11): p. 2160-2171.

63. Sánchez-Humanes, B., V.L. Sork, and J.M. Espelta, *Trade-offs between vegetative growth and acorn production in Quercus lobata during a mast year: the relevance of crop size and hierarchical level within the canopy.* Oecologia, 2011. **166**(1): p. 101-110.

64. Kohn, J.R., *Sex Ratio, Seed Production, Biomass Allocation, and the Cost of Male Function in Cucurbita foetidissima HBK (Cucurbitaceae).* Evolution, 1989. **43**(7): p. 1424-1434.

65. Martín, D., et al., *Trade-off between stem growth and acorn production in holm oak.* Trees, 2015. **29**(3): p. 825-834.

66. Stout, A.B., *Cyclic manifestation of sterility in Brassica pekinensis and B. chinensis.* Botanical Gazette, 1922. **73**(2): p. 110-132.

67. Salazar-García, S. and C.J. Lovatt, *Flowering of avocado (Persea americana Mill.) I. Inflorescence and flower development.* Revista Chapingo Serie Horticultura, 2002. **8**(1): p. 71-75.

68. Lockhart, J.A. and V. Gottschall, *Fruit-induced & apical senescence in Pisum sativum L.* Plant Physiology, 1961. **36**(4): p. 389-398.

69. Millington, W.F., *Shoot Tip Abortion in Ulmus americana.* American Journal of Botany, 1963. **50**(4): p. 371-378.

70. Garrison, R. and R.H. Wetmore, *Studies in Shoot-Tip Abortion: Syringa vulgaris.* American Journal of Botany, 1961. **48**(9): p. 789-795.

71. Leopold, A.C., E. Neidergang-Kamien, and J. Janicki, *Experimental modification of plant senescence.* Plant Physiology, 1959. **34**: p. 570-573.

72. Gross, H.L., *Crown deterioration and reduced growth associated with excessive seed production by birch.* Canadian Journal of Botany, 1972. **50**(12): p. 2431-2437.

73. Reece, P.C., *Differentiation of avocado blossom buds in Florida.* Botanical Gazette, 1942. **104**(2): p. 323-328.

74. Tappeiner II, J.C., *Notes: Effect of Cone Production on Branch, Needle, and Xylem Ring Growth of Sierra Nevada Douglas-Fir.* Forest Science, 1969. **15**(2): p. 171-174.

75. Koller, D., H.R. Highkin, and O.H. Caso, *Effects of Gibberellic Acid on Stem Apices of Vernalizable Grasses* American Journal of Botany, 1960. **47**(6): p. 518.

76. Hodson, H.K. and K.C. Hamner, *Floral inducing extract from Xanthium.* Science, 1970. **167**(3917): p. 384-385.

77. Garcia-Luis, A., et al., *The regulation of flowering and fruit set in Citrus: Relationship with carbohydrate levels.* Israel Journal of Botany, 1988. **37**: p. 189-201.

78. Luckwill, L.C., *Growth regulators in flowering and fruit development.* American Chem. Soc. Symp., 1977. **37**: p. 293-304.

79. Prang, L., et al., *Gibberellin signals originating from apple fruit and their possible involvement in flower induction*, in *Acta Horticulturae*. 1997, International Society for Horticultural Science. p. 235-241.

80. Wheaton, T.A., *Fruit thinning of Florida mandarins using plant growth regulators.* Proceedings International Society of Citriculture, 1982(1): p. 263-8.

81. Murneek, A.E., *New practices to regulate the fruit crop.* Missouri Agricultural Experiment Station Research Bulletin, 1940. **416**: p. 1-15.

82. El-Zeftawi, B.M., *Regulating preharvest fruit drop and the duration of the harvest season of grapefruit with 2,4-D and GA.* Journal of Horticultural Science & Biotechnology, 1980. **55**(3): p. 211-17.

83. Gawad, H.A. and L. Ferguson, *Growth regulator effects on alternate bearing of pistachios.* Proceedings of the Plant Growth Regulation Society of America, 1987. **14th**: p. 63-9.

84. Chacko, E.K., R.R. Kohli, and G.S. Randhawa, *Investigations on the use of (2-chloroethyl) phosphonic acid (ethephon, CEPA) for the control of biennial bearing in mango.* Scientia Horticulturae, 1974. **2**(4): p. 389-398.

85. Ogata, T., *The control of flowering and fruit-set in satsuma mandarin with plant growth regulators and the dynamics of endogenous plant hormones in their processes.* Bulletin of Osaka Prefecture University. Series B, 1997. **49**: p. 67-109.

86. Galliani, S., S.P. Monselise, and R. Goren, *Improving fruit size and breaking alternate bearing in 'Wilking' mandarin by ethephon and other agents.* HortScience, 1975. **10**(1): p. 68-69.

87. Basak, A., et al., *Apple thinning with NAA, carbaryl, and ethephon applied separately and in mixtures.* Pestycydy, 1986(3-4): p. 109-14.

88. Goldschmidt, E.E., *Endogenous abscisic acid and 2-trans-abscisic acid in alternate bearing 'Wilking' mandarin trees.* Plant Growth Regulation, 1984. **2**(1): p. 9-13.

89. Monselise, S.P., E.E. Goldschmidt, and A. Golomb, *Alternate bearing in citrus and ways of control.* Proceedings International Society of Citriculture, 1982(1): p. 239-42.

90. Jones, W.W., C.W. Coggins, Jr., and T.W. Embleton, *Endogenous Abscisic Acid in Relation to Bud Growth in Alternate Bearing `Valencia' Orange.* Plant Physiology, 1976. **58**(5): p. 681-682.

91. Takeda, F. and J.C. Crane, *Abscisic acid in pistachio as related to inflorescence bud abcission.* Journal of the American Society for Horticultural Science, 1980. **105**: p. 573-576.

92. Monerri, C., et al., *Relation of carbohydrate reserves with the forthcoming crop, flower formation and photosynthetic rate, in the alternate bearing Salustiana' sweet orange (Citrus sinensis L.).* Scientia Horticulturae, 2011. **129**(1): p. 71-78.

93. Feucht, W., *Sugar balances in organs of biennial bearing apple trees.* Gartenbauwissenschaft, 1964. **29**(3): p. 313-24.

94. van der Walt, M., S.J. Davie, and D.G. Smith, *Carbohydrate and other studies on alternate bearing Fuerte and Hass avocado trees.* South African Avocado Growers' Association Yearbook, 1993. **16**: p. 82-85.

95. Wilcox, J.C., *Some factors affecting apple yields in the Okanagan Valley. VI. Contents of nitrogen, phosphorus, and potassium in the terminal shoots.* Canadian Journal of Agricultural Science, 1949. **29**: p. 424-36.

96. Fernández-Escobar, R., R. Moreno, and M. García-Creus, *Seasonal changes of mineral nutrients in olive leaves during the alternate-bearing cycle.* Scientia Horticulturae, 1999. **82**(1-2): p. 25-45.

97. Hallé, F. and R. Martin, *Etude de la croissance rythmique chez Hevea brasiliensis Müll. Arg (Euphorbiaceae - Crotonoïdées).* Adansonia, 1968. **28**: p. 475-503.

98. Bugnon, P. and F. Bugnon, *Feuilles juvéniles et pousses multinodales chez le Pin maritime.* Bulletin de la Société d'Histoire Naturelle de Toulouse, 1951. **86**: p. 18-23.

99. Salazar-García, S., et al., *Crop Load Affects Vegetative Growth Flushes and Shoot Age Influences Irreversible Commitment to Flowering of 'Hass' Avocado.* HortScience, 2006. **41**(7): p. 1541-1546.

100. Godley, E.J., *Paths to maturity.* New Zealand Journal of Botany, 1985. **23**(4): p. 687-706.

101. Smith, H.M. and A. Samach, *Constraints to obtaining consistent annual yields in perennial tree crops. I: Heavy fruit load dominates over vegetative growth.* Plant Science, 2013. **207**(0): p. 158-167.

102. Vriezen, W.H., et al., *Changes in tomato ovary transcriptome demonstrate complex hormonal regulation of fruit set.* New Phytologist, 2008. **177**(1): p. 60-76.

103. Lee, T.D. and F.A. Bazzaz, *Maternal regulation of fecundity: non-random ovule abortion in Cassia fasciculata Michx.* Oecologia, 1986. **68**(3): p. 459-465.

104. Lee, T.D., *Patterns of fruits and seed production*, in *Plant Reproductive Ecology: Patterns and Strategies*, J.L. Doust and L.L. Doust, Editors. 1988, Oxford University Press: Oxford. p. 179-202.

105. Pozo, L.V., *Endogenous hormonal status in citrus flowers and fruitlets: relationship with postbloom fruit drop.* Scientia Horticulturae, 2001. **91**(3,4): p. 251-260.

106. Talon, M., et al., *Hormonal regulation of fruit set and abscission in citrus: classical concepts and new evidence*, in *Acta Horticulturae*. 1997, International Society for Horticultural Science. p. 209-217.

107. Dal Cin, V., R. Velasco, and A. Ramina, *Dominance induction of fruitlet shedding in Malus x domestica (L. Borkh): molecular changes associated with polar auxin transport.* BMC Plant Biology, 2009. **9**(1): p. 139.

108. Lee, T.D., *Patterns of Fruit and Seed Production in a Vermont Population of Cassia nictitans L. (Caesalpiniaceae).* Bulletin of the Torrey Botanical Club, 1989. **116**(1): p. 15-21.

109. Kitajima, A., et al., *Influence of seeded fruit on seedless fruit set in Japanese persimmon cv. Fuyu (Diospyros kaki L. f.).* Engei Gakkai Zasshi, 1992. **61**(3): p. 499-506.

110. Bangerth, K.F. and L.C. Ho, *Fruit Position and Fruit Set Sequence in a Truss as Factors Determining Final Size of Tomato Fruits.* Annals of Botany, 1984. **53**: p. 315-319.

111. Crane, J.C., I.M. Al-Shalan, and R.M. Carlson, *Abscission of pistachio inflorescence buds as affected by leaf area and number of nuts.* Journal of the American Society for Horticultural Science, 1973. **98**: p. 591-592.

112. Bangerth, K.F., *Dominance among fruits/sinks and the search for a correlative signal.* Physiologia Plantarum, 1989. **76**(4): p. 608-614.

113. Bangerth, K.F., C.-J. Li, and J. Gruber, *Mutual interaction of auxin and cytokinins in regulating correlative dominance.* Plant Growth Regulation, 2000. **32**(2): p. 205-217.

114. Stephenson, A.G., *Flower and fruit abortion: Proximate causes and ultimate functions.* Annual Review of Ecology and Systematics, 1981. **12**: p. 253-279.

115. Sachs, T., *Senescence of Inhibited Shoots of Peas and Apical Dominance.* Annals of Botany, 1966. **30**(3): p. 447-456.

116. Murneek, A.E., *Effects of correlation between vegetative and reproductive functions in tomato (Lycopersicon esculentum Mill.).* Plant Physiology, 1926. **1**(1): p. 3-56.

117. Stewart, J.P., *Factors Influencing Yield, Size, Color and Growth in Apples.* Pennsylvania State College Annual Report, 1910. **1910-1911**: p. 401-510.

118. Hooker, H.D., *Annual and biennial bearing in York Imperial apples.* Missouri Agricultural Experiment Station Research Bulletin, 1925. **75**: p. 3-16.

119. Lagasse, F.S., *The effect of applying nitrogen at various times and in various amounts to Yellow Transparent apple trees.* Transactions of the Peninsula Horticultural Society, 1934: p. 66-71.

120. Meland, M. and B. Gjerde, *The effect of hand thinning on return bloom of 'Summered' and 'Aroma' apples*, in *Acta Horticulturae*, A. Erez and J.E. Jackson, Editors. 1992, drukkerij Avanti: Zaltbommel, Netherlands. p. 219-222.

121. Schaffer, A.A., et al., *Fruit set and carbohydrate status in alternate and nonalternate bearing Citrus cultivars.* Journal of the American Society for Horticultural Science, 1985. **110**(4): p. 574-8.

122. Li, C.-Y., D. Weiss, and E.E. Goldschmidt, *Girdling affects carbohydrate-related gene expression in leaves, bark and roots of alternate-bearing Citrus trees.* Annals of Botany, 2003. **92**(1): p. 137-143.

123. Blanusa, T., et al., *Regulation of sweet cherry fruit abscission: the role of photo-assimilation, sugars, and abscisic acid.* Journal of Horticultural Science & Biotechnology, 2006. **81**(4): p. 613-620.

124. Mason, T.G., *Growth and abscission in sea island cotton.* Annals of Botany, 1922. **36**(144): p. 457-484.

125. Fulford, R.M., *Effect of chemical defoliation on the development of apple spurs.* Annals of Botany, 1970. **34**(138): p. 1079-88.

126. Martinez-Fuentes, A., et al., *Timing of the inhibitory effect of fruit on return bloom of 'Valencia' sweet orange (Citrus sinensis (L.) Osbeck).* Journal of the Science of Food and Agriculture, 2010. **90**(11): p. 1936-1943.

127. Murneek, A.E., *Physiology or reproduction in horticultural plants II. The physiological basis of intermittent sterility with special reference to the spider flower.* . Missouri Agricultural Experiment Station Research Bulletin, 1927. **106**: p. 3-37.

128. Williams, R.R., et al., *The effect of picking date on blossoming and fruit set in the following year for the apple cv. Bramley's seedling.* Journal of Horticultural Science, 1980. **55**(4): p. 359-362.

129. Muñoz-Fambuena, N., et al., *Fruit regulates seasonal expression of flowering genes in alternate-bearing 'Moncada' mandarin.* Annals of Botany, 2011. **108**(3): p. 511-519.

130. Roberts, R.H., *Off-year apple bearing.* Annual Report of the Wisconsin State Horticultural Society, 1920. **51**: p. 72-78.

131. Abou, R.M., et al., *Flowering of mango trees in relation to chemical composition of shoots.* Egyptian Journal of Horticulture, 1984. **11**(1): p. 19-30.

132. Ikeda, A., Y. Sonoda, and J. Yamaguchi, *Regulation of carbon source partitioning: all about regulation in response to internal ratio of C and N.* Tanpakushitsu Kakusan Koso, 2003. **48**(15, Zokango): p. 2103-2112.

133. Cozen and Wilkinson, *Control of lateral bud inhibition, flower emergence, and dormancy in the black currant.* Nature, 1966. **211**: p. 867-868.

134. Hemberg, T., *Growth-Inhibiting Substances in Terminal Buds of Fraxinus.* Physiologia Plantarum, 1949. **2**: p. 37-44.

135. Kachru, R.B., R.N. Singh, and E.K. Chacko, *Inhibition of flowering in mango (Mangifera indica L.) by gibberellic acid.* HortScience, 1971. **6**: p. 140-141.

136. Greene, D.W., *Reducing floral initiation and return bloom in pome fruit trees-applications and implications.* HortTechnology, 2000. **10**(4): p. 740-743.

137. Schmidt, T., et al., *Crop load overwhelms effects of gibberellic acid and ethephon on floral initiation in apple.* HortScience, 2009. **44**(7): p. 1900-1906.

138. Davis, L.D., *Flowering and alternate bearing.* Proceedings of the American Society for Horticultural Science, 1957. **70**: p. 545-556.

139. Chan, B.G. and J.C. Cain, *The effect of seed formation on subsequent flowering in apple*, in *Proceedings of the American Society for Horticultural Science*, S.H. Yarnell, Editor. 1967, American Society for Horticultural Science. p. 63-68.

140. Thompson, P.A. and C.G. Guttridge, *The role of leaves as inhibitors of flower Induction in strawberry: With one figure in the text.* Annals of Botany, 1960. **24**(4): p. 482-490.

141. Grochowska, M.J., *Identification of the growth inhibitor connected with flower bud formation in apple.* Bulletin de l'Acádemie Polonaise des Sciences. Série des sciences biologiques, 1964. **12**(9): p. 379-383.

142. Grochowska, M.J., *Natural growth regulators in apple trees in relation to biennial bearing.* Bulletin de l'Acádemie Polonaise des Sciences. Série des sciences biologiques, 1963. **11**(12): p. 589-90.

143. Grochowska, M.J. and W. Ciurzynska, *Differences between Fruit-Bearing and Non-Bearing Apple Spurs in Activity of an Enzyme System Decomposing Phloridzin.* Biologia Plantarum, 1979. **21**(3): p. 201-205.

144. Iwahori, S. and J.T. Oohata, *Control of flowering of satsuma mandarins (Citrus unshiu Marc.) with gibberellin.* Proceedings International Society of Citriculture, 1982(1): p. 247-9.

145. Salazar-García, S. and C.J. Lovatt, *GA_3 application alters flowering phenology of 'Hass' avocado.* Journal of the American Society for Horticultural Science, 1998. **123**(5): p. 791-797.

146. Grochowska, M.J. and A. Karaszewska, *The production of growth producing hormones and their active diffusion from immature, developing seeds of four apple cultivars.* Fruit Science Reports, 1976. **3**(2): p. 5-16.

147. Nitsch, J.P., *Growth and morphogenesis of the strawberry as related to auxin.* American Journal of Botany, 1950. **37**(3): p. 211-215.

148. Callejas, R. and K.F. Bangerth, *Is auxin export of apple fruit an alternative signal for inhibition of flower bud induction?*, in *Acta Horticulturae*, J.L. Guardiola, J.L. Garcia Martinez, and J.D. Quinlan, Editors. 1997, Kardinaal Mercierlaan: Leuven, Belgium. p. 271-277.

149. Hedden, P. and J. Graebe, *Inhibition of gibberellin biosynthesis by paclobutrazol in cell-free homogenates of Cucurbita maxima endosperm and Malus pumila embryos.* Journal of Plant Growth Regulation, 1985. **4**(1): p. 111-122.

150. Gianfagna, T.J. and P.J. Davies, *The transport of substances out of developing fruits in relation to the induction of apical senescence in Pisum sativum line G2.* Physiologia Plantarum, 1983. **59**(4): p. 676-84.

151. Grochowska, M.J., *The Free Movement of ^{14}C-labelled Organic Compounds from intact Apple Seeds to Growing Fruitlets and Shoots.* Biologia Plantarum, 1974. **16**(3): p. 194-198.

152. Hamilton, D.A. and P.J. Davies, *Sucrose and Malic Acid as the Compounds Exported to the Apical Bud of Pea following $^{14}CO_2$ Labeling of the Fruit.* Plant Physiology, 1988. **88**: p. 466-472.

153. Hamilton, D.A. and P.J. Davies, *Mechanism of export of organic material from the developing fruits of pea.* Plant Physiology, 1988. **86**: p. 956-959.

154. Zeevaart, J.A.D., *Flower formation as studied by grafting.* Mededelingen van de Landbouwhogeschool, 1958. **58**: p. 1.

155. Chailakhyan, M.K., *On the hormonal theory of plant development.* Doklady Akademii Nauk SSSR, 1936. **3**: p. 452.

156. Takada, S. and K. Goto, *TERMINAL FLOWER2, an Arabidopsis Homolog of HETEROCHROMATIN PROTEIN1, Counteracts the Activation of FLOWERING LOCUS T by CONSTANS in the Vascular Tissues of Leaves to Regulate Flowering Time.* Plant Cell, 2003. **15**(12): p. 2856-2865.

157. Notaguchi, M., et al., *Long-Distance, Graft-Transmissible Action of Arabidopsis FLOWERING LOCUS T Protein to Promote Flowering.* Plant Cell Physiology, 2008. **49**(11): p. 1645-1658.

158. Nishikawa, F., et al., *Isolation and characterization of a Citrus FT/TFL1 homologue (CuMFT1), which shows quantitatively preferential expression in Citrus seeds.* Journal Jpn. Soc. Hortic. Sci., 2008. **77**(1): p. 38-46.

159. Kotoda, N. and M. Wada, *MdTFL1, a TFL1-like gene of apple, retards the transition from the vegetative to reproductive phase in transgenic Arabidopsis.* Plant Science, 2005. **168**(1): p. 95-104.

160. Chapman, G.P., C.W. Fagg, and W.E. Peat, *Parthenocarpy and internal competition in Vicia faba L.* Zeitschrift fur Pflanzenphysiologie, 1979. **94**: p. 247-255.

161. Carbonell, J. and J.L. Garcia-Martinez, *Fruit set of unpollinated ovaries of Pisum sativum L. Influence of vegetative parts.* Planta, 1980. **147**: p. 444-450.

162. Hoad, G.V., *The role of seed derived hormones in the control of flowering in apple,* in *Acta Horticulturae*. 1978. p. 93-103.

163. Gälweiler, L., et al., *Regulation of Polar Auxin Transport by AtPIN1 in Arabidopsis Vascular Tissue.* Science, 1998. **282**(5397): p. 2226-2230.

164. Gomez-Roldan, V., et al., *Strigolactone inhibition of shoot branching.* Nature, 2008. **455**(7210): p. 189-U22.

165. Umehara, M., et al., *Inhibition of shoot branching by new terpenoid plant hormones.* Nature, 2008. **455**(7210): p. 195-200.

166. Stirnberg, P., K. van de Sande, and H.M.O. Leyser, *MAX1 and MAX2 control shoot lateral branching in Arabidopsis.* Development, 2002. **129**: p. 1131-1141.

167. Sorefan, K., et al., *MAX4 and RMS1 are orthologous dioxygenase-like genes that regulate shoot branching in Arabidopsis and pea* Genes & Development, 2003. **17**: p. 1469-1474

168. Booker, J., et al., *MAX3/CCD7 Is a Carotenoid Cleavage Dioxygenase Required for the Synthesis of a Novel Plant Signaling Molecule.* Current Biology, 2004. **14**(14): p. 1232-1238.

169. Alder, A., et al., *The Path from ß-Carotene to Carlactone, a Strigolactone-Like Plant Hormone.* Science, 2012. **335**(6074): p. 1348-1351.

170. Kohlen, W., et al., *The tomato CAROTENOID CLEAVAGE DIOXYGENASE8 (SlCCD8) regulates rhizosphere signaling, plant architecture and affects reproductive development through strigolactone biosynthesis.* New Phytologist, 2012. **196**(2): p. 535-547.

171. Mason, M.G., et al., *Sugar demand, not auxin, is the initial regulator of apical dominance.* Proceedings of the National Academy of Sciences, 2014. **111**(16): p. 6092-6097.

172. Lal, S., *Integration of Molecular Networks in the Shoot Apical Meristem that Controls Floral Specification in Arabidopsis thaliana*, in *Genetics, Genomics and Bioinformatics*. 2011, University of California: Riverside. p. 181.

173. Buechel, S., et al., *Role of A-type ARABIDOPSIS RESPONSE REGULATORS in meristem maintenance and regeneration.* European Journal of Cell Biology, 2010. **89**(2-3): p. 279-284.

174. Winter, D., et al., *An "Electronic Fluorescent Pictograph"□ Browser for Exploring and Analyzing Large-Scale Biological Data Sets.* PLoS One, 2007. **2**(8): p. e718.

175. Bleecker, A.B., *The ethylene-receptor family from Arabidopsis: structure and function.* Philosophical Transactions of the Royal Society of London, B, 1998. **353**: p. 1405-1412.

176. Aubert, S., et al., *Ultrastructural and biochemical characterization of autophagy in higher plant cells subjected to carbon deprivation: control by the supply of mitochondria with respiratory substrates.* The Journal of Cell Biology, 1996. **133**(6): p. 1251-1263.

177. Wang, R., et al., *Microarray Analysis of the Nitrate Response in Arabidopsis Roots and Shoots Reveals over 1,000 Rapidly Responding Genes and New Linkages to Glucose, Trehalose-6-Phosphate, Iron, and Sulfate Metabolism.* Plant Physiology, 2003. **132**(2): p. 556-567.

178. Scheible, W.-R., et al., *Genome-Wide Reprogramming of Primary and Secondary Metabolism, Protein Synthesis, Cellular Growth Processes, and the Regulatory Infrastructure of Arabidopsis in Response to Nitrogen.* Plant Physiology, 2004. **136**(1): p. 2483-2499.

179. Gao, H., T.L. Sage, and K.W. Osteryoung, *FZL, an FZO-like protein in plants, is a determinant of thylakoid and chloroplast morphology.* Proceedings of the National Academy of Sciences, 2006. **103**(17): p. 6759-6764.

180. Tzvetkova-Chevolleau, T., et al., *The light stress-induced protein ELIP2 is a regulator of chlorophyll synthesis in Arabidopsis thaliana.* Plant Journal, 2007. **50**(5): p. 795-809.

181. Kirik, A., et al., *The Chromatin Assembly Factor Subunit FASCIATA1 Is Involved in Homologous Recombination in Plants.* The Plant Cell, 2006. **18**(10): p. 2431-2442.

182. Smyth, D.R., J.L. Bowman, and E.M. Meyerowitz, *Early Flower Development in Arabidopsis.* Plant Cell, 1990. **2**(8): p. 755-767.

183. Hensel, L.L., et al., *The fate of inflorescence meristems is controlled by developing fruits in Arabidopsis.* Plant Physiology, 1994. **106**(3): p. 863-876.

184. Bleecker, A.B. and S.E. Patterson, *Last Exit: Senescence, Abscission, and Meristem Arrest in Arabidopsis.* Plant Cell, 1997. **9**(7): p. 1169-1179.

185. Yu, S.-M., *Cellular and Genetic Responses of Plants to Sugar Starvation.* Plant Physiology, 1999. **121**(3): p. 687-693.

186. Kader, J.-C., et al., *Formation of Autophagic Vacuoles and Accumulation of Deacylation Products of Membrane Polar Lipids During the Course of Sucrose Starvation in Higher Plant Cells*, in *Plant Lipid Metabolism*. 1995, Springer Netherlands. p. 188-196.

187. Guiboileau, A., et al., *Physiological and metabolic consequences of autophagy deficiency for the management of nitrogen and protein resources in Arabidopsis leaves depending on nitrate availability.* New Phytologist, 2013. **199**(3): p. 683-694.

188. Brouquisse, R., et al., *Asparagine Metabolism and Nitrogen Distribution during Protein-Degradation in Sugar-Starved Maize Root-Tips.* Planta, 1992. **188**(3): p. 384-395.

189. Moriyasu, Y. and Y. Ohsumi, *Autophagy in Tobacco Suspension-Cultured Cells in Response to Sucrose Starvation.* Plant Physiology, 1996. **111**(4): p. 1233-1241.

190. Brouquisse, R., Gaudillère, Jean-Pierre, and P. Raymond, *Induction of a Carbon-Starvation-Related Proteolysis in Whole Maize Plants Submitted to Light/Dark Cycles and to Extended Darkness.* Plant Physiology, 1998. **117**(4): p. 1281-1291.

191. Brouquisse, R., et al., *Study of Glucose Starvation in Excised Maize Root Tips.* Plant Physiology, 1991. **96**(2): p. 619-626.

192. Lea, U.S., et al., *Nitrogen deficiency enhances expression of specific MYB and bHLH transcription factors and accumulation of end products in the flavonoid pathway.* Planta, 2007. **225**(5): p. 1245-1253.

193. Cline, M.G., *Exogenous Auxin Effects on Lateral Bud Outgrowth in Decapitated Shoots.* Annals of Botany, 1996. **78**(2): p. 255-266.

194. Cline, M.G., S.P. Chatfield, and H.M.O. Leyser, *NAA Restores Apical Dominance in the axr3-1 Mutant of Arabidopsis thaliana.* Annals of Botany, 2001. **87**(1): p. 61-65.

195. Hempel, F.D. and L.J. Feldman, *Bi-directional inflorescence development in Arabidopsis thaliana: Acropetal initiation of flowers and basipetal initiation of paraclades.* Planta, 1994. **192**(2): p. 276-286.

196. Brewer, P.B., et al., *Strigolactone Acts Downstream of Auxin to Regulate Bud Outgrowth in Pea and Arabidopsis.* Plant Physiology, 2009. **150**(1): p. 482-493.

197. Morris, S.E., et al., *Mutational Analysis of Branching in Pea. Evidence That Rms1 and Rms5 Regulate the Same Novel Signal.* Plant Physiology, 2001. **126**(3): p. 1205-1213.

198. Beveridge, C.A., G.M. Symons, and C.G.N. Turnbull, *Auxin Inhibition of Decapitation-Induced Branching Is Dependent on Graft-Transmissible Signals Regulated by Genes Rms1 and Rms2.* Plant Physiology, 2000. **123**(2): p. 689-698.

199. Booker, J., et al., *MAX1 Encodes a Cytochrome P450 Family Member that Acts Downstream of MAX3/4 to Produce a Carotenoid-Derived Branch-Inhibiting Hormone.* Developmental Cell, 2005. **8**(3): p. 443-449.

200. Lazar, G. and H.M. Goodman, *MAX1, a regulator of the flavonoid pathway, controls vegetative axillary bud outgrowth in Arabidopsis.* Proceedings of the National Acadamy of Sciences of the United States of America, 2005. **103**(2): p. 472-476.

201. Crawford, S., et al., *Strigolactones enhance competition between shoot branches by dampening auxin transport.* Development, 2010. **137**(17): p. 2905-13.

202. Yoneyama, K., et al., *Nitrogen deficiency as well as phosphorus deficiency in sorghum promotes the production and exudation of 5-deoxystrigol, the host recognition signal for arbuscular mycorrhizal fungi and root parasites.* Planta, 2007. **227**(1): p. 125-32.

203. Yoneyama, K., et al., *Phosphorus deficiency in red clover promotes exudation of orobanchol, the signal for mycorrhizal symbionts and germination stimulant for root parasites.* Planta, 2007. **225**(4): p. 1031-1038.

204. Lopez-Raez, J.A., et al., *Tomato strigolactones are derived from carotenoids and their biosynthesis is promoted by phosphate starvation.* New Phytologist, 2008. **178**(4): p. 863-874.

205. Mickelbart, M.V. and M.L. Arpaia, *Rootstock influences changes in ion concentrations, growth, and photosynthesis of 'Hass' avocado trees in response to salinity.* Journal of the American Society for Horticultural Science, 2002. **127**: p. 649-655.

206. Eastmond, P.J., et al., *Trehalose-6-phosphate synthase 1, which catalyses the first step in trehalose synthesis, is essential for Arabidopsis embryo maturation.* Plant Journal, 2002. **29**(2): p. 225-235.

207. van Dijken, A.J.H., H. Schluepmann, and S.C.M. Smeekens, *Arabidopsis trehalose-6-phosphate synthase 1 is essential for normal vegetative growth and transition to flowering.* Plant Physiology, 2004. **135**(2): p. 969-977.

208. Wingler, A., et al., *Trehalose Induces the ADP-Glucose Pyrophosphorylase Gene, ApL3, and Starch Synthesis in Arabidopsis.* Plant Physiology, 2000. **124**(1): p. 105-114.

209. Fritzius, T., et al., *Induction of ApL3 Expression by Trehalose Complements the Starch-Deficient Arabidopsis Mutantadg2-1 Lacking ApL1, the Large Subunit of ADP-Glucose Pyrophosphorylase.* Plant Physiology, 2001. **126**(2): p. 883-889.

210. Krapp, A., et al., *Arabidopsis Roots and Shoots Show Distinct Temporal Adaptation Patterns toward Nitrogen Starvation.* Plant Physiology, 2011. **157**(3): p. 1255-1282.

211. Osuna, D., et al., *Temporal responses of transcripts, enzyme activities and metabolites after adding sucrose to carbon-deprived Arabidopsis seedlings.* Plant Journal, 2007. **49**(3): p. 463-491.

212. Bläsing, O.E., et al., *Sugars and Circadian Regulation Make Major Contributions to the Global Regulation of Diurnal Gene Expression in Arabidopsis.* The Plant Cell Online, 2005. **17**(12): p. 3257-3281.

213. Botton, A., et al., *Signaling pathways mediating the induction of apple fruitlet abscission.* Plant Physiology, 2011. **155**(1): p. 185-208.

214. Zhang, Y., et al., *Inhibition of SNF1-Related Protein Kinase1 Activity and Regulation of Metabolic Pathways by Trehalose-6-Phosphate.* Plant Physiology, 2009. **149**(4): p. 1860-1871.

215. Baena-González, E., et al., *A central integrator of transcription networks in plant stress and energy signalling.* Nature, 2007. **448**(7156): p. 938-942.

216. Chary, S.N., et al., *Trehalose-6-Phosphate Synthase/Phosphatase Regulates Cell Shape and Plant Architecture in Arabidopsis.* Plant Physiology, 2008. **146**(1): p. 97-107.

217. Holmstrom, K.-O., et al., *Drought tolerance in tobacco.* Nature, 1996. **379**(6567): p. 683-684.

218. Poethig, R.S., *Vegetative phase change and shoot maturation in plants.* Current Topics in Developmental Biology, 2013. **105**(Developmental Timing): p. 125-152.

219. Remay, A., et al., *A survey of flowering genes reveals the role of gibberellins in floral control in rose.* Theoretical and Applied Genetics, 2009. **119**(5): p. 767-781.

220. Furner, I.J. and J.E. Pumfrey, *Cell fate in the inflorescence meristem and floral buttress of Arabidopsis thaliana.* Plant Journal, 1993. **4**(6): p. 917-931.

221. HORRIDGE, J.S. and K.E. COCKSHULL, *Size of the Chrysanthemum Shoot Apex in Relation to Inflorescence Initiation and Development.* Annals of Botany, 1979. **44**(5): p. 547-556.

222. Thomas, R.G., *Correlations between Growth and Flowering in Chenopodium amaranticolor: I. Initiation of Leaf and Bud Primordia.* Annals of Botany, 1961. **25**(2): p. 138-151.

223. Gerber, A.I., K.I. Theron, and G. Jacobs, *Synchrony of Inflorescence Initiation and Shoot Growth in Selected Protea Cultivars.* Journal of the American Society for Horticultural Science, 2001. **126**(2): p. 182-187.

224. Foster, T., R. Johnston, and A. Seleznyova, *A Morphological and Quantitative Characterization of Early Floral Development in Apple (Malus x domestica Borkh.).* Annals of Botany, 2003. **92**(2): p. 199-206.

225. Jahn, O.L. and M.N. Dana, *Crown and Inflorescence Development in the Strawberry, Fragaria Ananassa.* American Journal of Botany, 1970. **57**(6): p. 605-612.

226. Green, K.A., et al., *CORONA, a Member of the Class III Homeodomain Leucine Zipper Gene family in Arabidopsis, Regulates Stem Cell Specification and Organogenesis.* Plant Cell, 2005. **17**: p. 691-704.

227. Melzer, S., et al., *Flowering-time genes modulate meristem determinacy and growth form in Arabidopsis thaliana.* Nature Genetics, 2008. **40**(12): p. 1489 - 1492.

228. Junttila, O., *Apical growth cessation and shoot tip abscission in Salix.* . Physiologia Plantarum, 1976. **38**(4): p. 278-286.

229. Suzuki, T., *Shoot-tip abscission and adventitious abscission of internodes in mulberry (Morus alba).* Physiologia Plantarum, 1991. **82**(4): p. 483-489.

230. Clearwater, M.J., et al., *Vigor-controlling rootstocks affect early shoot growth and leaf area development of kiwifruit.* Tree Physiology, 2006. **26**(4): p. 505-515.

231. Mueller, R.J., *Shoot Tip Abortion and Sympodial Branch Reorientation in Brownea ariza (Leguminosae).* American Journal of Botany, 1988. **75**(3): p. 391-400.

232. Sakai, S., *Sympodial and monopodial branching in Acer (Aceraceae): Evolutionary trend and ecological implications.* Plant Systematics and Evolution, 1990. **171**(1): p. 187-197.

233. Pigott, C.D., *Effect of Photoperiod and Water Supply on Apical Abscission of Long-Shoots of Tilia cordata Mill.* New Phytologist, 1984. **97**(4): p. 575-581.

234. Greathouse, D.C. and W.M. Laetsch, *Structure and Development of the Dimorphic Branch System of Theobroma cacao.* American Journal of Botany, 1969. **56**(10): p. 1143-1151.

235. Durzan, D.J., *Nitrogen reallocation during female bud abscission in alternate bearing of Pistachio.* Advances in Horticultural Science, 1996. **10**: p. 219-225.

236. Wang, N.N., M.-C. Shih, and N. Li, *The GUS reporter-aided analysis of the promoter activities of Arabidopsis ACC synthase genes AtACS4, AtACS5, and AtACS7 induced by hormones and stresses.* Journal of Experimental Botany, 2005. **56**(413): p. 909-920.

237. Thimm, O., et al., *Mapman: a user-driven tool to display genomics data sets onto diagrams of metabolic pathways and other biological processes.* Plant Journal, 2004. **37**(6): p. 914-939.

238. Usadel, B.r., et al., *Extension of the Visualization Tool MapMan to Allow Statistical Analysis of Arrays, Display of Coresponding Genes, and Comparison with Known Responses.* Plant Physiology, 2005. **138**(3): p. 1195-1204

239. Pfaffl, M.W., *A new mathematical model for relative quantification in real-time RT-PCR.* Nucleic Acids Research, 2001. **29**(9): p. e45.

Section 2: The Shoot Apical Meristem

The ability of plants to grow from seemingly nothing at all has fascinated people for millenia, and was perhaps most famously demonstrated by Johannes Baptista van Helmont's 1648 potted willow experiment. Although he incorrectly deduced that plants obtained their mass from water, it is known today that plants obtain much of their bulk from carbon dioxide in the atmosphere. This gas is then used by the plant to make sugars, cellulose and other molecules needed to grow and reproduce. However, it is also equally clear that plants do not simply swell up like a sponge, because their seedlings bear little resemblance to mature trees. Instead, plants actually confine much of their growth and development to very small parts of their anatomy, which can be found by tracing the stem from the ground up, so to speak. After passing the trunk, the larger branches, and the slender twigs, the actual tip of the branch is often found to be obscured by a dense cluster of small scales or leaves, collectively known as a bud. When these leaves are peeled off layer-by-layer, one will eventually find a smooth rounded dome in the center, often a mere fraction of a millimeter wide, surrounded by tiny organs in various stages of development. This is the primary unit of plant growth, and it is known as the shoot apical meristem (SAM).

Appearances can be deceiving however, as the SAM actually performs many critically important activities necessary for survival. The more obvious of these include the production of all new leaves, branches, and flowers, which replace lost or damaged organs, and are necessary to produce the next generation. The SAM is also the site of many developmentally important decisions, regulating aspects such as how fast the plant grows, how many leaves are produced, and when to flower. These decisions are in turn are based on a wide variety of information sources, such as temperature, photoperiod, disease, age, and the current nutritional state of the plant.

Unlike an animal brain though, very little of this decision-making process is evident in the cellular anatomy of the SAM. When examined from longitudinal sections, its tissues are slightly smaller and denser than average, but there is otherwise little to attract attention. The most obvious feature is a subtle layered arrangement of cells near the surface, which are distinguishable by the fact that their cells always divide at right angles to the surface. In most flowering plants, two such layers are present, each of which is a single cell thick, and both are draped over an interal dome-shaped mound of irregularly shaped cells.

For the sake of convenience, the layers are numbered from the outside-in starting with Layer 1 (L1), and then proceeding through L2, L3, and so on. However, this system becomes less useful with tissue depth, because the presence of the irregularly shaped cells deep inside the SAM make it increasingly difficult to identify the individual layers. As a result, many authors simply stop counting at L3, but it is commonly accepted that "L3" refers to the entire inner volume of irregularly shaped cells, rather than to a single layer (Figure 2.0). The three-layered description has some support in terms of known gene expression patterns, and to avoid confusion the remainder of this dissertation will also stop counting at L3. The only exception occurs in chapter 4, where a longitudinal analysis of protein distributions made it necessary to describe cell layers as deep as L11 (see Figure 3.5).

In addition to the cell layers, there is also another discrete set of patterns in the SAM that cannot be seen by the naked eye. They are instead recognized by differences in gene expression patterns and cell division rates. The very center of the SAM for example, contains a vertical column of cells that divide at rates 2-3x slower than those in the periphery [1]. This division rate, along with the appearance of new organs on the periphery, have long served as landmarks to identify the meristem structure, and they are conveniently known as the Central Zone (CZ) and Peripheral

Zone (PZ). Typically the CZ is further subdivided into upper and lower portions, such that cells in the L1 and L2 are recognized as the "upper" CZ, while those in the underlying L3 are known as the Rib Meristem (RM). The astute student however, will note that this interpretation is not quite universal, as some researchers further postulate the existence of a fourth "Organizing Center" (OC) inserted between the CZ and RM tissues. Although not shown in Figure 2.0, the OC is equivalent to the rounded apex of L3, pushing the remaining part of the RM somewhat deeper into the stem. Until better genetic evidence is available though, only CZ, PZ, and RM will be used for the remainder of this dissertation.

While the numbering system shown in Figure 12 does provide a useful set of spatial coordinates, it is also somewhat misleading as it implies that the SAM is static structure, unchanging over time. This could not be further from the truth. Instead, it must be remembered that the SAM is a site of plant growth, and as a result its cells are in a state of constant flux as they divide, grow, and differentiate. For example, the repeated perpendicular divisions that occur in L1 and L2 actually cause these layers to expand sideways, where the displaced cells eventually bend around the curve of the apical dome and become part of the cylindrical stem surface. The motion is reminiscent of the path taken by water droplets in an umbrella-shaped fountain, though the individual plant cells move considerably slower. If growth by lateral displacement is followed to its logical extremes, it is important to note that all of the founding cells will be pushed off to the sides over time, while new ones take their place in the middle. No single cell in the SAM is a permanent resident. The overall shape and size of an SAM is perhaps more analogous to a standing wave, where stability is the illusion caused by a dynamic equilibrium.

Maintaining that wave is of course a difficult challenge, as the inputs to that equilibrium (cell division) must be precisely matched to its outputs (organ differentiation) at all times. Failure to

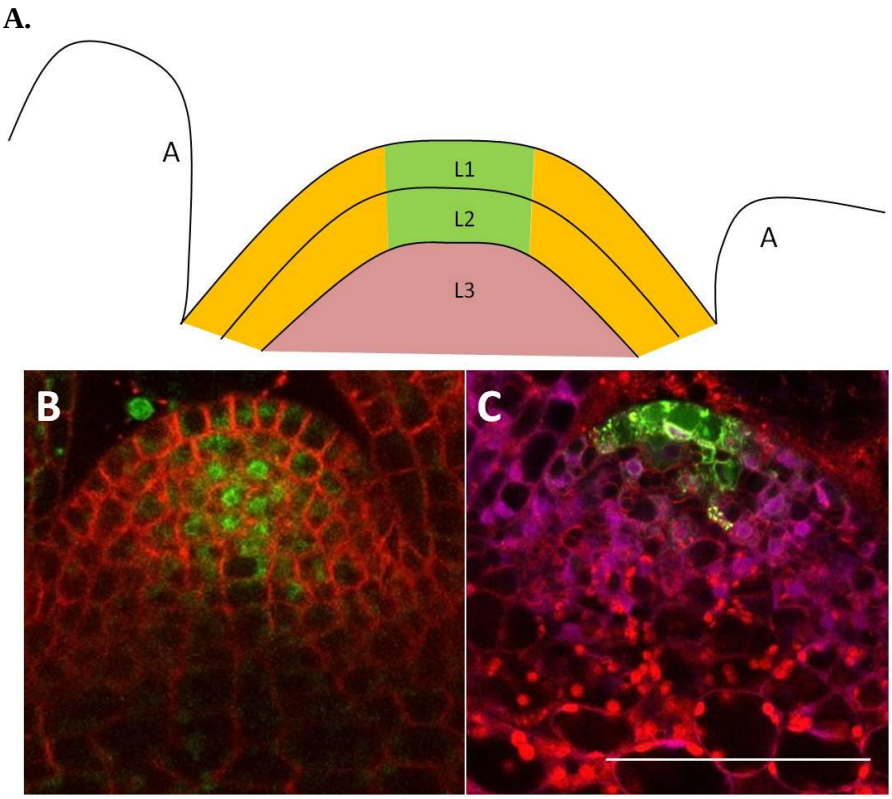

Figure 2.0. Structure of the SAM. **(A)** Diagrammatic longitudinal section of the SAM showing tissue organization. B, C Actual longitudinal section of *A. thaliana* SAM showing WUS and CLV3 expression patterns, as shown using the GFP fluorescent reporters (green). **(B)** pWUS:eGFPWUS **(C)** pCLV3:mGFP5-ER. L1 = Layer 1, L2=Layer 2, L3= Layer 3, A = lateral primordia, Green = Central Zone, Orange = Peripheral zone, Pink = Rib Meristem. Scale bar = 50 μm.

do so would quickly rob the plant of its ability to grow, with obvious consequences for survival. Exactly how this balance is maintained is not fully understood, but the motion of the cells makes at least one part of the process perfectly clear: the cells must change their identity as they are moved from one place to another. Those that start in the CZ for example, switch to PZ gene expression patterns as they move further away from the middle, and may later adopt leaf and flower identities as they are incorporated into mature organs. Cell identity in the SAM is thus largely an issue of location rather than its developmental history.

The ability of a cell to determine its location within the SAM structure is thus of paramount importance, yet it must do so in the absence of any stationary reference point. So far as currently understood, each cell solves this problem in exactly the same way a person would do so: it talks to its neighbors. Based on what the individual cell sees and what its neighbors report seeing, it is possible to work out exactly where the cell is located in the overall plant structure. Of course in actual plant tissues such communication occurs largely through to the exchange of proteins, hormones, and RNA molecules, though increasingly evidence suggests that mechanical forces in the cell wall may also contribute some information [2]. Some molecules can travel further distances than others, some are modified en-route in order to become functional, and still others move from cell to cell in precise patterns, much like the knight in a game of chess. When these molecules are produced in different areas of the plant, the surrounding cells can estimate their relative locations to each other simply by reading the chemical bar-code in their local milieu, and then develop accordingly.

Hormone Regulation

At the present time, only a few such routes of chemical communication have been identified, two of which are plant hormones: auxin and cytokinin. Auxin is best known for increasing the volume of cells, though it also has roles in apical dominance and tropism growth patterns. Cytokinin meanwhile is known for stimulating cell division, in addition to other roles in senescence and pathogen responses. Together the function of the two hormones would appear to complement each other very well in terms of overall growth, yet within the SAM they appear to mix about as well as oil and water. Cells that respond to auxin often don't respond to cytokinin, and vice versa. Why this should be so is not well understood, but studies of root vasculature development suggest that their mutual exclusion is actually used to generate spontaneous patterns

that help guide plant development [3, 4]. In callus tissue, the two hormones are often found to have response patterns arranged in a polka-dot like arrays, where each hormone "dot" is surrounded by a circular field belonging to the other [5]. The SAM is organized around a single such dot, where cytokinin responses occur in the RM [6], and auxin responses occur in the PZ [7] which often occur in discrete foci corresponding to new lateral organs [7, 8]. The CZ cells in contrast, do not appear to be sensitive to either hormone [9], but instead express both auxin and cytokinin biosynthesis genes [5, 10-13]. The production of cytokinin in the L1 and L2 is also consistent with the distribution of bioactive cytokinin concentrations observed with immunological techniques [14] and with GFP reporter systems [11]. This suggests a stable arrangement of three mutual exclusion zones within the SAM, which closely correspond to the known CZ, PZ, and RM tissues. Root apical meristems (RAM) in contrast, appear to be based on the reciprocal arrangement, as roots have an auxin response dot in the middle [15] surrounded by cytokinin responses in the overarching root cap, concentrated in the root cap columella cells [6].

The WUS-CLV3 feedback loop

Another potential communication system that has been extensively studied involves a potential feedback loop between the CZ and RM cells, thought to be carried out by WUS [16, 17] and CLV3 [18, 19]. WUS is a homeodomain transcription factor produced exclusively within the RM, but is capable of moving 2-5 cell diameters away from its center of origin [20, 21]. WUS has also been shown to activate transcription of *CLAVATA3* in the overlying CZ cells by directly binding to the *CLV3* promoter [20]. CLV3 in turn, is thought to be a small secreted oligopeptide [22-25] that is modified with a few arabinose sugars [25]. The mature glycoprotein then travels through the apoplast to reach leucine-rich receptor kinases in the RM, such as CLV1 [26, 27] or *BARELY ANY MERISTEM1* (*BAM1*) [28], thereby triggering a signaling cascade that ultimately

suppresses WUS transcription [29]. Many of the intermediate biochemical steps however, have not yet been fully identified, which makes it difficult to fully reject the feedback loop null hypothesis.

There is also evidence of a more complex set of feedback loops, as WUS has been found to regulate components of the cytokinin signal transduction pathway [30], and exogenous cytokinin are able to stimulate *WUS* transcription [31, 32]. Altered cytokinin signalling pathways have also been shown to affect *CLV3* expression patterns [33]. *WUSCHEL-LIKE HOMEOBOX5* (*WOX5*), which is closely related to WUS, is known to participate in auxin pathways within the root [34], while the generation of SAMs from callus or root tissue has repeatedly been shown to require a pre-incubation on auxin rich media [5, 35, 36], where it may actually stimulate auxin transport [37, 38]. Micro RNA molecules may also be involved, as a variant of *AUXIN RESPONSE FACTOR 10* (*ARF10*) that was resistant to miR160a was able to increase WUS and CLV3 expression patterns [39].

Clearly, there is a lot going on. To help clarify how such cross-talk contributes to SAM structure, the research presented in this dissertation explores two closely related subjects. The first is the regulation of *CLV3*, which was studied by resolving the promoter structure of this gene in chapter 3. The results suggest that *CLV3* is regulated in part by auxin responses, while activation and/or repression is likely to be controlled complicated set of cis-motifs in the 3' enhancer region. The presence of these 3' motifs in a known transposon also suggests a novel origin of the WUS/CLV3 feedback loop. Chapter 4 meanwhile, explores the possibility that WUS and cytokinin responses form a second feedback loop necessary for SAM structure. This was done by narrowing down the possible cellular and biochemical routes by which cytokinin could affect *WUS* transcription, translation, and protein movement. The results however, suggest that the two pathways are at

largely independent of each other, though cytokinin responses may increase WUS stability in the RM. Unexpectedly, the data also found that the *absence* of cytokinin responses in the CZ is a critical part of SAM structure. The cytokinin response-free cells were also found to have an enhanced protein degradation mechanism, which may help shape the WUS protein gradient. Interestingly, WUS proteins were found to be rapidly degraded following auxin treatments, suggesting a model in which the SAM structure is defined by cytokinin-induced stability in the RM, and auxin-induced protein degradation in the surrounding CZ and PZ cells.

Chapter 2 CLV3 promoter characterization

Introduction

The WUS-CLV3 feedback loop [18, 29] has long been an attractive model to explain how SAM structure is maintained in a dynamically changing cellular environment. Simply by combining activation of CLV3 with the repression of *WUS*, computer simulations have repeatedly shown that this is sufficient to maintain constant population of cells with CZ and RM identity [40-42]. However, despite the simplicity of this model, the molecular mechanisms that carry out the feedback loop have instead revealed a number of potential complications. On the forward path for example, WUS is known to be a bi-functional transcription factor, activating and repressing several hundred different target genes [30, 42, 43]. Currently it is not currently known exactly how WUS switches from activator to repressor, but it has been shown to directly bind to DNA motifs in *AGAMOUS* [44] and *CLV3* [20] regulatory regions, where it activates their transcription. Additional binding sites on repressed targets such as *KANADI1*, *YABBY3*, *ASYMMETRIC LEAVES2* have also been identified [42]. Complicating this model of is the observation that CLV3 activation requires both WUS and SHOOTMERISTEMLESS in leaf tissues [22], suggesting that the presence of WUS alone is not sufficient. In addition WUS has also found to directly interact with the GRAS domain transcription factor HAM1 [45, 46], as well as the potent transcriptional repressor *TOPLESS* (*TPL*) [47, 48]. TPL itself further has been shown to assemble a protein complex with Sin3 ASSOCIATED PROTEIN (SAP18) and HISTONE DEACETYLASE 19 (HDA19) [49, 50], suggesting a potential link between WUS and chromatin modification.

In order to discriminate between the two models, this study began by attempting to identify the cis-regulatory environment around the *CLV3* locus. The *CLV3* expression pattern was first

carefully recorded with a GFP reporter, which in contrast to previously published RNA in-situ's, found layer-specific differences in *CLV3* transcriptional output. The regulatory regions of *CLV3* were then annotated by mapping predicted transcription factor binding sites and computationally significant cis-motifs, which were further resolved with phylogenetic footprinting.

This analysis found that *CLV3* has a very simple 5' promoter, containing an auxin responsive element, suggestive of ubiquitous expression. The 3' enhancer in contrast, contained at least 3 large cis-regulatory modules, two of which were found within a naturally occurring transposon, while the 3rd included several known WUS binding sites. On the basis of promoter deletion experiments, all three cis-regulatory modules were found to be required for *CLV3* activation. The existence of the transposon in turn, has several implications for the evolution of the WUS-CLV3 feedback loop and Brassicaceae plant anatomy.

Results

Predicted cis motifs

Previous reports of the CLV3 expression pattern have consistently found it localized to the apex of the SAM, where it is often used as an indicator of CZ cell identity. Within this region, the expression pattern is somewhat variable, as previous RNA in-situ revealed a narrow inverted cone-shape [27, 33], while GFP and GUS reporters often produce more indistinct rounded shape 3-4 cell layers deep [51, 52]. In contrast, the present study found a slightly more complex pattern when viewed as a longitudinal section. In perfectly centered sections, the pCLV3:mGFP5-ER reporter often appears in an inverted cone shape, but the expression zone is noticeably broader than the previous RNA in-situ results (Figure 2.1). As the section plane is displaced from the central axis and becomes more tangential, a conspicuous gap is frequently visible, where the L2 cells have less fluorescence than those immediately above and below. This suggests a bi-partite

expression pattern where a flat, circular domain occurs specifically in the L1, and a second spherical domain occurs underneath in the L3 cells (Figure 2.1).

In order to identify the *CLV3* regulatory structure, this work began by annotating all known regulatory motifs on an 8kb genomic sequence centered on At2g27250. Transcription factor binding sites were identified by consulting multiple online prediction tools which quickly found over two hundred predicted cis-motifs, many of which had low probability scores. The odds of identifying functional cis-motifs were increased in a few select cases by adding 5bp sequences on either side of the core motif, based on previously identified target sites for *WUS* [20], *ARF1* [53], and *ARR1* [54]. The enlarged biding sites were then mapped to the *CLV3* genomic sequence, tolerating up to 2 mis-matches in the flanking regions. In order to account for the presence of transcription factors whose cis-motifs are not currently known, MEME analysis [55] were employed to identify motifs shared between genes that are co-expressed with CLV3.

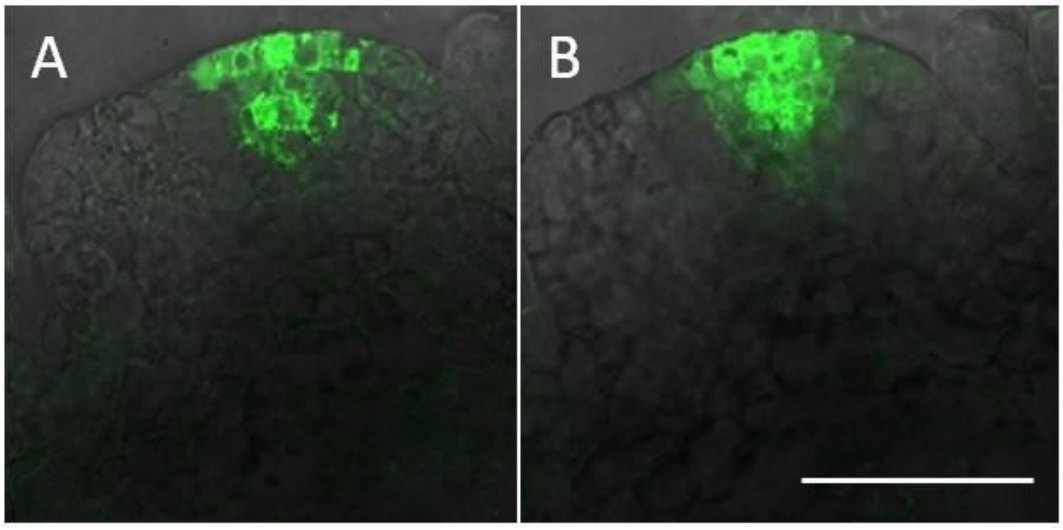

Figure 2.1 CLV3 expression pattern. A-B: pCLV3:mGFP5-ER reporter in two optical sections of the same meristem. **(A)** tangential section, showing the L2 "gap". **(B)** Centered longitudinal section. Scale bar = 50 μM.

Fifty-one genes (Table 3.2) were selected based on flow-cytometry data [9] (see methods), and 1000 bp their upstream, and downstream sequences were analyzed. In the upstream regions, two MEME motifs were found to display non-random patterns that might suggest functional relevance (Figure 2.2). Motif 2 (GCCCA) occurred in pairs spaced 40-80bp apart in 22% of the genes that had at least one occurrence, and Motif3 (ACGGnnnnnA), was found within the first 300 bp of the Transcriptional Start Site (TSS) in 15 out of 17 the genes that contained this sequence. Neither motif clearly matched known *A. thaliana* transcription factors, but the GCCCA sequence of Motif 2 is similar to the target site recognized by *PCF1* and *PCF2* in rice [56], which are part of the TCP domain transcription factor family [57] involved in cell proliferation [58-60]. In the 3' enhancer region, MEME analysis identified only a single recognizable pattern, where Motif 10 and Motif 7 occurred in several tandem repeats in the 3' region of At4g12720. Based on the near-identical expression patterns between *CLV3* (Figure 2.1) and the auxin biosynthesis gene *YUCCA4* (*YUC4*) [5], a third MEME analysis was performed using only these two genes. This identified the palidromic sequence CCAGTGG, located -385bp upstream of the *YUC4* TSS, and -360bp upstream of CLV3. No currently recognized plant transcription factors are known to recognize this motif.

Overall, 231 potential cis-motifs and transcription factor binding sites were identified. Most were randomly distributed over the entire *CLV3* genomic sequence, but irregular clusters could be recognized near the coding region. The largest cluster occurred in the upstream 500bp of the 5' promoter, while up to three smaller clusters occurred in the 3' enhancer region (Figure 2.5). The list of potential factors was then filtered to include those found inside the previously identified *CLV3* regulatory regions (1.5kb upstream and 1.2kb downstream) [22], which left just 157 predictions (See Table 3.1). Many of the remaining predictions were found to have overlapping

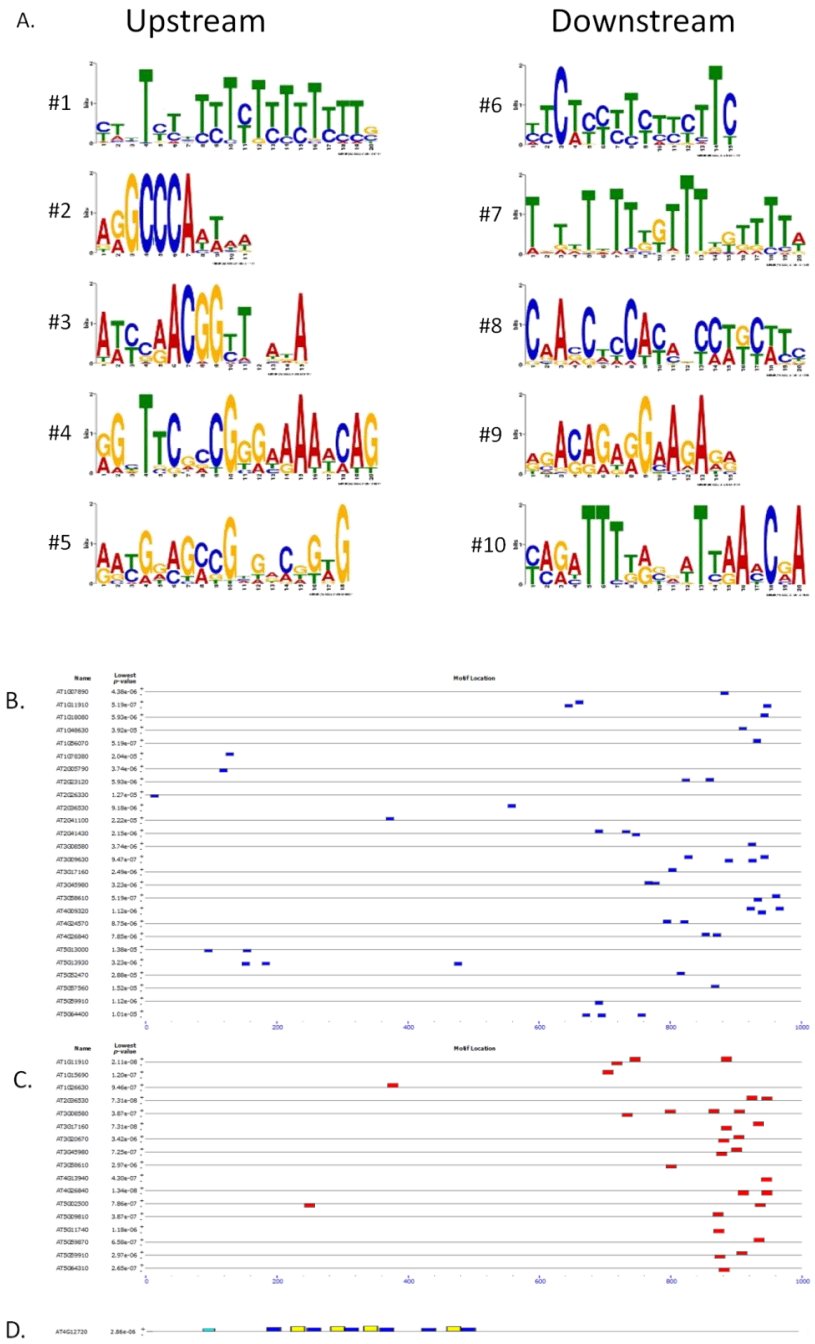

Figure 2.2. MEME motifs, identified from 51 genes co-expressed with At*CLV3*. (A) Identified motifs, found within 1000bp upstream and downstream of the coding sequence. **(B)** Clustering of Motif 2 in the promoter of 26 co-expressed genes. **(C)** Clustering of Motif 3 in the promoter of 17 co-expressed genes. **(D)** Tandem repeats of motifs #7 (blue) and #10 (yellow) in the 3' enhancer region of At4g12720. All scales are 1000bp, shown 5'-3'.

sequences, though it is unclear how well this might predict their actual function in-vivo. One notable example of this phenomenon is a predicted MYB-like binding site located at -155bp, which was predicted by four different databases. In other cases, two structurally different transcription factors were predicted to have overlapping cis-motifs, such as the bZIP/homeodomain pair Opaque-2/*ALFIN-1* in the 3' enhancer region. Interestingly, the data also revealed four partial miR414 targets, three of which overlapped with the DNA/Mariner family transposable element At2gTE50670 in the 3' enhancer (Figure 2.5), and the fourth occurred in the 3rd exon.

Footprinting

In an alternative approach to identify unknown cis-motifs, phylogenetic footprinting was used to compare *CLV3* orthologous sequences from different species. In this method, functional regulatory structures can be identified by their conservation over evolutionary time, which often requires little more than performing a sequence alignment. The method is also quite robust, as previous studies found that the identified footprints matched 80 and 85% of known transcription factor binding sites [61, 62]. To begin this analysis, three *CLV3* orthologs (*A. thaliana, A. lyrata, B. rapa*) were identified by their syntenic relationships within the Brassicaceae using the tools in the Brassica Genome.org database [63]. Their cDNA sequences were aligned with 27 CLE family paralogs identified in *A. thaliana* [64] (Figure 2.3) in order to identify features that were unique to *CLV3* orthologs, before expanding the search to additional species. This analysis revealed three potentially unique traits that might be used to distinguish orthologs from the multitudes of closely related CLE genes. These included three consecutive histidines at the C terminal end of the CLE motif, a C-terminal oligo extension, and a 3-exon gene structure, all of which had been previously identified in the *CLV3* sub-group [64]. Additional orthologs were

then identified using tBlastn searches against the At*CLV3* protein, for which nine species which met the criteria described above: *Brachypodium distachyon, Oryza sativa*, *Ricinus communis, Glycine max, A. thaliana, Arabidopsis lyrata* and *Brassica rapa, Capsella grandiflora, and Camelina sativa*. No At*CLV3* orthologs were identified in the gymnosperms, basal angiosperms, or the Asteriids using these search parameters. The Euphorbiaceae and Fabaceae each contributed one species in the closely related Eurosiids I [65], while the monocots are represented by two species in the Poaceae. As a result, this sampling is heavily biased towards the Brassicaceae family (Eurosiids II), which provide more than half of the total number of species.

In order to footprint the promoter regions, initial sequence alignments were performed using 8kb genomic fragments, containing up to 5kb of upstream and downstream sequences on either side of the coding region. However, little or no homology was found when all nine orthologs were aligned simultaneously. This was not improved by removing monocot clade, as the two grass orthologs (Os*CLV3*, Bd*CLV3*) failed to align with each other. Repeating this pattern, both *R.*

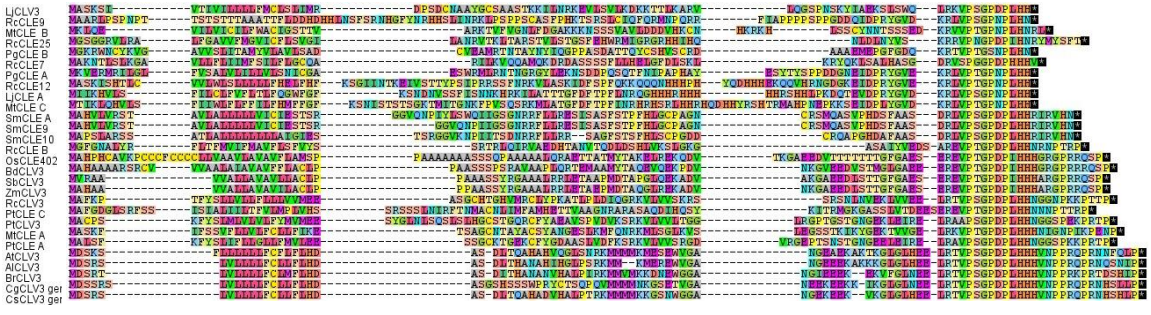

Figure 2.3. CLV3 character identification. Twenty eight putative CLV3 orthologous protein sequences were aligned and then adjusted according to hydropohic patterns. The left two columns correspond to the signal peptide sequence, the middle column is largely produced by the 2nd exon, and the right two columns represent the CLE motif plus N-terminal and C-terminal extensions. Lj = *Lotus japonicus*, Rc = *Ricinus communis*, Mt = *Medicago truncatula*, Pg = *Picea glauca*, Sm = *Selaginella moellendorffii*, Os = *Oryza sativa*, Bd = *Brachypodium distachyon*, Sb = *Sorghum bicolor*, Zm= *Zea mays*, Pt = *Populus trichocarpa*, At = *Arabidopsis thaliana*, Al = *Arabidopsis lyrata*, Br = *Brassica rapa*, Cg = *Capsella grandiflora*, Cs = *Camelina sativa*, * = stop codon. Amino acids were arbitrarily colored to enhance visual pattern recognition.

communis and *G. max* also failed to alignment with each other, or with any of the remaining orthologs. In contrast, conserved regions became clearly visible when the five Brassicaceae species were aligned separately (Figure 2.4). This result appears to reflect the optimum degree of sequence divergence for this gene, as previous studies have found that orthologs outside of the Brassicaceae were less informative due excessive divergence [62, 66], whereas sequences obtained entirely within the Brassicaceae have been found to have too little divergence [62, 67].

Three of the remaining species (*A. thaliana, A. lyrata, C. sativa*) had complete genomic sequences, while the other two (*B. rapa* and *C. grandiflora*) consisted of two contigs separated by a gap of unknown size. In the *B. rapa* ortholog, the gap was located in the 3' region, and was flanked by 256 and 452 base pair sequences that did not align with any of the other Brasssicaceae orthologs, despite strong sequence conservation in the surrounding regions. This indicates the recent insertion of a large DNA fragment, potentially >700bp in size. Attempts to locate the source of the two end-fragment sequences in the *B. rapa* genome with BLAST searches, unexpectedly found that each was present in multiple copies, and were distributed across several different chromosomes. No evidence of transposable element sequences were found, so the flanking regions were here interpreted to be contaminating scaffold sequences from the original genome assembly [68]. A similar gap of unknown size occurred in *C. grandiflora*, where one contig aligned with the CDS and 3' UTR, while the entire 5' upstream contig failed to align with any other ortholog. In both cases, the non-aligning sequences were removed from the analysis, providing a final alignment consisting of four orthologs in the 5' promoter region, and five orthologs spanning the CDS and 3' UTR.

Overall, the five orthologs shared between 27% and 65% sequence similarity, and grouped into two closely related pairs. One pair contained *C. grandiflora* and *C. sativa*, and the other

contained *A. thaliana* and *A. lyrata*. In contrast, *B. rapa* was found to be distinct from all other Brassicaceae orthologs, which accurately recapitulates its predicted evolutionary relationship with the rest of the family [69]. Upon closer inspection, the coding regions were found to be 79-93% similar, which dropped to just 14-34% in regions with no significant alignments.

The initial alignment was considerably fragmented, with many insertions, deletions, and isolated nucleotides. In many cases, the position of these features varied with the settings in the alignment software, and were here interpreted to be artifacts of the alignment procedure. To correct such artifacts, isolated nucleotides were manually adjusted left or right to maximize local sequence alignments within ±5bp. Where variation in the length of tandem repeats was apparent, gaps were introduced into one or more ortholog sequences to accommodate the largest number of repeats present. Conserved regions were then identified by using a 5bp sliding window to identify regions with more than 60% identity. This window is unusually small compared to previous studies that have used 15-50bp sliding windows [62, 70-72], but was chosen here to more accurately reflect the minimum size of known transcription factor binding sites. Where large contiguous conserved regions were found, the presence of small 1-3bp indels within their sequences were used to break them into smaller fragments, as disruption of these sites indicates that they do not contain functional cis-motifs. scattered in the 3' UTR. Several predicted transcription factor sites were found within the coding regions, but these were interpreted to be non-functional, as previous GUS-reporter systems did not reveal any significant regulatory elements within this region [22]. Among other notable features was a predicted signal peptide in the first exon, identified with signal P 4.0[73], which was almost entirely conserved and is consistent with the secretion of the mature CLV3 oligopeptide [74]. In addition, the second exon was found to be completely conserved with no In all, 42 conserved regions were identified, ranging in size from 5 to over 111bp long. Fourteen footprints were found in the coding

sequence, of which nine of were clustered around the three exons. Only one footprint was found entirely within in the 5' UTR, and the remaining four were intervening gaps. The second exon also completely overlapped with several predicted transcription factors, including HOX2a, as

A.

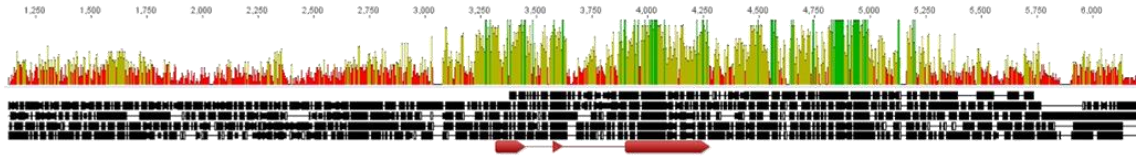

B. C.

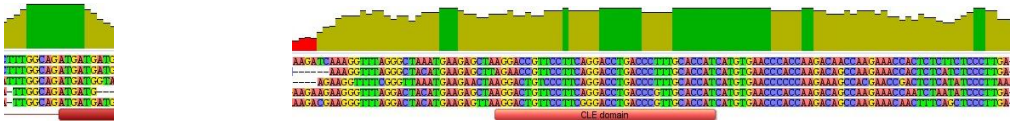

D.

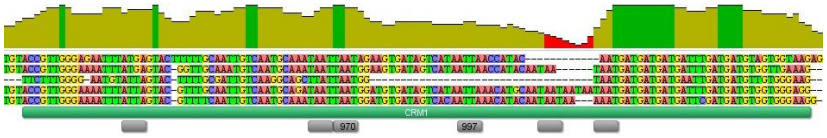

E.

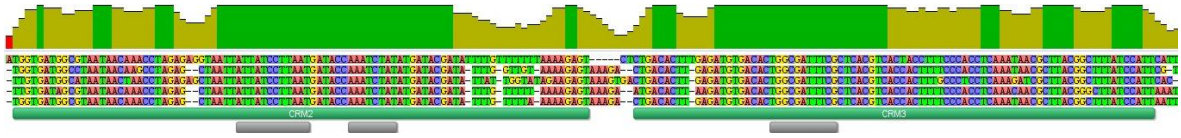

Figure 2.4. **Phylogenetic footprinting**. Orthologous sequences are shown in order from top to bottom: *Capsella grandiflora*, *Camelina sativa*, *Brassica rapa*, *Arabidopsis lyrata*, *Arabidopsis thaliana*. **(A)** Alignment of all five Brassicaceae species. Sequence conservation is shown on top both in height and color, where green=100% identity, off-green=30-99%, red=0-29% identity. The three exons of At*CLV3* mRNA are indicated below with red arrowheads, while contiguous DNA segments are shown in black for each ortholog below. The scale is in reference to the consensus. **(B)** Example of sequence conservation across an intron/exon boundary. **(C)** Third exon coding sequence, ending with the stop codon. **(D)** CRM1. The *WUS* binding sites +970 and +997 are labeled, while other TAAT core sequences shown in gray. **(E)** CRM2 and CRM3. Three BLAST identified motifs are shown below in gray. Nucleotide positions are color-coded A=red, T=green, G=yellow, C=blue.

well as cytokinin (ARR1) and gibberellic acid (GAMYB) responsive motifs. This suggests as-yet unrecognized functional role for the second exon, which might explain why it has been retained in a family that consists largely of single exon genes [64]. The 3rd exon was also highly conserved, although curiously the most conserved region only partially overlapped with the CLE motif [64] and instead included part of the C-terminal extension. In the 3' UTR, the footprints were found to overlap with potential zinc-finger and MYB binding sites, as well as a cytokinin-responsive ARR10 site.

In the upstream regulatory region, the 5' promoter contained ten conserved footprints, eight of which formed a large and nearly contiguous block near the TSS. The two isolated footprints were located at -204bp and -167bp upstream, corresponding to the palindromic Motif#2 and the redundantly predicted MYB binding site, respectively. In the remaining footprints, additional predictions were found for an overlapping AGL15/CBF site, an auxin response element [53], overlapping GT1 and AGAMOUS (AG) sites, and one prediction for a TATA-less promoter. The latter may be related to the position of the only recognizable TATA box-like sequence, which at -68bp upstream, which is more than double the usual 25-35bp described for other TATA-based promoters [75].

In contrast, the 3' enhancer region contained seventeen footprints arranged in roughly three clusters, spanning a region nearly 600 bp long. Two of these clusters closely corresponded with the previously noted clusters of predicted transcription factor sites, while the third was distinctly isolated and had no predicted transcription factors. Together, the footprints contained one of the three known WUS binding sites (+970), two predicted AtHB1 binding sites, a cytokinin responsive element (ARR1), several bZIP motifs, a KNOX-like site, and a predicted cis-motif for

NPR1. Strikingly, the majority of the footprints also overlapped with a DNA transposable element in *A. thaliana*, At2TE50665 (see Figure 2.5a).

It has previously been implied that WUS controls *CLV3* expression in a concentration dependent manner [20, 76], which is consistent with the close proximity of two demonstrated WUS binding sites (+970, +997). The region around these two sites also contains several other TAAT cores within a single stretch about 100bp long, much of which is represented by four conserved footprints, which together might form a WUS binding site cluster. However, only the +970 WUS binding site [20] was found to be perfectly conserved, while the other TAAT cores displayed mutations or were interrupted by indel sequences in one or more orthologs. Instead, when the region around the known WUS binding sites was examined in more detail with a 5bp sliding window, a strikingly periodic pattern was observed, where four different conserved motifs were found to be regularly spaced about 15 bp apart. In order from 5'-3', these motifs were identified as CCGTTGGG, AGTAC, TTGTCAA, and TAATTAATGG (Figure 2.4), the latter two of which correspond to a predicted W-box motif, and the +970 WUS binding site. In addition, a perfectly conserved sequence was found just 25-36 bp downstream in all orthologs, which consisted almost entirely of tandem repeats containing ATG. The ATG repeats also overlapped with a predicted ALFIN-1 homeodomain/Opaque-2 binding site, suggesting that this sequence may actually represent a modified bZIP motif, or perhaps an atypical homeodomain binding site containing a TGAT core motif [77].

It is not clear how many potential binding sites are present in these ATG repeats, but in consideration of the size of the conserved region, it seems likely that they could accommodate up to three transcription factor proteins simultaneously. This interpretation correlates well with the position of three TGAT core motifs. The potential functional role of the TGAT motifs is further

supported by the observation that they are 4x over-represented in the surrounding 124 bp conserved region, while the TAAT cores actually are 5x under-represented. In addition, pair-wise distance measurements between the two cores revealed a skewed distribution, where few sites were found closer together than the median value of 5bp. When several median-length pairs were aligned, this corresponded to the 13bp motif TAATnnWnnTGAT. When this motif was subjected to Patmatch (v1.1) searches of the *A. thaliana* genome, it was found to be 26x over-represented among the genes directly targeted by WUS [42]. Multiple copies of the 13bp motif were also found in several target genes, including two in the 3' enhancer of At*CLV3*. Together, this evidence suggests the presence of a larger cis-regulatory module that may include up to five other transcription factors besides WUS.

Slightly further downstream, another conspicuous feature of the 3' enhancer is the presence of two large and perfectly conserved sequence blocks, spanning 42 and 32 bp, respectively (Figure 2.4). Both the size and the degree of sequence conservation in these two regions were exceptional in that they exceeded those found in the coding region of At*CLV3*. The two regions also overlapped with the DNA family transposable element At2TE50665, suggesting that these may represent coding sequences of the transposon, rather than At*CLV3* regulators. When examined with the 5bp sliding window, the two conserved blocks were found to be surrounded on both sides by a strikingly periodic arrangement of three cis-motifs, spaced 11bp apart, strongly reminiscent of the pattern associated with the WUS-binding region. Superficially, the region around the two conserved blocks resembled an inverted repeat (Figure 2.4), though the underlying sequence in each half showed little or no sequence similarity. The repeated occurrence of this pattern suggests that the cis-motifs are organized around a higher-ordered protein structure, each of which may bridge up to 5-7 unique transcription factors. Such clusters

of cis-motifs can be described as cis-regulatory modules, which in recognition of their similar structure, are provisionally identified here as CRM 1, 2, and 3 (Figure 2.4).

Of the three modules, evidence from the WUS binding sites [20] and a promoter deletion analysis [78], suggests that only CRM1 has a direct role in AtCLV3 activation. Although CRM2 and CRM3 might belong to a transposable element, the overall sequence of At2TE50665 is poorly conserved. It is also an old transposon, which likely shared a common ancestor with all five orthologs more than 20mya [79]. Suspecting functional diversification, the two large sequence blocks were subjected to additional BLAST searches in order to similar motifs in the *A. thaliana* genome. The genes located next to the motifs were identified, and there expression patterns of a select subset of identified genes were compared using microarray data using the eFP browser [80]. In all, 32 genes were identified, most of which contained only one of the two conserved blocks. The only genes that shared both conserved blocks were the pair formed by At2g27250 (*CLV3*) and At2G27240. Unexpectedly, this analysis revealed that many genes had similar expression patterns in the lateral root cap, the columella, and root procambium tissue (Table 3.3). This root expression pattern was also found to be shared between At2G27240 and At*CLV3* [80], though the root expression of *CLV3* was much reduced compared to its levels in the SAM.

Further alignment of the oligomers returned by the blast searches identified three potential cis-motifs, each of which was found to correlate with these expression patterns. Motifs (AAATCTAT and TGGCGATTTCG) were clearly related to root expression patterns, whereas the third motif (ATTATCCTTAAT) was less tissue specific, but associated with several disparate structures in the shoot.

However, the predicted transcription factor binding sites found within CRM2 and CRM3 did not strongly support any of these putative functions. The AAATCTAT motif overlapped with a predicted cytokinin response element (ARR1), and an AGAMOUS binding site. Cytokinin

responses occur in both root and shoot tissues [6], though *AGAMOUS* expression is clearly confined to the flowers [81], indicating a shoot-related function. The root-related function of the TGGCGATTTCG motif was at least partially supported by a predicted "right part of the root hair cis-element" motif [82], but the associated transcription factor is unknown. Finally, the ATTATCCTTAAT motif overlapped with two predicted targets, one for AtHB-2/HAT4, which has root and shoot expression patterns, and the other was a computer identified "sucrose response element" originally identified from lateral buds [83].

CLV3 Promoter Deletions

To test the function of the identified regulatory regions, a series of deletions were performed in the pCLV3m:H2B-YFP reporter construct (Figure 2.7). This construct containes three previously described mutated WUS binding sites [20], which enhanced expression of the reporter by 120% (data not shown). Five large deletions, each about 500bp long were initially performed in the regulatory regions, three of which occurred in the upstream 1.5kb region (Deletions 1-3) and two in the downstream 1.2kb (Deletions 4-5). Based on initial findings, two of the initial deletions were subdivided into smaller segments, identified here as 3.1, 5.1, and 5.2 (Figure 2.6). Most deletions produced a binary on-off response in the SAM, though a faint signal remained in the flower meristems of deletions 4 and 5, which occurred in 25% of all independent alleles. Only deletion 5.1 produced an intermediate fluorescent signal, though the pattern indicates reflection off the surface of the SAM, rather than actual fluorescence. Overall the deletions revealed that the AtCLV3 promoter is located in a small region between -154 and +25 bp TSS, while the 3' enhancer required sequences between +584 and +1389 bp TSS (Figure 2.6). These regions closely correspond to the previously identified conserved footprints, and contained 8 out of 10 footprints in the 5' promoter, all four footprints in the 3'UTR, and 14 out of 18 in the 3'enhancer region.

A

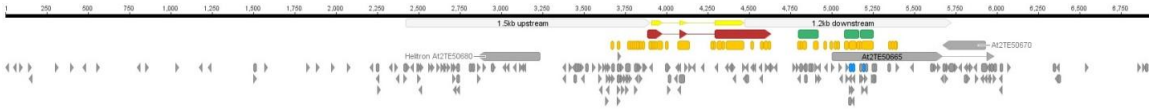

.

B.

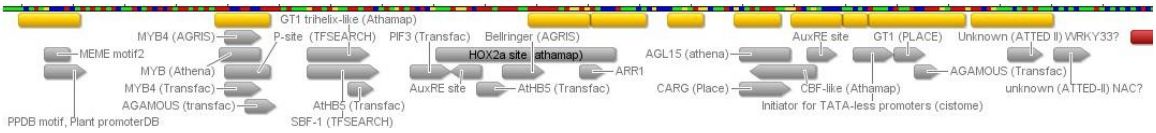

C.

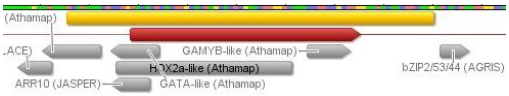

D.

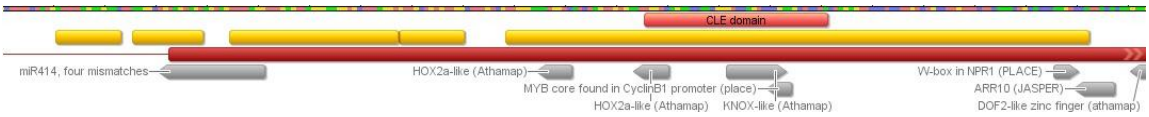

E.

F.

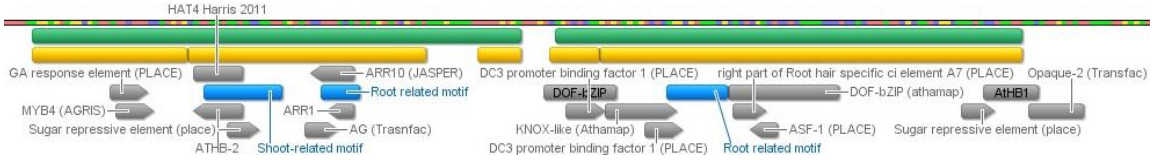

Figure 2.5. Consensus of footprinting and transcription factor predictions. **(A)** Overall view of regulatory regions covering ~7kb. B-F close ups of significant features. **(B)** 5' promoter, showing 225bp. The red square shows the beginning of CLV3 mRNA. **(C)** second exon. **(D)** third exon **(E)** CRM1 **(F)** CRM2 and CRM3. Adjacent, but discontinuous footprints reflect the presence of indels between orthologous sequences. Red=mRNA, green = cis-regulatory region, orange=conserved footprint, gray=predicted cis-motifs, blue=motifs identified by BLAST searches. Color-coded DNA sequences shown in line across top, A=red, T=green, C=blue, G=yellow.

Discussion

Overall structure

Previous deletions of At*CLV3* [78] found the 5' promoter region was less than 812 bp long, and detected a large 3' enhancer approximately 950bp long. These findings are broadly consistent with the results of the present study, where deletions 1, 2, 3, and 3.1 further narrowed down the 5' promoter to just 154bp, and deletions 4, 5, 5.1 and 5.2 support the existence of a regulatory region just 805bp long in the 3' enhancer. However, the two studies disagree in the functional annotation of these regulatory regions, as the present analysis found only positive regulatory regions (deletions 4, 5, and 5.1), while both positive and negative regulatory functions were found in a previous deletion analysis [78]. Disregarding the 5' end of deletion V1 [78] which had no significant footprint in the present analysis, a comparison of the two studies revealed that the previously identified negative regulatory region, corresponds to a 334 bp sequence containing CRM2 and CRM3. Meanwhile, the positive regulatory region corresponded to a 290 bp sequence containing CRM1. The source of the discrepancy is obscure, but might potentially be related to the different techniques used to observe CLV3 expression. The previous deletion analysis relied on a GUS reporter system that used whole plant extracts [78], which might have missed ectopic expression patterns, while the present study did not attempt to observe any other tissue outside of the SAM. Thus it would be of interest to examine similar deletion constructs in a future study, to see if ectopic expression patterns actually occur following the loss of negative regulatory region(s).

The slight increase in the reporter expression in the mutant control compared to a wild-type pCLV3:H2B-YFP reporter (Figure 2.6) is consistent with the repressive function of WUS transcription factors, but suggests that WUS alone is insufficient to repress *CLV3* expression.

A.

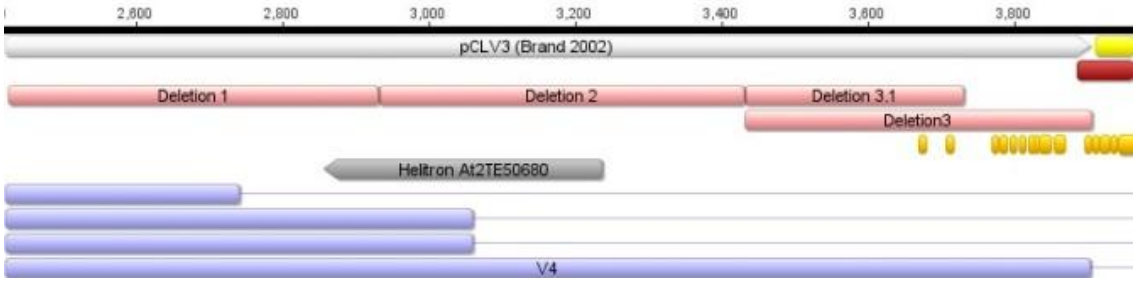

B.

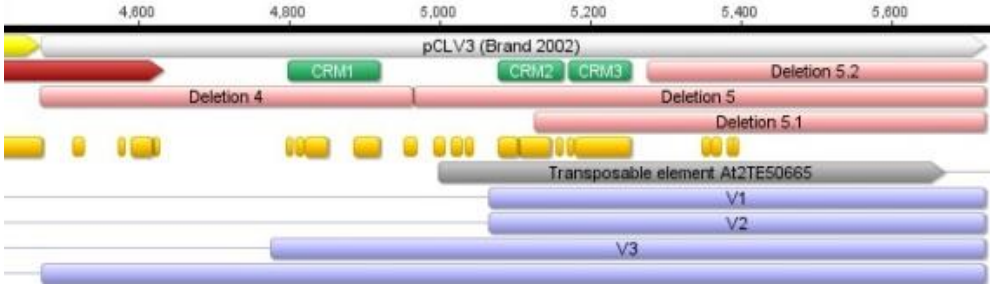

C.

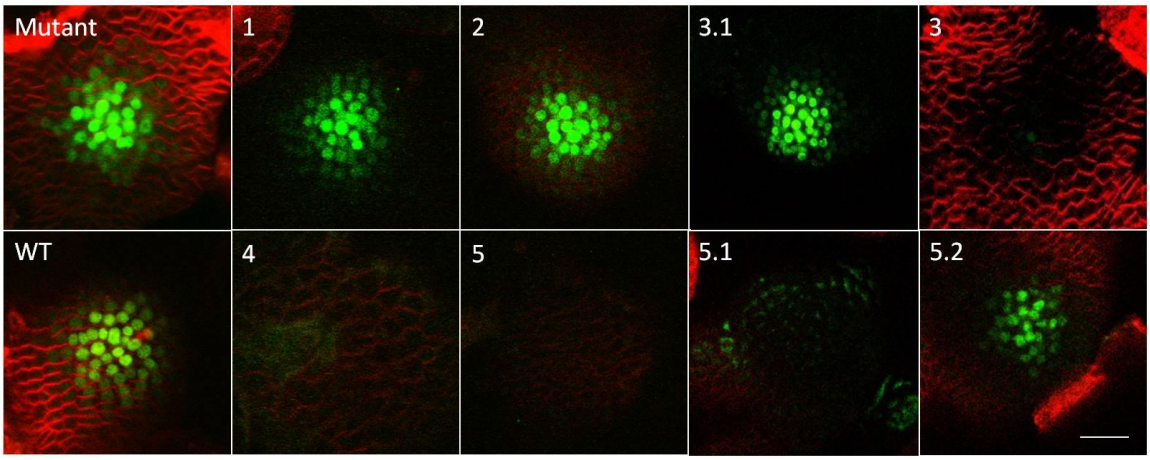

Figure 2.6. Deletion analysis of the At*CLV3* regulatory regions. A-B. Outline of deletion regions and relevant features. Deletions from the present study are shown in pink, deletions V1-V4 are shown in blue, according to their previously described locations [78]. **(A)** Deletions 1-3.1 occur in the 5' promoter. **(B)** Deletions 4-5.2 occur in the 3' enhancer. The numbers correspond to the same regions shown above. Yellow= CDS, Red = mDNA, Green = cis-regulatory modules, Orange = conserved footprints, Light Gray = CLV3 regulatory regions 1.5kb upstream and 1.2 kb downstream, as previously identified [22], Dark gray = naturally occurring transposons. Scale bar = 50 μM

The failure to detect strong reporter activity in deletions 5 and 5.1 might also indicate an interaction between their regulatory modules, as the presence of CRM1 alone could not activate the reporter in the absence of CRM2 and CRM3. The reverse is also true, as CRM2/3 were not able to activate the reporter in the absence of CRM1 (Deletion 4). It is not clear how the modules might interact with each other, as CRM1 is separated from CRM2/3 by 280-335bp, indicating that they are located on non-adjacent nucleosomes. There are however, four conserved regions located between CRM1 and CRM2 (Figure 2.5), which if recognized by additional DNA binding proteins, might help bridge the nucleosome gap.

5' Promoter regulation

The AtCLV3 expression pattern occurs in an inverted cone-shaped domain in the apex of the SAM, and displays layer-specific patterns. The L1 is often strongest, while the signal intensity fades with tissue depth. In tangential sections, L2 cells often have noticeably weaker expression levels (Figure 13). However, the L2 "gap" often disappears in perfect longitudinal sections, suggesting that AtCLV3 is actually expressed in two closely spaced domains: a broad L1 sheet in the CZ, and a smaller, but roughly spherical domain directly underneath. Ideally, it would be possible to predict these two patterns using the conserved cis-motifs identified in this study, but unfortunately the function of individual regulatory regions often cannot be completely determined with the available data. Deletion 3.1 for example (Figure 2.6), suggests that Motif #2 and the redundantly predicted MYB site have no apparent function in the 5' promoter, yet this contrasts with their unique and strongly conserved footprints. There is also predicted cytokinin-response element located at -102bp, but it is poorly conserved among the four orthologous sequences. A predicted AGL15 binding site might produce the L1 pattern by partially suppressing L2-L4 expression, as AGL15 is known to interact with transcriptional repressors such as TOPLESS [84]

and SAP18 [85]. However, an examination microarray data with the eFP browser [86] suggests that AGL15 is only transcribed in a small subset of root tissues [80], where it is unlikely to affect the SAM. However, considering that the AGAMOUS-LIKE gene family contains more than 100 members [87, 88], it is possible that one or more of them might function redundantly to suppress AtCLV3 in a subset of SAM cells.

If these four cis-elements are removed from consideration, the remaining portion of the At*CLV3* 5' promoter is surprisingly small, and is potentially less than 66bp long. Within this small region are three predicted cis-motifs, in addition to the previously noted initiator for a TATA-less promoter, and several conserved regions around the transcriptional start site. Two of the cis-motifs, GT-1 and AGAMOUS, partially overlap with each other and are clear transcriptional activators. The presence of the AG site might also explain the weak expression pattern found in the flower meristems of deletions 4 and 5. The role of GT-1 is harder to explain though, as it is homogenously expressed in most plant tissues, and presumably would lead to widespread ectopic expression of AtCLV3.

However, the absence of such ectopic expression patterns might be explained in terms of a nearby auxin response element, which is recognized by the AUXIN RESPONSE FACTOR1 (ARF1) [53]. Based on the pDR5rev:3xVENUS-N7 reporter, no auxin responses occured in the SAM itself, but they can be readily detected in the apices of lateral anlagen [8, 89, 90]. Although it is not immediately clear how this might relate to AtCLV3 expression patterns in the CZ, a review of the ARF gene family finds that it includes 5 activators and 17 repressors [91]. The cone-shaped expression domain of At*CLV3* is thus most consistent with repressive auxin responses in the peripheral zone, and might even suggest that the "cone" shape is actually pyramidal based on the auxin response foci observed with the pDR5rev:3xVENUS-N7 reporter [8]. This model is also

consistent with the peripheral expression of *ARF3* and *ARF9*, both of which have been demonstrated to be transcriptional repressors [5, 9, 92]. However, this interpretation is at odds with the transcriptional activator ARF5/MONOPTEROS, which is also largely expressed in the peripheral zone, and trace amounts extend into the CZ [33]. As At*CLV3* itself is known to be up regulated by auxin responses at least within the narrow confines of the CZ [33], the potential functional significance of the GT-1 site might be questioned by an alternative regulatory hypothesis. It is equally probable for example, that At*CLV3* is activated in the CZ primarily by ARF5 or other ARF paralogs, and repressed though an unrelated molecule produced in the peripheral zone. So long as this occurs at levels below the detection threshold of the pDR5rev:3xVENUS-N7 reporter, this model would be indistinguishable from the GT-1 activation/peripheral auxin repression model. Currently, the only evidence that might be able to discriminate between these two hypothesis is rather indirect, and relies on the enhancement of cytokinin responses through the alcohol inducible RNAi system to silence *ARR7/15* expression [33]. Interestingly, the CLV3 expression level was reduced in this system [33], which is consistent with auxin-based activation.

3' enhancer

In contrast with the promoter, the 3' enhancer region of At*CLV3* is quite large, with conserved regions spanning a minimum of 460 bp. This region quite likely contains three cis-regulatory modules, each of which may contain 5-7 unique cis-motifs, and together they might support upwards of 20 different transcription factors from multiple gene families. Clearly, regulation of At*CLV3* from the 3' enhancer is likely to be complicated. One hint about how this might occur lies in the regular spacing of cis-motifs 11-15 bp apart, which is suggestive of helical phasing. The motifs themselves show little or no sequence similarity between modules, implying that

transcription factors themselves are interchangeable, while their spacing pattern is governed by a higher-order protein complex that bridges all 5-7 cis-motifs simultaneously. Disregarding a poorly conserved insertion in CRM1 (Figure 2.4), all three modules are almost exactly the same size at 85-90bp long, further supporting the existence of a higher-order structure. Although the identity of this structure cannot be determined from the present data, its functional significance appears to be reflected in CRM1, where the ATG repeats/TGAT cores sequence appears to be re-evolving in the ~36bp inserted sequence that displaced the original conserved block (Figure 2.4). Research in the Drosophila model suggests that the organizing proteins may in fact be PcG and/or TRX proteins, which are thought to be recruited to regulatory modules by a platform of multiple DNA binding proteins [93]. In the Drosophila example however, the "platform" was spread over several hundred base pairs. In plants, a more comparable example might be the PcG binding site demonstrated in *LEAFY COTYLEDONS2*, where PcG proteins recognized an RLE motif that contained several cis-motifs in a region 50bp long [94]. Interestingly, analysis of *FERTILIZATION INDEPENDENT* (*FIE*) target sites found in *A. thaliana* found that they were enriched in four cis-motifs [95], and at least one of each can be identified in the three CRM's revealed by the present study.

The possibility of chromatin regulation also immediately suggests a plausible mechanism by which the 3' enhancer region might repress *CLV3* transcription. The three CRM's may serve as a nucleation site for a chromatin silencing mechanism, allowing the silenced chromatin to spread in both directions until it blocks the 5' promoter of AtCLV3, and presumably the promoter of the neighboring gene At2g27240 as well. However, this model is only weakly supported by the plant literature, as only as a single tenuous chain of evidence supports such an interaction: The TAAT core-motifs in CRM1 are bound by WUS proteins [20], which in turn recruits TOPLESS [47], SAP18 [49], and ultimately the histone deacetylase HDA19/SIN3-LIKE [96]. This evidence is at

least consistent with the repressive portion of WUS transcriptional activities. Although the biochemical details regarding how WUS activates transcription are not yet known, another example from the Drosophila model suggests that such bifunctional activity might be an emergent property of chromatin regulation. Transcription factors that recruit PcG proteins to transcriptional start sites were found to prefer H3K4me3 chromatin modifications [93]. If interpreted correctly, this suggests that transcriptionally active promoters directly recruit their own repressor complex. When a similar model is extrapolated to plants, it is tempting to speculate that the reverse situation might also true: WUS as a repressive transcription factor, may recruit TRX proteins to silenced chromatin, thus activating *CLV3* expression.

The spread of chromatin silencing is also known to involve insulator motifs that limit the spread of such silencing, but the asymmetric structure of the three CRM's makes it tempting to speculate that they have polarized activity. Interestingly, such directional specificity has been observed in fission yeast centromeres, where strand specific repression depended on which Sin3 homolog was used to assemble a histone deacetylase complex [97]. However, no comparable examples are known from plants.

Chromatin looping

Another possible mechanism by which the 3' enhancer region might affect At*CLV3* transcription is through chromatin looping. This typically involves 8-70kb stretches of DNA [98], all of which are considerably larger than the 1.5kb that separates the At*CLV3* promoter from the three cis-regulatory modules. Considering that this small region only supports 5-8 nucleosomes, such short-distance looping might be difficult to achieve before transcriptional activation due to stearic interference. The possibility of looping with a distant enhancer element is also unlikely, as the

previously identified 1.5kb +1.2 kb regulatory regions were sufficient to reproduce the At*CLV3* expression pattern [22].

RNA silencing

The presence of a potential miR414 site in the coding sequence of *CLV3* is intriguing, as it may also offer another level of control. If this microRNA were to be expressed in the RM, its presence would be sufficient to explain the weak expression of AtCLV3 in L2-L4 tissues. This interpretation is consistent with the finding that miR414 is up regulated by cytokinin responses [99], and strong cytokinin responses are known to occur in the Rib Meristem [6]. However, the putative target site in the 3rd exon is poorly conserved among the five orthologs (Figure .4), and others have suggested that the miR414 gene product itself does not fold properly [100]. Still, it may be premature to dismiss miR414 as a pseudo-gene, as several additional target sites were also found in a naturally occurring transposon (At2TE50670), just past the *CLV3* regulatory region.

Regulatory genes

Between the three CRM's identified in this study, it is possible that they can recruit up to 20 different transcription factors simultaneously. Currently, only WUS proteins have clearly been demonstrated to be part of this group, though a few other candidates can be inferred based on known protein interactions. The recognition that SAP18 binds to the EAR-domain of ERF3 [96] for example, clearly suggests that WUS can interact with SAP18 through its own EAR-like domain, in addition to the previously established WUS-TPL interaction [47, 84]. Although TPL did not bind to HDA19 [48], the observation that TOPLESS RELATED1 (TPR1) and HDA19 co-immunoprecipitated suggests that they are at least part of the same protein complex [101]. Thus

it would be interesting to identify the proteins that co-immunoprecipitate with WUS, as these may include the adjacent transcription factors and the higher order protein complexes.

Among transcription factors, one likely candidate might be *HAIRY APICAL MERISTEM1* (*HAM1*) At2g45160, a GRAS domain transcription factor. Originally identified in *Petunia hybrida*, the GRAS domain HAM1 is known to cooperate with the WUS ortholog TERMINATOR [102], and was later shown to physically interact with WUS in *A. thaliana* [45]. This pattern is consistent with the structure of the cis-regulatory modules, particularly if HAM1 should bind to one of the cis-motifs on either side of the conserved +970 WUS binding site. It is also possible that STM might be another co-factor, as both WUS and STM were required to ectopically express AtCLV3 in leaf tissue [22].

Evolution

The WUS-CLV3 feedback loop has long been predicted to be an essential part of meristem structure within *A. thaliana* [18, 29], yet evidence from the present study suggests that *CLV3* orthologs are rather poorly conserved outside of the Brassicaceae. The lack of conservation may be related to the size of the CLE gene family, where current evidence suggests that most plant species have twenty or more paralogs [64, 103, 104]. Many of these are co-expressed in the same tissues [52], and at least some are functionally interchangeable [105, 106].

However, it is also difficult to reconcile the WUS-CLV3 feedback loop with the number of evolutionary clades in each gene family, which would be expected to closely correspond if they represent a conserved feedback loop. Instead, the *WOX* gene family is organized into 3 recognizable clades [107, 108], whereas CLE genes are divided into 13 distinct groups [64]. Their functions are also diametrically opposed, as *WOX* genes tend to be expressed in or near stem cells, while CLE genes are typically expressed in tissues that display terminal

differentiation, such as trichomes, vasculature, stamens, the placenta, and abscission zones [109]. If WUS is an activator of *CLV3*, it is also difficult to explain why *CLV3* expression occurs as much as 24 hours after the appearance of WUS, a phenomenon that has been repeatedly observed plant embryos [17, 22], and callus tissue studies [35, 110]. Although WUS and CLV3 do have reciprocal phenotypes in mutant backgrounds [29, 111], and when ectopically expressed [18, 29, 112], it is surprising that the importance of the hypothesized feedback loop has not left a stronger evolutionary imprint.

Instead, there are hints that the two genes may actually operate in different, but related pathways. One such pathways appears to involve an auxin-CLE connection, which is supported by the similarity of auxin responsive tissues and CLE gene family expression patterns in vasculature tissue, leaf tips, guard cells, and trichomes [52]. This is consistent with the proposed CLV3 regulation by an auxin response element, and is futher supported by the synergistic interaction between auxin and exogenous CLE oligopeptides found in developing *Zinnia elegans* tracheids [113]. Another pathway appears to involve a WUS-cytokinin connection, as WUS has been found to directly regulate cytokinin signaling by repressing A-type ARRs [30, 42], and potentially has a role in activating cytokinin biosynthesis in *A. thaliana* [10]and rice [114]. In turn, these two mechanisms might be linked by the mutually exclusive pattern of auxin and cytokinin responses, which seem to be involved in pattern formation in different parts of the plant [4, 115-118]. Together these observations suggest that WUS and CLV3 might simply respond to the patterns produced by these hormones, providing sharper boundaries between zones and imparting tissue-specific cell identities.

In the present study, the fortuitous finding that several significant *CLV3* regulatory regions lie entirely within a naturally occurring transposon immediately suggests a novel hypothesis that

could unite many different observations. A transposition event that introduced the cis-regulatory modules to AtCLV3 could easily explain the difficulty of identifying *CLV3* orthologs outside of the Brassicaceae, as it implies that it occurred independently in other lineages, where similar transpositions may have involved other CLE paralogs. Repression of the transposon via siRNA pathways might also trigger chromatin silencing, leading to the repression of nearby genes, while replicative transposition might explain why the 13-bp TAATnnWnnTGAT motif seems to be widespread in the *A. thaliana* genome. On a more macroscopic level, the sudden introduction of the cis-regulatory modules might also immediately reduce the size of the SAM, as ectopic activation of *CLV3* in the CZ would partially stimulate terminal differentiation by the CLE pathway, and thus indirectly suppress WUS expression. Such a mechanism would produce smaller plants overall, which is consistent with the size of *A. thaliana* and related species.

Methods

Bioinformatic cis-element searches

Potential transcription factor binding sites were annotated on the *CLV3* locus using Athamap [119], Geneious [120], PLACE [121], Con-site: http://consite.genereg.net/, Cistrome [122], Plant TFDB [123], Jaspar [124] and Athena [125] databases. MicroRNA target sites were confirmed with MiRbase [126]. CLV3 co-expressed genes were identified from a previous flow-cytometry data set [9], which was filtered to include CZ-specific genes that had expression levels at least 4x higher than their expression levels in the RM. Histones and ribosome related genes were excluded from the analysis. Upstream and downstream sequences were extracted from TAIR, and subjected to MEME cis-motif searches [55]. Searches were set to include "any number of repetitions", motif width-6-20bp, and to return a maximum of 10 motifs.

Phylogenetic footprinting

Putatively homologous *CLV3* genes were identified in *A. thaliana*, *A. lyrata*, and *Brassica rapa* databases using the synteny tool in the Brassica database: http://brassicadb.org/brad/. Additional genes were identified by conducting tblastn searches with the At*CLV3* protein sequence, by consulting Phytozome: http://phyto5.phytozome.net/, and by searching the Ancestral Angiosperm Genome Project: http://ancangio.uga.edu/content/aagp-home. Putative ortholog and paralog coding sequences that lacked introns or contained multiple stop codons were rejected. Sequence alignments were initially performed using MUSCLE [127], then adjusted manually using the Geneious software package version 6.1.5 [120].

Deletions

Construct pCLV3m:H2B-YFP (Figure 2.7) was provided courtesy of Mariano Peralez, containing 1.5kb of upstream and 1.2 KB downstream regulatory sequences [22]. Three WUS binding sites in this construct were mutated as described [20] prior to generating deletions by inverse PCR. Followed re-circularization by ligation, the deleted plasmid was first amplified in *E. coli*, then in agrobacterum strain GV310, and finally transformed into wild-type L*er* Arabidopsis plants using the floral dip technique [128]. T1 plants were identified by BASTA selection, and meristems were imaged from 2-4cm tall bolting shoots from 12-16 day old plants. Images were taken with a Zeiss 510 confocal microscope using a 40x objective, 363µM pinhole, HFT 458nM, NFT 545nM, Channel 2 used a BP500-530 filter, Channel 3 used a BP565-615 filter. FM4-64 dye was used for contrast.

Table 2.1. List of predicted TF, cis-motif and other structures. All distances are relative to the Transcriptional start site, using TAIR10 annotations.

Annotation	Minimum	Maximum	Length	Direction	Footprint	Location
Bellringer	-1,470	-1,463	8	forward	No	5' enhancer
+970 WUS-like	-1,468	-1,461	8	none	No	5' enhancer
Sugar RE	-1,451	-1,446	6	forward	No	5' enhancer
AP2/ERF-like	-1,428	-1,421	8	reverse	No	5' enhancer
SEF4	-1,391	-1,383	9	forward	No	5' enhancer
SPL8-like	-1,391	-1,375	17	forward	No	5' enhancer
AG	-1,379	-1,374	6	forward	No	5' enhancer
AP1	-1,378	-1,372	7	reverse	No	5' enhancer
GT1 trihelix-like	-1,372	-1,361	12	forward	No	5' enhancer
Bellringer	-1,320	-1,313	8	forward	No	5' enhancer
ARR10	-1,301	-1,293	9	forward	No	5' enhancer
E2F	-1,268	-1,261	8	forward	No	5' enhancer
MYB core	-1,242	-1,238	5	forward	No	5' enhancer
ARR1	-1,237	-1,233	5	reverse	No	5' enhancer
GT1 trihelix-like	-1,231	-1,219	13	forward	No	5' enhancer
ARR10	-1,207	-1,200	8	forward	No	5' enhancer
HOX2a-like	-1,180	-1,173	8	forward	No	5' enhancer
MEME motif3	-1,176	-1,167	10	forward	No	5' enhancer
HOX2a-like	-1,169	-1,163	7	forward	No	5' enhancer
ARR1	-1,168	-1,164	5	reverse	No	5' enhancer
TGA1a bZIP-like	-1,150	-1,140	11	none	No	5' enhancer
ABRE-like	-1,147	-1,141	7	none	No	5' enhancer
DC3	-1,147	-1,141	7	reverse	No	5' enhancer
ERF2-like	-1,077	-1,067	11	none	No	5' enhancer
WUS -1080	-1,057	-1,052	6	none	No	5' enhancer
At2TE50680	-1027	-647	381	reverse	No	5’ enhancer
ARR1	-1,021	-1,017	5	forward	No	5' enhancer
ARR10	-1,021	-1,014	8	forward	No	5' enhancer
Sugar RE	-988	-983	6	forward	No	5' enhancer
MYB2	-940	-935	6	none	No	5' enhancer
ARR1	-929	-925	5	forward	No	5' enhancer
ARR10	-869	-862	8	reverse	No	5' enhancer
ARR10	-848	-841	8	reverse	No	5' enhancer
GT1 trihelix-like	-809	-798	12	reverse	No	5' enhancer
DC3	-770	-764	7	forward	No	5' enhancer
Bellringer	-758	-751	8	reverse	No	5' enhancer
MYB1	-746	-742	5	reverse	No	5' enhancer
W-Box motif	-506	-501	6	reverse	No	5' enhancer
W-box in NPR1	-505	-501	5	reverse	No	5' enhancer

Annotation	Minimum	Maximum	Length	Direction	Footprint	Location
AP2/ERF-like	-470	-463	8	forward	No	5' enhancer
HOX2a-like	-446	-440	7	reverse	No	5' enhancer
+970 WUS-like	-440	-435	6	none	No	5' enhancer
MYB2	-432	-427	6	none	No	5' enhancer
T-box motif	-419	-414	6	none	No	5' enhancer
Unknown (PPDB)	-396	-389	8	forward	No	5' enhancer
MYB core	-395	-391	5	reverse	No	5' enhancer
MEME from YUC4	-367	-361	7	none	No	5' enhancer
abaA	-329	-315	15	forward	No	5' enhancer
ARR10	-290	-283	8	forward	No	5' enhancer
MYB	-288	-280	9	forward	No	5' enhancer
Bellringer	-285	-278	8	reverse	No	5' enhancer
AtHB9	-266	-261	6	forward	No	5' enhancer
AGP1-like	-247	-239	9	forward	No	5' enhancer
ARR10	-247	-240	8	forward	No	5' enhancer
ARR1	-245	-241	5	forward	No	5' enhancer
ARR1	-244	-240	5	reverse	No	5' enhancer
SPL8	-238	-222	17	forward	No	5' enhancer
AGL3	-228	-223	6	forward	No	5' enhancer
Unknown (PPDB)	-211	-204	8	forward	Yes	5' promoter
MEME motif2	-211	-207	5	none	Yes	5' promoter
MYB	-177	-170	8	none	Yes	5' promoter
P-site	-176	-168	9	none	Yes	5' promoter
MYB4	-176	-170	7	forward	Yes	5' promoter
MYB4	-176	-170	7	forward	Yes	5' promoter
AGAMOUS	-172	-167	6	forward	Yes	5' promoter
GT1 trihelix-like	-160	-149	12	forward	No	5' enhancer
SBF-1	-160	-147	14	forward	No	5' enhancer
AtHB5	-152	-148	5	forward	No	5' enhancer
PIF3	-140	-133	8	forward	No	5' promoter
HOX2a site	-135	-101	35	none	No	5' enhancer
AuxRE site	-132	-127	6	reverse	No	5' enhancer
AtHB5	-127	-122	6	forward	No	5' enhancer
Bellringer	-122	-115	8	forward	Partial	5' enhancer
ARR1	-107	-103	5	forward	Partial	5' enhancer
AGL15	-76	-67	10	none	Yes	5' promoter
CARG	-76	-67	10	forward	Yes	5' promoter
CBF-like	-74	-62	13	reverse	No	5' promoter
AuxRE site	-63	-58	6	forward	Yes	5' promoter
Initiator for TATA-less promoter	-54	-47	8	forward	Partial	5' promoter
GT1	-46	-41	6	forward	Yes	5' promoter

Annotation	Minimum	Maximum	Length	Direction	Footprint	Location
AGAMOUS	-42	-38	5	forward	Yes	5' promoter
Unknown	-24	-18	7	forward	Yes	5' promoter
unknown	-15	-9	7	forward	No	5' promoter
AP1	19	25	7	reverse	Partial	5' UTR
Unknown	114	120	7	none	Yes	1st Intron
CPC1	125	133	9	forward	No	1st Intron
bZIP2/53/44	128	133	6	forward	No	1st Intron
SORLREP5	128	137	10	none	No	1st Intron
GA response	170	176	7	reverse	No	1st Intron
GT1 trihelix-like	175	186	12	reverse	Partial	1st Intron
ARR10	189	196	8	reverse	Yes	2nd Exon
GATA-like	189	198	10	reverse	Yes	2nd Exon
HOX2a-like	190	225	36	none	Yes	2nd Exon
GAMYB-like	229	237	9	forward	Yes	2nd Exon
bZIP2/53/44	256	261	6	forward	No	2nd Intron
DC3 factor 1	279	285	7	reverse	No	2nd Intron
DOF2-like	329	339	11	reverse	No	2nd Intron
miR414, partial	405	425	21	reverse	Partial	3rd Exon
HOX2a-like	479	485	7	reverse	Yes	3rd Exon
HOX2a-like	498	504	7	reverse	Yes	3rd Exon
KNOX-like	516	527	12	forward	Yes	3rd Exon
MYB core	524	528	5	reverse	Yes	3rd Exon
W-box in NPR1	580	584	5	forward	Yes	3rd Exon
ARR10	584	591	8	reverse	No	3' UTR
DOF2 zinc finger	595	606	12	reverse	No	3' UTR
AtHB-1 site	600	613	14	none	No	3' UTR
DOF2 zinc finger	630	640	11	reverse	Yes	3' UTR
GT1 trihelix-like	641	652	12	reverse	No	3' UTR
MYB4	683	689	7	reverse	No	3' UTR
AG	684	688	5	reverse	No	3' UTR
ARR10	719	726	8	forward	Yes	3' UTR
MYB4	732	738	7	reverse	Yes	3' UTR
ARR10	754	761	8	forward	No	3' enhancer
ARR10	774	781	8	reverse	No	3' enhancer
DC3	886	892	7	forward	No	3' enhancer
AP2/ERF-like	907	915	9	forward	Partial	3' enhancer
CRM1	912	1,034	123	none	Partial	CRM1
MYB core	913	917	5	reverse	Yes	CRM1
W-box in NPR1	946	950	5	reverse	Yes	CRM1
AtHB1	957	966	10	none	Yes	CRM1
WUS 970	957	964	8	none	Yes	CRM1

Annotation	Minimum	Maximum	Length	Direction	Footprint	Location
WUS 997	981	984	4	none	Yes	CRM1
Opaque-2	1,018	1,027	10	forward	Yes	CRM1
ALFIN1 HD-like	1,021	1,030	10	forward	Yes	3' enhancer
Sugar RE	1,034	1,039	6	reverse	No	3' enhancer
Bellringer	1,038	1,045	8	forward	No	3' enhancer
W-box in NPR1	1,078	1,082	5	reverse	Yes	3' enhancer
CRM2	1,106	1,240	135	none	Partial	3' enhancer
At2TE50665	1114	2098	985	Forward	Partial	CRM2/3
YPF1	1,119	1,127	9	forward	Partial	3' enhancer
ARR10	1,167	1,174	8	forward	No	3' enhancer
Evening Element	1,167	1,175	9	reverse	No	3' enhancer
GA response	1,206	1,212	7	forward	Yes	CRM2
MYB4	1,207	1,213	7	forward	Yes	CRM2
ATHB-2	1,221	1,229	9	reverse	Yes	CRM2
HAT4	1,221	1,229	9	none	Yes	CRM2
Sugar RE	1,227	1,232	6	forward	Yes	CRM2
AG	1,241	1,246	6	forward	Yes	CRM2
CRM3	1,241	1,369	129	none	Partial	CRM2
ARR10	1,242	1,249	8	reverse	Yes	CRM2
ARR1	1,245	1,249	5	reverse	Yes	CRM2
DOF-bZIP	1,284	1,296	13	none	Yes	CRM3
DC3	1,288	1,294	7	forward	Yes	CRM3
KNOX-like	1,295	1,307	13	forward	Yes	CRM3
DC3	1,302	1,308	7	forward	Yes	CRM3
DOF-bZIP	1,317	1,336	20	none	Yes	CRM3
right part of RHE	1,318	1,323	6	forward	Yes	CRM3
ASF-1	1,321	1,325	5	reverse	Yes	CRM3
Sugar RE	1,359	1,364	6	forward	Yes	CRM3
AtHB1	1,363	1,372	10	none	Partial	CRM3
Opaque-2	1,371	1,380	10	none	No	3' enhancer
AtHB1	1,458	1,467	10	none	Partial	3' enhancer
W-box in NPR1	1,512	1,516	5	forward	No	3' enhancer
Bellringer	1,600	1,607	8	reverse	No	3' enhancer
SBF site	1,719	1,728	10	none	No	3' enhancer
Bellringer	1,738	1,745	8	forward	No	3' enhancer
AG	1,762	1,767	6	forward	No	3' enhancer
AtHB5	1,781	1,788	8	reverse	No	3' enhancer
miR414, partial	1,785	1,805	21	none	No	3' enhancer
At2TE50670	1786	2049	264	Reverse	No	3’ enhancer
SEF4	1,804	1,812	9	forward	No	3' enhancer
ARR2-like	1,812	1,821	10	forward	No	3' enhancer

Annotation	Minimum	Maximum	Length	Direction	Footprint	Location
miR414, partial	1,823	1,854	32	none	No	3' enhancer
miR414, partial	2019	2055	37	none	No	3' enhancer

Table 2.2. **Fifty-one genes co-expressed with CLV3 in *A. thaliana.*** *G*enes were selected from a flow-cytometry data set[9] and filtered by relative transcript levels such that $CZ \geq 4(RM)$.

Gene #	Locus	Gene #	Locus	Gene #	Locus
1	At1g07890	21	At3g08580	41	At5g13000
2	At1g09070	22	At3g08770	42	At5g13930
3	At1g11910	23	At3g09630	43	At5g48480
4	At1g15690	24	At3g17160	44	At5g52470
5	At1g18080	25	At3g20670	45	At5g57560
6	At1g26630	26	At3g45980	46	At5g59820
7	At1g27770	27	At3g56880	47	At5g59870
8	At1g28290	28	At3g58610	48	At5g59910
9	At1g48410	29	At4g03210	49	At5g64310
10	At1g48630	30	At4g08950	50	At5g64400
11	At1g56070	31	At4g09320	51	At5g00470
12	At1g78380	32	At4g12720		
13	At2g05790	33	At4g13940		
14	At2g23120	34	At4g24570		
15	At2g23810	35	At4g26840		
16	At2g26330	36	At4g29030		
17	At2g27040	37	At4g29780		
18	At2g36530	38	At5g02500		
19	At2g41100	39	At5g09810		
20	At2g41430	40	At5g11740		

Table 2.3. CRM2 and CRM3 Functional assessment. Blast search results used to identify similar motifs elsewhere in the *A. thaliana* genome, and the expression pattern of adjacent genes were estimated using the eFP Browser [86].

Blast probe: TAATTATTATCCTTAATGATACCAAATCTATATGATACGATA

Locus	Gene ID	Sequence match	Estimated expression pattern
At2g27250	CLV3	100%	SAM in CZ, lateral root cap, root procambium
At2g27240	Malate transporter	100%	Lateral root cap, root procambium
At2g33230	YUCCA7	CCAAATCTATATGAT	Root cap columella
At2g23320	WRKY15	GATACCAAATCTAT	Base of root cap columella
At2g36090	F-box protein	AAATCTATATGATA	Root Procambium
At2g37900	Unknown	AAATCTATATGATA	Root Procambium, shoot phloem
At2g19830	SNF7.2	TAATGATACCAAAT	Root Procambium
At4g30080	ARF16	AATGATACCAAATCTA	Lateral root cap, base of root cap columella
At2g29400	PP1.1	ATTATTATCCTTAAT	SAM excluding the CZ, abaxial leaf epidermis
At2g15960	Unknown	ATTATCCTTAATGAT	Leaf mesophyll
At2g02070	IDD5	ATTATCCTTAATGAT	Carpel, lateral root cap, root endodermal initials
At2g15930	Unknown	ATTATCCTTAATGAT	Pollen
At2g29390	AtSMO2-2	ATTATTATCCTTAAT	Leaf epidermis, pollen, root cortex

Table 2.3 continued. CRM2 and CRM3 Functional assessment, continued.

Blast probe: AGATGTGACACTGGCGATTTCGCTCACGTCAC

Locus	Gene ID	Sequence match	Estimated expression pattern
At2g27250	CLV3	100%	SAM in CZ, lateral root cap, root procambium
At2g27240	Malate transporter	100%	Lateral root cap, root procambium
At2g05140	Phosphoribosyl-aminoimidazole carboxylase family	ACTGGCGATTTCG	SAM, root cortex initials
At2g05160	CCCH-type zinc finger	ACTGGCGATTTCG	Root epidermis, pollen
At2g36790	UGT73C6	TGGCGATTTCGCT	Lateral root cap
At2g03150	RSA1	TTTCGCTCACGT	Root epidermis initiation zone
At2g05294	unknown	CTGGCGATTTCG	Root cap,nearly homogenous
At2g17060	unknown	CACTGGCGATTT	Lateral root cap, root procambium
At2g21140	PRP2	CTGGCGATTTCG	Lateral root cap, root procambium, stem epidermis
At2g28110	IRX7	ATTTCGCTCACG	Root xylem
At2g30010	TBL45	CTGGCGATTTCG	Root protophloem, stem epidermis
At2g30020	AP2C1	CTGGCGATTTCG	SAM, base of root cap columella
At2g33860	ARF3	TGGCGATTTCGC	Lateral root cap

Table 2.4. List of primers used for deletions.

Name	Sequence
1.0 Forward	ATAATTTAAGCATATAACTGTTTCCAGATT
1.0 Reverse	CGATATCAAGCTTATCGATACCGTCG
2.0 Forward	TGTTAGACTTAGGAATTAATTA
2.0 Reverse	ATTGAACAATATGGATGATACCTTAATCGG
3.0 Forward	ATCCACAATGGCGAAGGCAG
3.0 Reverse	TGCTGTGGAGGTTCACAACTAATAC
3.1 Forward	TTAATAACTACGATACACGTTTAGG
4.0 Forward	CAAAGACAACCATTTGTAGTCACTATTTCT
4.0 Reverse	GCGGCCGCTCTAGAACTAGTGG
5.0 Forward	GAGCTCCAGCTTTTGTTCCCTTTAG
5.0 Reverse	ACACTGACACTGCCTGTCACTG
5.1 Reverse	CATTAAGGATAATAATTAGCTCTAGGTTTG
5.2 Reverse	CTTAAAATTATACTTAGAATTAATGGATAAAGGC

Figure 2.7. Map of pCLV3m:H2B-YFP used for deletions. This sequence also contains three mutated WUS binding sites, as previously described [20].

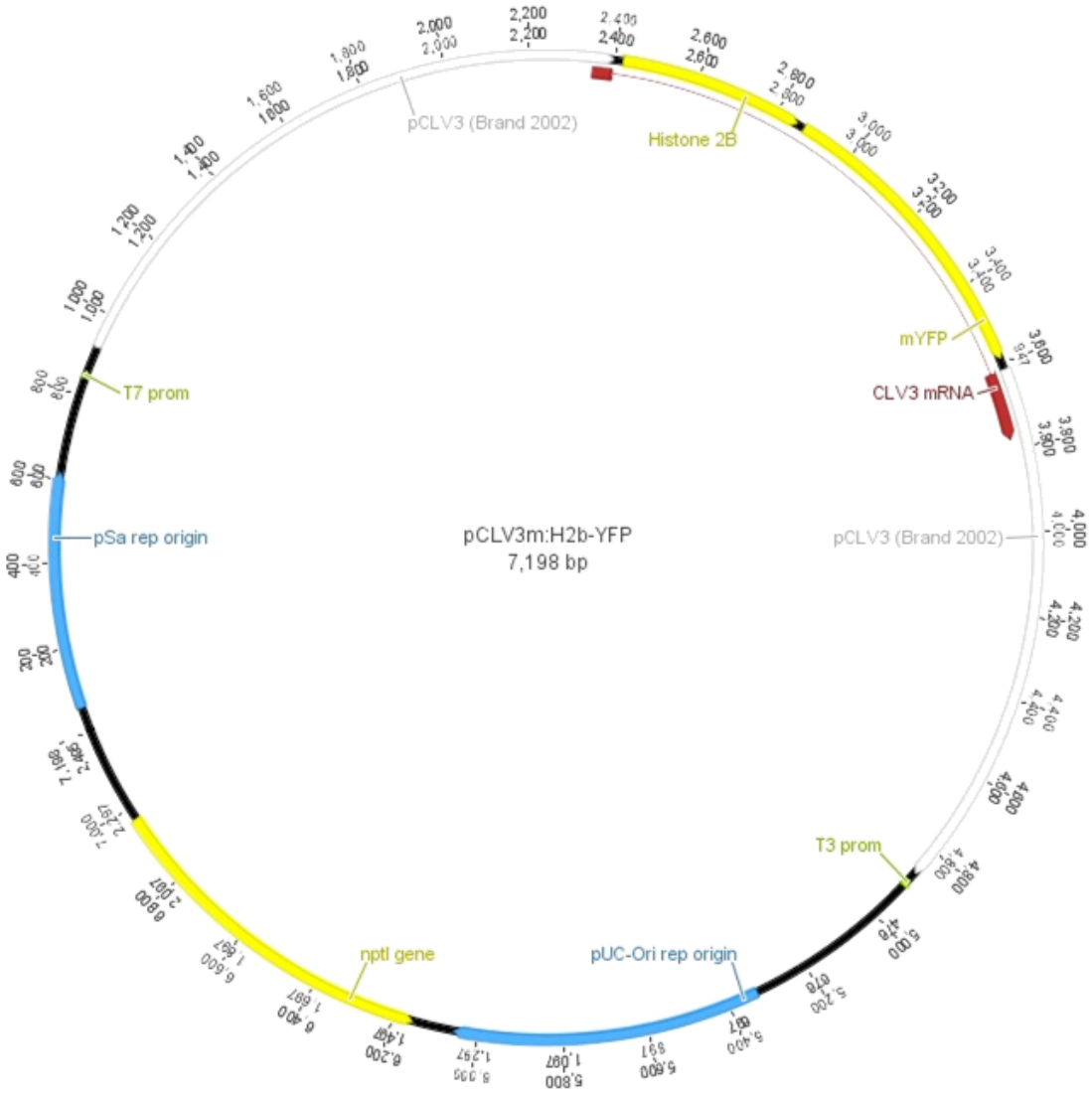

Chapter 3 WUS and cytokinin hormone interactions

Introduction

Plant growth is heavily dependent on the continuous function of the SAM. In order to maintain the dynamic structure of the SAM, a feedback loop between WUSCHEL (WUS) and CLAVATA3 (CLV3) has been proposed to be an integral part of meristem maintenance [22, 29]. Research over the past decade has successfully clarified many aspects of this model by identifying some of the intermediate steps between *CLV3* transcription, perception and signal transduction pathways, though it is not yet known how this controls *WUS* transcriptional repression. In contrast, studies of WUS regulated genes have identified several hundred candidates [30, 42], and have shown that WUS binding to *CLV3* regulatory sequences is necessary for *CLV3* expression [20].

However, there is an increasing amount of evidence to suggest that this feedback loop is at least partially influenced by hormone signaling pathways. One of the most striking examples of this occurs in rice, where cytokinin biosynthesis mutants produce a flower phenotype that is almost identical to the *wus-1* mutant phenotype in *A. thaliana* [12]. A more direct route of cross-talk was found through microarray experiments, which found that WUS repressed *ARABIDOPSIS RESPONSE REGULATOR7* (*ARR7)* and *ARR15* [30], both of which are negative regulators of the cytokinin response pathway [129]. This interaction is fully consistent with the strong pattern of cytokinin responses that occurs in the RM [6], and suggests that this pattern might be a result of WUS repression of a repressor, leading to activation. In addition, exogenous cytokinin treatments can increase *WUS* transcript levels [31, 32], and *WUS* transcripts are increased when cytokinin catabolism is reduced in *ckx3/ckx5* double mutant [130]. Similar positive correlations have also been found in callus tissues [5, 35] and in microarray studies [33]. More directly, WUS has even

been found to activate *ARR1* transcription, a positive regulator of cytokinin responses [11], which in turn might explain why both *WUS* and *ARR15* are simultaneously up regulated in SAM regeneration studies [36]. However, this interpretation is somewhat inconsistent with the expression pattern of *ARR7* and *ARR15*, which have been found to strongly overlap with the RM in numerous studies [18, 30, 33, 131, 132]. How this is possible in a tissue that also expresses their direct negative regulator indicates that this system is not well understood.

Auxins are involved in the WUS-CLV3 feedback loop, as this hormone has repeatedly been found to reduce WUS transcript levels [133-135]. There also appears to be a tight correlation between the auxin transporter PIN1 and WUS induction during somatic embyogenesis [5, 38], while mutation alleles of the auxin-sensitive *POPCORN* gene are known to disrupt *WUS* expression patterns [136]. This relationship is perhaps most strongly supported by studies in root meristems, where the closely related *WOX5* gene is known to participate in a complex feedback loop involving auxin biosynthesis with YUCCA6, auxin signal transduction with IAA17, auxin efflux with PIN1, and auxin influx with LAX3 carriers [34, 115]. In SAM tissues, the close juxtaposition of *WUS* and the *YUC4* biosynthesis domain in the overlying CZ [5] is also at least reminiscent of the activation of *YUC1* by pWOX5:WOX-GR in the root meristemss [34].

The work presented in this chapter is thus an attempt to narrow down the most likely mechanism that cytokinin uses to affect WUS transcription, translation, and protein distribution. Surprisingly, the results found that elevated levels of cytokinin did not directly affect *WUS* transcription, nuclear localization, or stability, nor did cytokinin have any significant effect on *CLV3*, eliminating a possible indirect mechanism. Instead, a novel absence of cytokinin response was identified in the CZ, and evidence suggests that this zone is maintained both by the lack of transcription, and by an unknown repressive mechanism that can affect B-type ARR proteins.

Cytokinin responses were also correlated with WUS protein stability, starting roughly 12 hours after exogenous treatment. Auxin however, dramatically reduced WUS protein levels within just 4 hours, suggesting that this hormone has a more direct effect on protein stability. This suggests a model where auxin responses in the CZ and PZ cells stimulate protein degradation pathways that confine WUS proteins to the RM, where cytokinin responses may favor protein stability.

Results

CZ tissue does not respond to cytokinin

In order to identify which part of the WUS-CLV3 feedback loop is affected by cytokinin responses, this work began by crossing the pTCSn1:mGFP5-ER reporter [6] was crossed into *wus-1* and *clv3-2* mutant backgrounds. In untreated plants, both *clv3-2* and WT meristems were found to have strong cytokinin responses in the RM, with a faint fluorescent signal extending deep into the pith and provascular tissue (Figure 3.1). The *wus-1* mutant was similar, though its fluorescent signal did not become faint in the deeper tissue layers, presumably because this mutant meristem did not produce pith or provascular tissue. Treatment with exogenous 6-benzylaminopurine (6-bap) for 24 hours did not change the location of the cytokinin response in WT meristems, or in the meristems of either mutant. Instead, the strength of the fluorescent signal was more than tripled in all three backgrounds, suggesting that endogenous cytokinin response mechanism is able to function over a wide range of concentrations. The enhanced signal was most easily detected in the weakly fluorescent pith cells, but interestingly, the immature leaves, young anlagen, and the apex of the SAM all failed to produce any fluorescent response at all. In both WT and *clv3-2* mutants, the absence of cytokinin responses occurred in a circular patch at the apex of the Central Zone and extended two cell layers deep. In *wus-1* homozygous

mutants, a similar response-free zone was found to be variable, but was detected in 84% of sectioned meristems, and extended only one cell layer deep (Figure 3.1).

The near-complete lack of cytokinin responses in the CZ was unexpected, though presence of this function indicates a previously unrecognized feature of meristem organization involving two opposite and adjacent cytokinin response fields. As exogenous cytokinin applications were not able to induce pTCSn1:mGFP5-ER expression in the response-free zone to any significant degree, the two-component system pCLV3:GR-LhG4 x p6xOP:ARR1ΔDDK-GR [11] was used to ectopically stimulate cytokinin responses specifically in the CZ tissue. As previously described, the ARR1ΔDDK-GR construct is a modified version of *ARABIDOPSIS RESPONSE REGULATOR 1* (*ARR1*), which activates cytokinin response genes following exposure to dexamethasone [137]. Plants containing both constructs were then crossed to three different lines containing the fluorescent reporters: pTCSn1:mGFP5-ER, pCLV3:mGFP5-ER, and pWUS:eGFP-WUS.

Surprisingly, when observed over a 48 hour time course of dexamethasone treatment, the pTCSn1:mGFP5-ER reporter did not immediately occur in the middle of the CZ as expected. For comparison, the pCLV3:mGFP5-ER reporter uses an identical promoter, indicating that the induced cytokinin response should occur in a pattern similar to the middle row in Figure 3.2. Instead, the pTCSn1:mGFP5-ER signal first appeared at the extreme edges of the peripheral zone, where it progressively appeared in adjacent cells in a centripetal manner, slowly constricting the cytokinin response-free zone until it disappeared between 24 and 48 hours later. The centripetal pattern was visible in both L1 and L2 cells, though the L2 signal was weaker and lagged behind the L1 by 1-3 cell diameters. By 48 hours, the response-free zone was completely lost, and pTCSn1:mGFP5-ER expression become nearly homogenous throughout the SAM.

The pCLV3:mGFP5-ER reporter in contrast, was expressed in the apical pattern as expected for the *CLV3* promoter. The fluorescent pattern occurred in conical patch of cells at the apex of the SAM, and extended up to four cells deep. The fluorescence levels were mostly uniform, though the L2 frequently had significantly less expression than the other layers. The expression pattern was already fully formed in the absence of dexamethasone treatment, and remained unchanged through at least 24 hours. The fluorescent pattern became broader in proportion to the size of the meristem at 48 hours, but the longitudinal pattern did not significantly change. Deep inside the SAM tissues however, a faint pCLV3:mGFP5-ER signal could be detected, which produced a central hourglass-shaped column more than 20 cell layers deep. This column was surrounded on

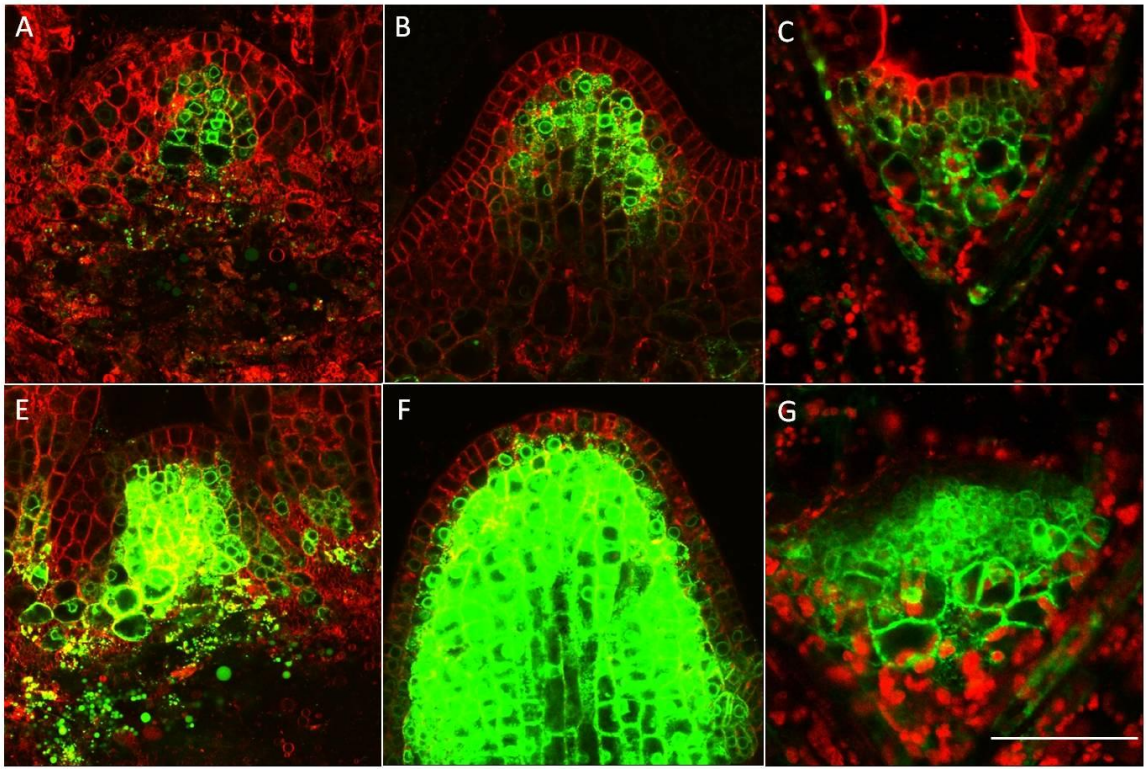

Figure 3.1. Longitudinal section of WUS and CLV3 mutant SAM'scontaining the pTCSn1:mGFP5-ER cytokinin response reporter. Top row = Mock treated, bottom row = 24 hour treatment with 6-benzylaminopurine. A,F =Wt L*er*. B,E =*clv3-2* mutant C,F = *wus-1*mutant. Scale bar = 50 μM.

either side by elongate elliptical voids that had little or no detectable fluorescence.

At the beginning of the time course, the pWUS:eGFP-WUS reporter produced a nuclear-localized pattern centered on the RM, with a radial concentration gradient spreading into all adjacent cells as expected. This pattern did not change after 6 hours of dexamethasone treatment, but by 12 hours a subtle increase in the number of cells displaying the pWUS:eGFP-WUS fluorescent reporter was apparent. The number of small meristem-like cells also began to increase over time, accumulating in a rootward direction at a rate directly proportional to the loss of the underlying large pith cells. The pWUS:eGFP-WUS expression pattern followed the downward appearance of the new cells, eventually producing a brightly visible fluorescent column extending more than 20 cells deep. Elongate voids with no fluorescence were visible on either side, similar to the faint column produced by pCLV3:mGFP5-ER.

Interestingly, long term ectopic induction of the pCLV3:GR-LhG4 x p6xOP:ARR1ΔDDK-GR system did not significantly change the volume of the SAM over the first 24 hours, but by 48 hours the SAM volume had quadrupled. This exponential growth pattern continued in plants subjected to prolonged 120 hour treatments, eventually producing a spherically swollen SAMs 1-2mm in diameter, with frequent superficial cracks (data not shown). Curiously, while the change in cell proliferation appeared to be abrupt in the pTCSn1:mGFP5-ER and pCLV3:mGFP5-ER reporter backgrounds, the proliferation rate in the pWUS:eGFP-WUS background was more gradual, beginning at least 12 hours earlier than in the other two lines. This precocious behavior may be related to the concentration of WUS proteins in this line, as the presence of the pWUS:eGFP-WUS construct can complement *wus-1* mutants[20], and likely double doubles the concentration of WUS proteins in the presence of the WT copy of WUS.

While CLV3 does not appear to induce or respond to cytokinin to any significant extent, WUS proteins displayed a more complicated pattern as shown by pWUS:eGFP-WUS reporter in Figure 3.4: Part of the WUS pattern overlaps with the cytokinin-response-free zone, and typically no WUS was found in either the deep RM or the PZ, where cytokinin responses were clearly present at comparable time points. The failure of WUS to activate cytokinin responses in the CZ is somewhat surprising, as 24 hours of exogenous 6-bap treatment moderately increased pWUS:eGFP-WUS fluorescent levels in both WT and *clv3-2* mutant backgrounds (Figure 3.3). On the other hand, if cytokinin is required to activate WUS transcription, the presence of WUS

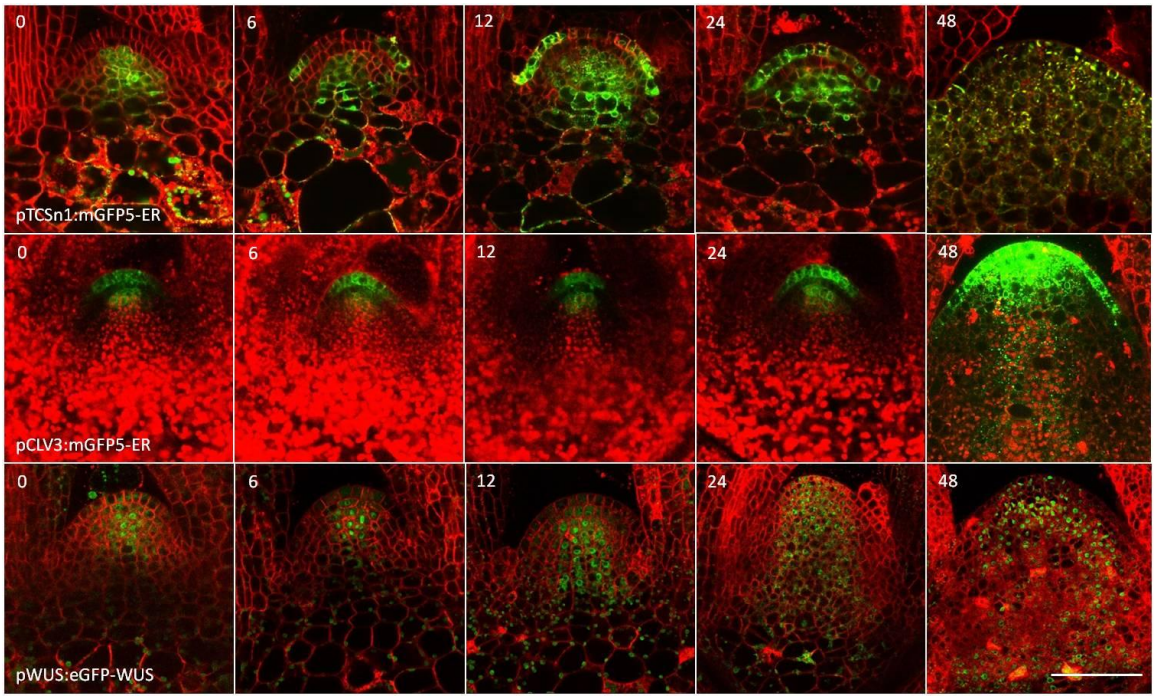

Figure 3.2. **Time course of ectopic cytokinin response activation in the CZ.** Longitudinal sections of seven day old pCLV3:GR-LhG4 x p6xOP: ARR1ΔDDK-GR seedlings, with the fluorescent reporters shown in green. The hours of dexamethasone treatments are indicated. The 48hour pCLV3:mGFP5-ER signal was enhanced to make the faint expression pattern more visible. The granular signal seen in the large pith cells below the SAM in pWUS:eGFP-WUS reporter correlates to the chloroplasts, which are still green in 7 day old seedlings. Scale bar = 50 μm.

expression in tissues that lack a clear cytokinin response is equally difficult to explain.

When cytokinin responses are eliminated with the cytokinin receptor triple mutant *ahk2/3/4*, only trace amounts of pWUS:eGFP-WUS fluorescent signal could be detected in seven day old plants. The lack of cytokinin responses was further confirmed by treating pWUS:eGFP-WUS x *ahk2/3/4* plants with exogenous 6-bap, which did not significantly change the fluorescent pattern (Figure 3.3). However, the *ahk2/3/4* mutant was quite variable, as 74% of examined SAM tissues displayed no fluorescence, while the remaining 26% ranged from faint GFP patterns to nearly full WT-like patterns (n = 19).

To deplete native cytokinin in WT meristems without the physical defects of the *ahk2/3/4* mutant, the dex-inducible construct p35S:GR-LhG4::p6xOP:CKX3 was used to over-expresses CYTOKININ OXIDASE 3 (CKX3), which degrades native cytokinin molecules [11]. Following 24 hours of dexamethasone treatment in this background, the pCLV3:mGFP5-ER reporter showed no significant change in expression (Figure 3.3). Parallel attempts to study pWUS:eGFP-WUS in the p35S:GR-LhG4::p6xOP:CKX3 background produced extremely variable results during the first 24 hours, ranging from the complete absence of fluorescent signal, to near-WT patterns, but became consistent by 48 hours of dex treatment.

WUS transcription is independent of the Cytokinin response

When *WUS* transcription was checked with RT-PCR however, both WT and *ahk2/3/4* mutants background were found to have detectable WUS transcription localized to the RM (Figure 3.4). The expression pattern of *WUS* also largely unchanged in *ahk2/3/4* mutant RNA in-situ's, suggesting that cyokinin responses primarily affect WUS protein. Further RNA in-situ's following the time course treatment of the pCLV3:GR-LhG4 x p6xOP:ARR1ΔDDK-GR system found that cytokinin did not significantly increase WUS transcription in the CZ cells (Figure 3.4).

This indicates that the pWUS:eGFP-WUS fluorescence observed in CZ cells is a product of protein movement, not local transcription. The RNA in-situ's further revealed that WUS transcription patterns also expanded in a rootward direction, similar to the pWUS:EGFP-WUS pattern shown in Figure 3.2. By 48 hours, WUS expression was clearly found throughout the entire volume of the enlarged RM, with the exception of L1 and L2, which had little or no WUS transcripts. In many cases, large elliptical voids appeared in the peripheral zone, which corresponded to the presence of lateral anlagen. When two voids were present simultaneously (Figure 3.4), the central RNA expression pattern is reminiscent of the central column displayed by the pWUS:eGFP-WUS reporter in Figure 3.2. Though WUS is known to be non-cell autonomous, the close correlation between RNA and GFP patterns suggests that WUS proteins has a short mobile range, here estimated at 3 cell diameters.

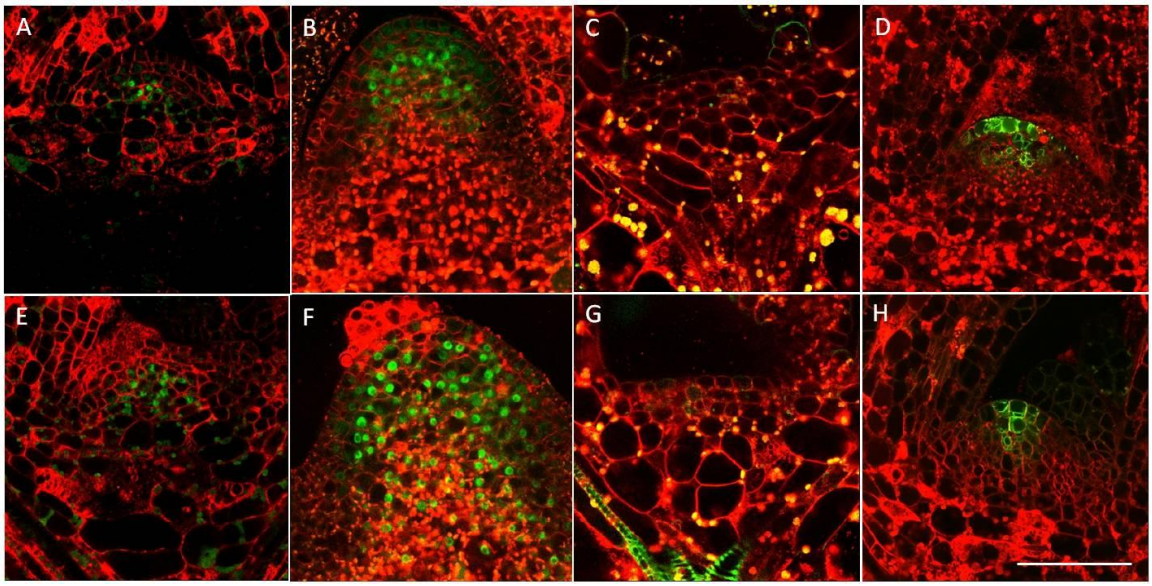

Figure 3.3. Response to altered cytokinin concentration. Top row= Mock treated, Bottom row= 24 hour treatments. E,F,G cytokinin treated, H dexamethasone treated. **(A,E)** = pWUS:eGFP-WUS in Ler WT. **(B,F)** = pWUS:eGFP-WUS in *clv3-2* mutant background. **(C,G)** = pWUS:eGFP-WUS in *ahk2/3/4* mutant background. **(D,H)** = p35S:GR-LhG4::p6xOP:CKX3 x pCLV3:mGFP5-ER. Scale bar = 50 μm.

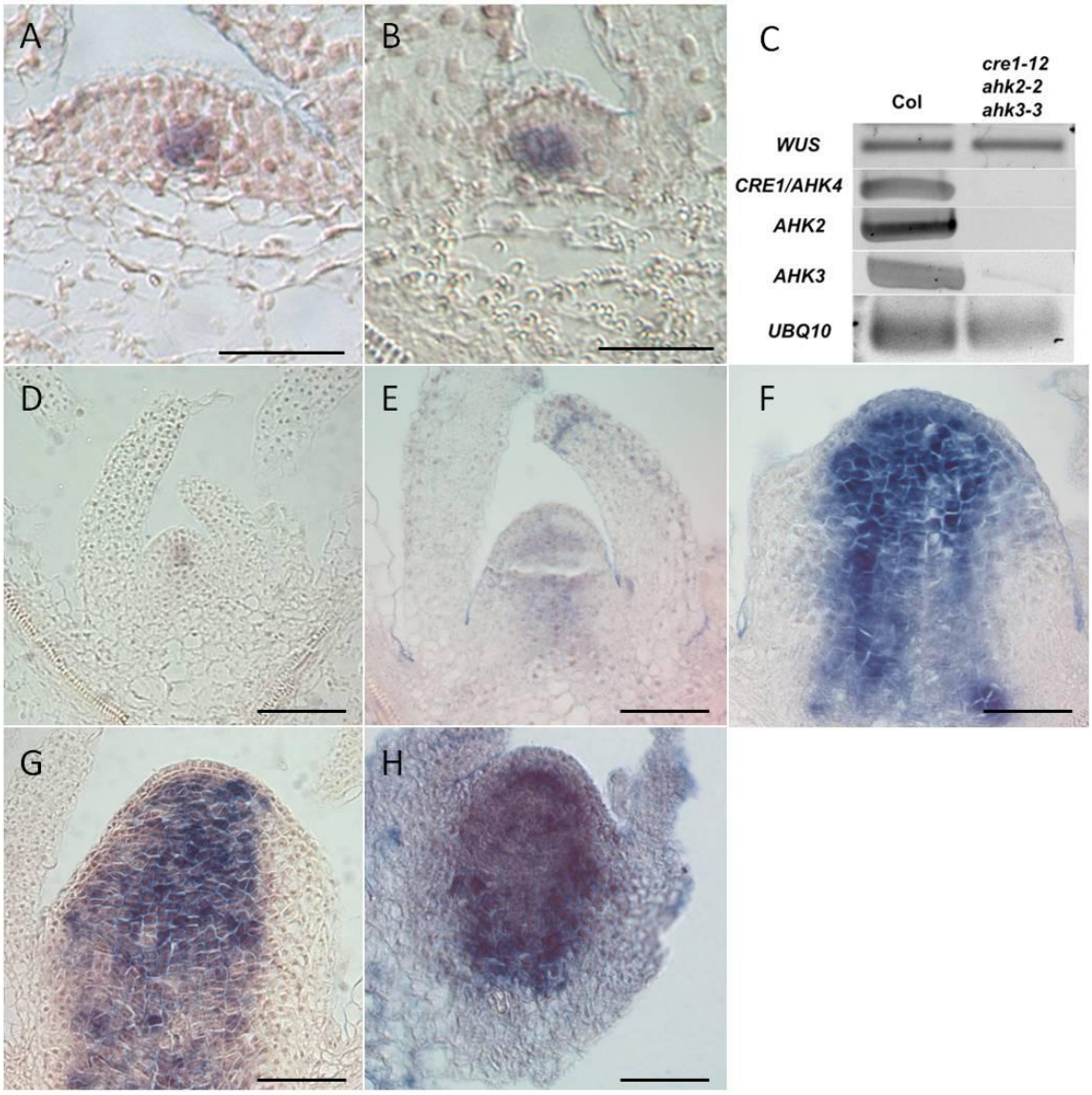

Figure 3.4 WUS transcript patterns in response to cytokinin levels. A-C cytokinin reduction in the *ahk2/3/4* triple mutant, data provided courtesy of Kaori Miyawaki. D-F = time course of cytokinin activation with the pCLV3:GR-LhG4 x p6xOP: ARR1ΔDDK-GR two component system. (**A**) WT Col-0 plant. (**B**) *ahk2/3/4* triple mutant. (**C**) RT-PCR showing WUS transcripts in both WT and the *ahk2/3/4* triple mutant. (**D**) 0 hours (**E**) 24 hours (**F**) 48 hours with two marginal voids. (**G**) 48 hours with one marginal void, (**H**) 48 hours with 0 marginal voids. Scale bars = 50 μM.

Cytokinin affects WUS protein distribution

Previous research has shown that the non-cell autonomous movement of WUS protein does not have tissue-specific patterns [21], suggesting that the plasmodesmata are unlikely targets of cytokinin regulation. In order to explore other possible means of protein movement regulation, this study began by performing hand-cut longitudinal sections of pWUS:eGFP-WUS plants, providing an un-biased view of the WUS concentration profile in the deeper layers of the SAM, thereby avoiding the loss of signal associated with tissue depth. Special care was taken to avoid saturating the pWUS:eGFP-WUS reporter during imaging, so that semi-quantitative analysis might reveal subtle patterns (see methods).

In untreated plants, the pWUS:eGFP-WUS reporter revealed a nearly symmetrical concentration profile, with a triangular peak centered on the RM, tapering off over 3-4 cell diameters (Figure 3.5). The location of the peak varied between L3-L5 in different sections, which likely reflects error introduced by tangential or oblique cuts. Above the peak, the fluorescent gradient was strongly linear, tapering to near undetectable levels in L1 cells. In the deep meristem tissues, the rootward gradient was equally linear and symmetric for the first 2-3 cell diameters, but then began to flatten out into a low but relatively constant background signal. It is not clear how much of the deep-layer signal reflects the presence of WUS, as the pWUS-eGFP-WUS reporter did not display its characteristic nuclear-localized pattern in these cells. Instead, the fluorescent signal largely co-localized with the developing chloroplasts in deepest cells layers, suggesting that this background signal is at least partially derived from chlorophyll auto-fluorescent noise. However, no such noise can be detected in the absence of pWUS-eGFP-WUS, or when histone or ER-tagged fluorescent proteins are used (data not shown), strongly implying that this background signal reflects the actual WUS protein distribution. When pWUS:eGFP-WUS plants were treated

with exogenous 6-bap for 48 hours, no significant changes were observed in the upper gradient (L1-L3), either in the slope or in the total fluorescent concentration. The signal started to diverge by L4 however, where fluorescent signal became as much as 2x brighter down through at least L10 (Figure 3.5).

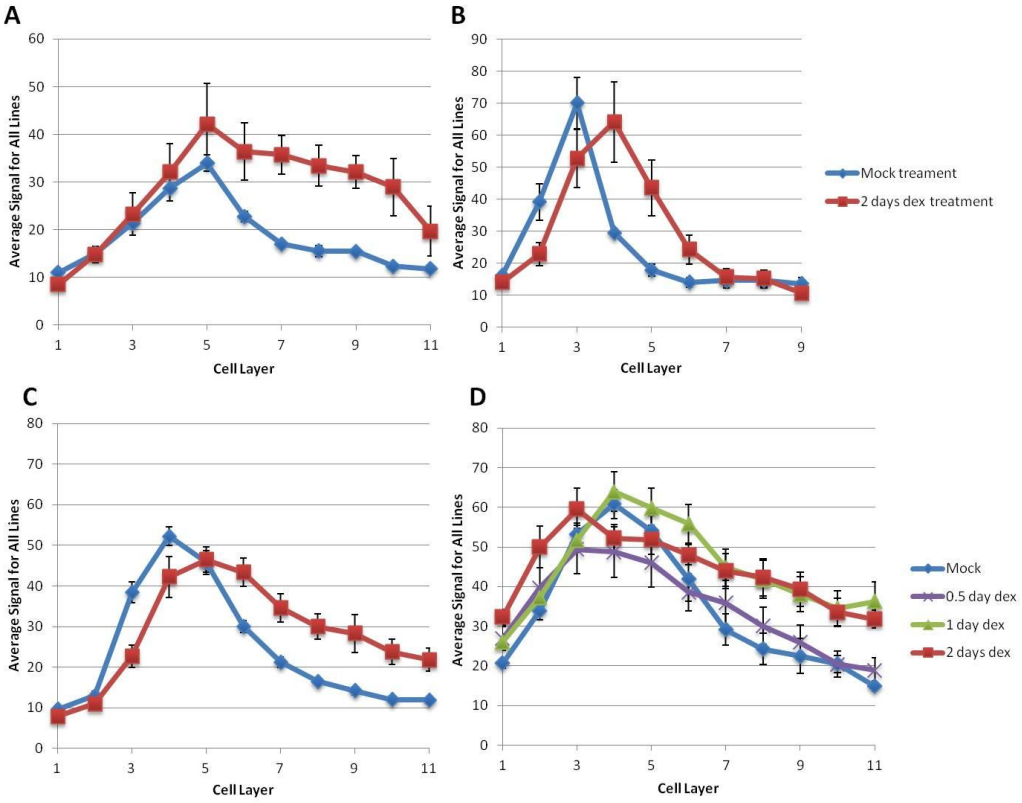

Figure 3.5. Semi-quantitative analysis of WUS protein distribution. Average fluorescent units are calculated on a layer by layer basis, measured along the median longitudinal axis of the SAM (see methods). The longitudinal axis is here shown horizontally, with the SAM apex on the left, and the roots towards the right. A, C were treated with 6-benzylaminopurine, B,D were treated with dexamethasone. A,B,D = pWUS:eGFP-WUS reporter. **(A)** Wt Ler plant **(B)** p35S:GR-LhG4::p6xOP:CKX3 **(C)** WT Ler with a modified nuclear-localized reporter pWUS:NLS-eGFP-WUS **(D)** pCLV3:GR-LhG4 x p6xOP:ARR1ΔDDK-GR time course over 48 hours. Standard error bars shown. N=4 meristems/treatment.

When cytokinin responses were ectopically induced in the pCLV3:GR-LhG4 x p6xOP: ARR1ΔDDK-GR background, the pWUS:eGFP-WUS reporter produced patterns very similar to the exogenous cytokinin treatments. The upper gradient remained unchanged, while the deeper cell layers starting at roughly L5 doubled their fluorescent signal. A time-course analysis further revealed that the deep-meristem signal began to appear after 12 hours, and was fully formed by 24 hours. Interestingly, by 48 hours the gradient in L1-L3 cells suddenly increased their fluorescent amplitude by 140%, yet the slope of the gradient in these cells remained unchanged.When cytokinin responses were reduced with the p35S:GR-LhG4::p6xOP:CKX3 construct, a slightly different pattern emerged. Rather than increasing the fluorescent signal in the deep cell layers, the entire triangular pattern of pWUS:eGFP-WUS shifted down by one cell layer. This occurred with little or no loss in fluorescent amplitude, though the slope of the upper gradient became slightly shallower in proportion to greater distance separating L1 cells from the new concentration peak.

Cytokinin do not affect WUS nuclear localization patterns

WUS proteins are known to occur in a nuclear localized pattern [17], which suggests involvement with nuclear pore trafficking mechanisms. To determine if cytokinin regulate WUS movements through the nuclear pore, two modified version of the pWUS:eGFP-WUS reporter were obtained, which contained nuclear import and nuclear export sequences tags: pWUS:NLS-eGFP-WUS, which was previously described by [20], and pWUS:eGFP-NES-WUS. If cytokinin favors nuclear import over export, or vice versa, one of these constructs should amplify the nuclear/cytoplasmic distribution of the fluorescent signal, producing a significantly different fluorescent pattern. As seen in Figure 3.6 however, the only significant change produced by 24 hour cytokinin treatments was a doubling of the fluorescent signal, which affected both modified

reporters and the pWUS:eGFP-WUS control alike. Expression of pWUS:NLS-eGFP-WUS was more clearly nuclear localized than pWUS:eGFP-WUS as expected, while pWUS:eGFP-NES-WUS produced very little fluorescent signal under either treatment.

To more accurately estimate the nuclear/cytoplasmic ratio, these resulting confocal images were further analyzed in order to estimate the relative concentration of fluorescent molecules in each subcellular compartment. First the average fluorescent concentration was measured in a portion of each subcellular compartment, and these figures were then multiplied by the volume of the cytoplasm and nucleus, respectively. Nuclei were assumed to be spherical, and their volume was calculated directly from the largest observable diameter. The volume of the whole cell was more difficult to obtain however, as optical sections often only allowed measurements of their length and width, as 3-D optical reconstructions frequently did not include the entire cell volume. Instead, "depth" was estimated using the average of the length and width measurements, reflecting the approximately cubic-rectangular shape of the cells in L1-L3.

However, when compared to presumably more accurate cell volumes measured using a tessellation method [138], the volumes calculated by the present study were on average 2x larger than expected. The present volume estimates did not change significantly when "depth" values were substituted with measurements from unrelated SAM images (data not shown), suggesting that these volume estimates are at least reasonably accurate, even if they lack precision. Curiously, the smallest volumes produced by the tessellation method closely approach the largest nuclear volumes obtained in the present analysis (50μm^3 vs. 39 μm^3, respectively), raising the possibility that this computer-automated method may have occasionally measured nuclei and/or vacuoles instead of entire cells.

Overall, pWUS:NLS-eGFP-WUS plants were found to produce about 15% smaller cells, 15% smaller nuclei, and 15% less total fluorescence when compared to pWUS:eGFP-WUS plants, but otherwise both reporters displayed similar subcellular distribution patterns: The L1 and L2 cells had identical nuclear/cytoplasmic ratios, and these values were independent of the total fluorophore concentration in each cell. In contrast, L3 cells had a distinctly elevated nuclear/cytoplasmic ratio that was on average almost twice as large as the upper two cell layers, and as much as 5x more in a outlier data. All nuclei held 2-4x more fluorescent units than would be expected based on their volume alone, yet counter-intuitively, this was just a small fraction of the total number of fluorescent units within the cell. Instead, the majority of fluorescent units were found in the larger volume of the cytoplasm, though at a lower concentration than what occurs inside the nucleus.

Cytokinin treatments did not significant change the nuclear/cytoplasmic ratios for either reporter, nor were any layer-specific patterns induced by this treatment. The only clear response to cytokinin treatment was a change in nuclear volume, which increased by an average of 154% in all three layers in both backgrounds. The change in nuclear volume apparently occurred at the expense of the cytoplasm, as the total cell volume remained constant (Figure 3.6).

Unexpectedly, the pWUS:NLS-eGFP-WUS reporter was found to have nuclear/cytoplasmic ratios that was essentially identical to those produced by pWUS:eGFP-WUS. This is inconsistent with the idea that the NLS tag drives nuclear import, though analysis of the pWUS:NLS-eGFP-WUS longitudinal gradient did find that protein movements into the L1 and L2 was slightly restricted (Figure 3.6), consistent with NLS trapping it inside the nucleus. However, this data also suggests an interesting paradox, as it implies that nuclear trapping occurs without significant nuclear enrichment.

Cytokinin affect transcription and protein stability of WUS

Another possible way in which cytokinin responses might affect the distribution of WUS protein is by regulating WUS translation and degradation rates. To study this possibility, the pWUS:eGFP-WUS reporter was exposed to the chemical inhibitors cyclohexmide and MG132, blocking protein translation and proteosome-mediated decay, respectively. Following 4 hour treatments with cycloheximide, no significant loss of fluorescence was found. Unexpectedly, the comparable treatment with MG132 led to the rapid loss of the fluorescent signal. When these chemical treatments were supplemented with exogenous 6-benzylaminopurine to boost the cytokinin response above a basal level however, these patterns were completely reversed.

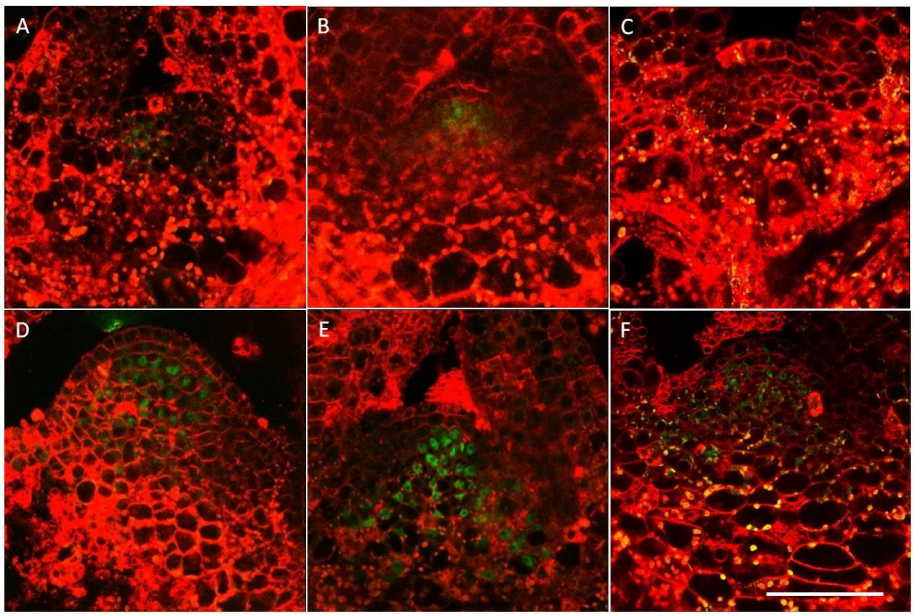

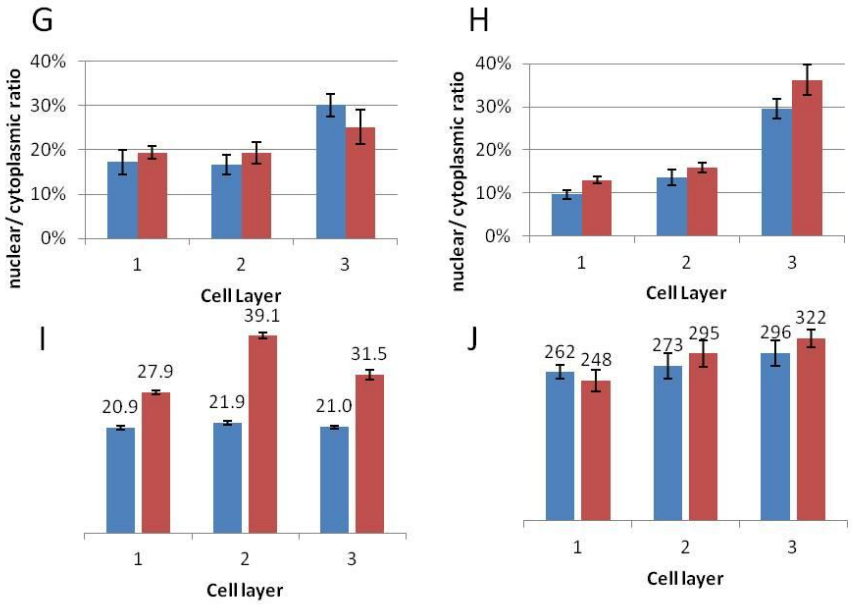

Figure 3.6. The nuclear/cytoplasmic distribution of WUS proteins. A-F longitudinal sections of SAM. Top row = mock treated, Bottom row = 6-benzyladenine treated. G-J Semi-quantitative analysis of subcellular fluorophore concentrations. **(A,D,G,I,J)** pWUS:eGFP-WUS. **(B,E,H)** pWUS:NLS-eGFP-WUS. **(C,F)** pWUS:eGFP-NES-WUS. **(G)** Nuclear/cytoplasmic ratio measured in pWUS:eGFP-WUS **(H)** Nuclear/cytoplasmic ratios measured in pWUS:NLS-eGFP-WUS. **(I)** Nuclear volume (μm^3) of pWUS:eGFP-WUS. **(J)** Total cell volume (μm^3) of pWUS:eGFP-WUS. Blue bars = Mock, Red bars = 24 hour 6-bap treatment. Standard Error bars shown, n = 12 cells/layer, averaged over at least 4 separate meristems. Scale bar = 50µm.

Cycloheximide plus 6-BAP led to the rapid loss of fluorescence, while the loss of signal seen with MG132 became strongly enhanced in the presence of MG132 plus 6-BAP, resembling the enhanced signal seen in 6-BAP treated WT plants (Figure 3.7).

Auxin stimulates WUS degradation

Although the mechanisms that might reduce WUS protein levels are not clearly understood, reports that induced variation in WUS transcript levels suggest an inverse correlation with auxin hormone responses [5, 33]. To test this possibility, a time course of NAA-treated pWUS:eGFP

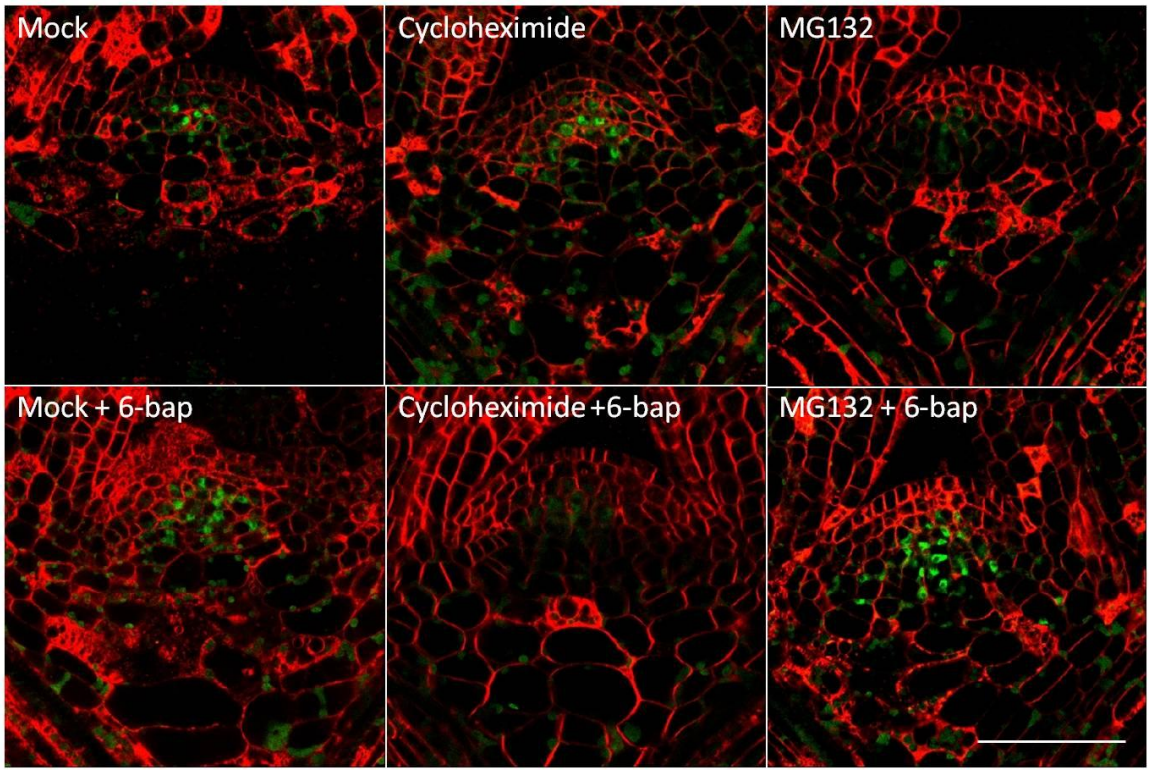

Figure 3.7. Cytokinin influences WUS translational and degradation. Longitudinal sections through the SAM of pWUS:eGFP-WUS seedlings treated for 4 hours as shown. Chloroplast autofluorescence appears as a pale green speckle in the pith tissues. Small, bright red vesicles indicate damage by the sectioning procedure. Scale bar = 50µm.

-WUS plants was performed over a 24 hour time period. The results indicate that the majority of the fluorescent signal is lost within 4 hours, while a faint residual signal persisted at least through 24 hours (Figure 3.8). Chemical treatment with cycloheximide however, was able to prevent the loss of fluorescence caused by the presence of exogenous NAA.

A.

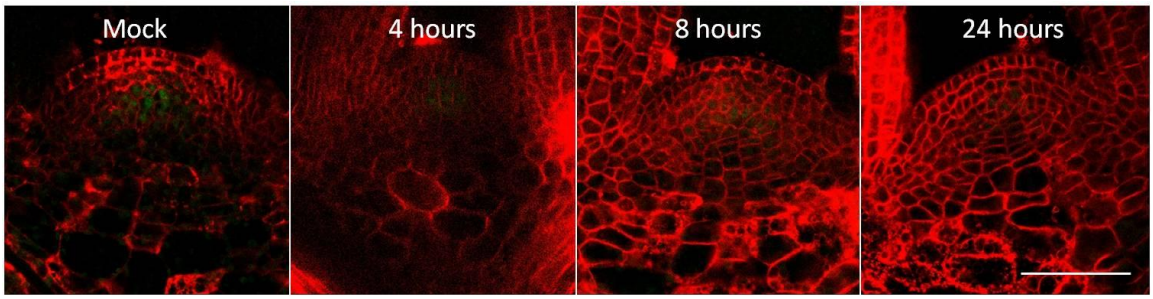

B.

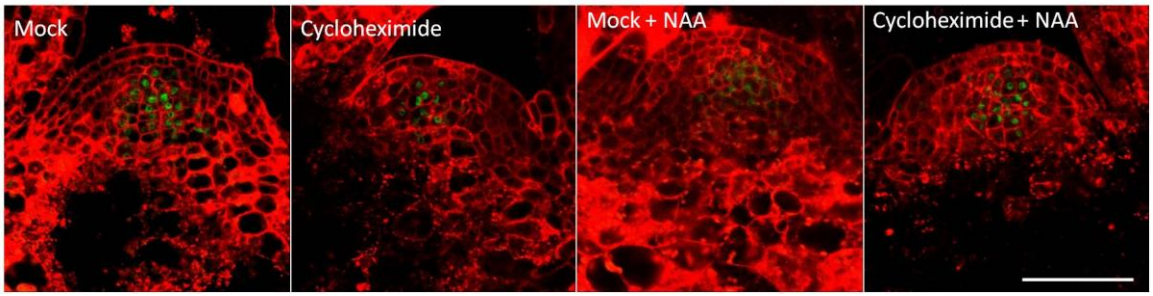

Figure 3.8. Auxin treatment degrades WUS. Longitudinal sections through the SAM of pWUS:eGFP-WUS seedlings. **(A)** Time course of NAA-treated plants. **(B)** Chemical inhibition of translation and degradation. 4 hour treatments are shown. Scale bar = 50µm.

Discussion

The CZ cells contain a potent protein degradation mechanism

The absence of cytokinin responses in the CZ is a novel feature of SAM organization, whose existence was clearly revealed by the distinct absence of pTCSn1:mGFP5-ER expression in response to exogenous cytokinin (Figure 3.1). Although it has been shown that this tissue lacks significant expression of hormone-response genes [9], the centripetal spread of pTCSn1:mGFP5-ER expression following pCLV3:GR-LhG4 x p6xOP: ARR1ΔDDK-GR induction indicates that the absence of a cytokinin response is also accompanied by a repressive mechanism as well. Presumably this mechanism works on a protein level, as the ARR1ΔDDK-GR protein is

unaffected by cytokinin signaling pathways. Given the appearance of cytokinin activity in the peripheral zone of pCLV3:GR-LhG4 x p6xOP: ARR1ΔDDK-GR plants following just 6 hours of dexamethasone treatment, this also argues against a radial degradation gradient, because the ARR1ΔDDK-GR hybrid protein would likely be destroyed before it ever reached the PZ, and degradation alone would likely still allow faint pTCSn1:mGFP5-ER activity in the CZ. Instead, it seems more likely that the ARR1ΔDDK-GR simply can't bind to its DNA target sites, perhaps due to chromatin silencing, which might also explain the lack of hormone signalling pathway expression in these cells. However, a degradation model is consistent with the linear pWUS:eGFP-WUS concentration gradients observed in the L1-L3 tissues, whose slopes were rigidly maintained despite fluctuations in total protein concentrations (Figure 3.5). The present data however, are not sufficient to distinguish between these possibilities,

WUS and the cytokinin-response free zone are independent

The cytokinin-response-free tissue is also unusual in that it seems to exist independently of the WUS-CLV3 feedback loop. While stem cell identity is known to require the migration of WUS proteins into the overlying CZ cells [20, 21], the response-free zone continues to be clearly visible even in *wus-1* mutants. The zone was also present in *clv3-2* mutants, and the lack of response by pCLV3:mGFP5-ER to a variety of different cytokinin treatments strongly suggests that *CLV3* expression is not regulated by cytokinin responses. One possible exception is the reduced expression levels of CLV3 in *ahk2/3/4* plants [139], though the near-absence of WUS proteins in this mutant background might suggest that *CLV3* is simply not strongly activated.

The potential link between cytokinin and WUS transcription is a bit harder to dis-entangle though, as ectopic cytokinin responses produced by the pCLV3:GR-LhG4 x p6xOP: ARR1ΔDDK-GR system did significantly increase the number of WUS-expressing cells, all of

which also had strong cytokinin responses by 48 hours. Close examination of RNA in-situ images however, reveals that WUS is expressed even in the complete absence of cytokinin responses, both in subsets of SAM tissue in the two-component system, and in the *ahk2/3/4* mutant. However, this pattern may be tissue-specific, as the RNA in-situ images also show that WUS is not strongly expressed in the L1 and L2 of the pCLV3:GR-LhG4 x p6xOP: ARR1ΔDDK-GR system, which is true whether or not cytokinin responses occur in those cells. In addition, the pWUS-eGFP-WUS fluorescence level was also largely unchanged when cytokinin levels were reduced with the p35S:GR-LhG4::p6xOP:CKX3 construct. Based on these observations, it seems quite likely that WUS transcription responds directly to cytokinin responses. Although the number of WUS-expressing cells does dramatically increase following prolonged induction of cytokinin responses in the response-free zone, this appears to be a secondary effect that occurs after the cells have acquired stem cell identity.

A model of cytokinin-free zone repression

In the conditions used by the present study, elimination of the cytokinin-response free zone could only be achieved with the pCLV3:GR-LhG4 x p6xOP: ARR1ΔDDK-GR system. This does not rule out a negative regulatory pathway though, as weak pTCSn1:mGFP5-ER expression patterns were found in the L1 and L2 cells of *clv3-2* mutants (Figure 3.1). In addition, the weak expression pattern also produced a gradient from L3 up to L1 cells, which is consistent with non-cell autonomous movement of cytokinin response proteins. Although the present data cannot identify which proteins might be involved, the most likely candidates would be members of the cytokinin signal transduction pathway, including Arabidopsis Histidine Phosphatase (AHP) and ARR family proteins. However, in most cases the movements of these native proteins have not

yet been studied. The sole exception is *ARR7*, which when ectopically expressed in L1 cells, was found to move by at least one cell layer [131].

Presumably, if exogenous cytokinin were applied at high enough concentrations, such non-cell autonomous movement might be sufficient to repress the response-free zone even in WT plants, eventually inducing cell proliferation and WUS expression. Although this experiment was not attempted by the present study, it is interesting to note when extremely high cytokinin concentrations have been used, the SAM has been shown to have higher WUS transcript levels [31, 32]. Exogenous cytokinin applications have even been found to produce a downward expansion of the WUS-expressing cell volume [139], similar to the results of the pCLV3:GR-LhG4 x p6xOP: ARR1ΔDDK-GR system in the present study. Thus it would thus be of interest to determine if the cytokinin-induced increase in WUS transcript levels is due to an increase in the number of cells expressing WUS, or if this reflects an increase in the amount of WUS transcripts per individual cell.

A developmental role for the absence of cytokinin responses?

From a developmental standpoint, the cytokinin-response free zone appears to be required in order suppress cell division in the underlying RM. This is supported by the massive cell proliferation observed following the loss of the response-free zone in induced pCLV3:GR-LhG4 x ARR1ΔDDK-GR plants. While it is tempting to speculate that the response-free zone is needed to produce a downwardly mobile morphogen that stimulates such proliferation, the elimination of the source would likely produce shoot-ward patterns as the morphogen concentration gradient decays, rather than the rootward pattern that is actually observed. Instead, the suppression of both *WUS* and *CLV3* expression around lateral anlagen even after prolonged dexamethasone treatment in the pCLV3:GR-LhG4 x ARR1ΔDDK-GR background suggests that the repressive signal

actually originates in the PZ. As the CZ is known to produce auxin biosynthesis genes CZ [5, 140, 141], and that cytokinin has repeatedly been found to reduce auxin transport [117, 142-145], a likely model suggests that the ectopic cytokinin response in the CZ blocks auxin transport to the PZ. The subsequent failure to activate repressive auxin response factors in the PZ might then favor proliferation over cell elongation.

Cytokinin regulaton of WUS nuclear localization

In a developmental context, nuclear trapping has repeatedly been shown to restrict the movement of transcription factors to a single cell layer [146-148]. The extended range of WUS protein movement over 3-5 cell layers is somewhat inconsistent with a full nuclear trapping model, though the pWUS:eGFP-WUS reporter does clearly show a moderate nuclear pattern. However, the nuclear localization of WUS was found to be largely independent of cytokinin responses, though two other patterns were found instead. The first of these was the enlarged nuclear volume, which was clearly cytokinin-dependent. Similar enlarged nuclei in other angiosperms have been correlated with endo-reduplication [149], and this is consistent with the enhanced cell proliferation rates seen under prolonged chemical treatments. The absence of any change in the WUS nuclear/cytoplasmic ratio is most easily explained a passive process, as dilution of WUS in an enlarged nucleus would be precisely balanced by an increase in WUS concentration in the cytoplasm, so long as the total cell volume itself did not change.

The failure of protein re-distribution to occur following the nuclear volume is harder to explain, as active transport mechanisms through the nuclear pore should presumably restore the original concentrations within a few minutes. No such equilibrium adjustment was detected in the present study, which counter-intuitively suggests that WUS only has a limited ability to move through the nuclear pore. This may reflect the mass of the eGFP-WUS protein, which at 64kDa, is much

larger than the 40kDa passive diffusion limit of the nuclear pore [150, 151]. The presence of nuclear fluorescent patterns however, clearly shows that at least some hybrid fluorescent proteins are actively transported into the nucleus Surprisingly, the addition of an extra NLS tag in the pWUS:NLS-eGFP-WUS reporter did not significantly enrich the nuclear localized pattern compared to pWUS:eGFP-WUS. Such a pattern might be expected to occur if WUS has a native NLS motif, which would make the added NLS tag is functionally redundant. The present data however, cannot rule out the possibility that NLS tag is blocked by some aspect of WUS structure. The NLS-eGFP-WUS protein is 8% larger than eGFP-WUS, and this figure is reminiscent of the 15% reduction found in pWUS:NLS-eGFP-WUS meristems, and might suggest that the limited mobility of the NLS construct reflects a size-dependent fractionation process, rather than nuclear trapping.

The continued presence of WUS in the cytoplasm however, requires the existence of a nuclear export mechanism to balance out the effects of nuclear import. Although such a function has not been attributed to the WUS protein, the EAR-like motif present in its C-terminus closely resembles a lysine rich NES motif [152]. The same motif is also recognized by TPL [49], though it is not clear which function predominates in WUS. Even if EAR-like motif functions as a nuclear exit sequence (NES) however, a system based exclusively on nuclear pore transport would likely shift the equilibrium to one extreme state or another rather than be perfectly balanced at an intermediate state. One clue about how a stable intermediate is achieved comes from the pWUS:eGFP-NES-WUS construct, whose fluorescent pattern is very weak, but is not zero (Figure 3.6), suggesting that WUS is rapidly degraded in the cytoplasm. This observation also indicates that WUS EAR-like motif has at best a weak NES function, as the added NES tag could only have such a strong impact if the native WUS molecule lacked a strong native NES function.

Together these observations indicate that only small fraction of WUS proteins are transported into the nucleus, while those that remain in the cytoplasm are degraded. Rather than being nuclear enriched, this situation is probably more accurately described as cytoplasmic depletion. Interestingly, the WUS subcellular pattern closely parallels a similar situation for Cytidylyltransferase (CCTα) proteins in the Mouse model, where mono-ubiquitination of the NLS motif was demonstrated to prevent nuclear import, and was further associated with higher rates of proteolytic degradation of CCTα in the cytoplasm [153].

Cytokinin do not directly control WUS protein stability

On the basis of current evidence, it seems likely that cytokinin responses are necessary for WUS protein stability. This may reflect a common trend for SAM expressed genes, as cytokinin exposure is also known to increase the stability of ACS [154] and ARR1 [155]. Evidence of a positive relationship is perhaps best seen in the *ahk2/3/4* receptor mutant background, where WUS mRNA is transcribed normally in the complete absence of cytokinin responses (Figure 3.4), yet the translated GFP reporter is barely detectable (Figure 3.3). Conversely, when cytokinin responses are induced by pCLV3:GR-LhG4 x ARR1ΔDDK-GR, we see an increase in WUS proteins in the L1 and L2 cells after 48 hours, but little or no WUS transcription in these cells (Figure 3.4). This suggests that the WUS proteins that move into the L1 and L2 cells are rapidly degraded in the absence of strong cytokinin responses, but become protected following ectopic cytokinin activation.

However, the idea of a positive correlation begins to break down when p35S:GR-LhG4::p6xOP:CKX3 induction is considered, because this did not obviously reduce pWUS:eGFP-WUS fluorescent levels (Figure 3.5). The fact that the peak fluorescence shifted down by one layer might indicate that the response-free zone became larger, but the variability of

this construct makes it difficult to draw firm conclusions. Another potential problem can be found in pCLV3:GR-LhG4 x ARR1ΔDDK-GR x pWUS:eGFP-WUS plants that have been induced with dexamethasone for 48 hours. Although cytokinin responses are homogenously distributed in these meristems, the pWUS:eGFP-WUS pattern does not clearly show strong WUS expression in the peripheral regions where cytokinin induced stability might be expected.

The results of cycloheximide and MG132 treatments do not help clarify this situation, as the alternating patterns of stability and instability cannot easily be explained in terms of the cytokinin signaling pathway alone. To do so requires assuming that the cytokinin phosphor-relay system has a previously undetected branch pathway, potentially regulating a protease with equally unusual phospho-dependent activity. However, this model is not much different than the observation that cytokinin influences WUS stability through both protein translation protein pathways, as both models require multiple steps with poorly known intermediates. Attempts to identify the possible intermediates using lists of cytokinin-targeted genes do not clearly help resolve this situation, as a meta-analysis [99] found only five translation related genes, two of which modify mRNA, one that modified tRNA, and two that are involved with ribosomal RNA processing. The same list of cytokinin targets also contains six protease genes (three up-regulated, three down-regulated), while a single representative from the ubiquitin/proteosome pathway was down-regulated [99]. In the absence of a clearly direct cytokinin-WUS connection, it is quite tempting to speculate that protein stability is a secondary effect of cytokinin responses. If so, stability may be a generic feature of cytokinin responses, which has the potential to affect all proteins simultaneously.

WUS is degraded in the presence of auxin

Experiments with auxin on the other hand, suggest a much more direct link with WUS stability. Four hours of exogenous NAA treatment dramatically reduced pWUS:eGFP-WUS fluorescent levels, while comparable treatments with cytokinin took a minimum of 12 hours to show the slightest response in WUS expression. The auxin–induced degradation was also readily blocked by cycloheximide treatments (Figure 3.8), indicating that the response requires protein translation. Still, exactly which proteins are translated, and how they affect WUS stability is not clear. Auxin induced degradation may have a functional significance for lateral anlagen though, as the concentration of auxin responses in distinct foci [8], would help rapidly reprogram the anlagen cells by degrading conflicting developmental proteins. This hypothesis is consistent with the large marginal voids of WUS and CLV3 expression found when cytokinin responses are ectopically induced with the pCLV3:GR-LhG4 x p6xOP:ARR1ΔDDK-GR system (Figure 3.2), which were often correlated to the presence of leaf primordia and sites of auxin accumulation. Similar marginal voids can also be seen in WT meristems treated with exogenous cytokinin [139]. Although not quite as direct, other research has also shown that WUS transcript levels are indirectly linked to auxin transport [5, 33, 136]. In addition callus tissue studies have found that induction of SAMs does not require cytokinin alone, but instead requires an appropriately high concentration of auxin [38] or a balanced auxin/cytokinin ratio [110], clearly implying that auxin is a significant part of the process.

Considering the overall organization of the SAM, this suggests a model where WUS helps stabilize the mutually exclusive pattern of auxin and cytokinin responses in the PZ and RM by activating the biosynthesis of both hormones and auxin transport genes within the CZ. The lack of hormone responses in the very cells that produce them is consistent with a similar pattern in

root development [4], and given the often symplast-like environment in the SAM, a repressive mechanism may be necessary to prevent hormone response proteins from spreading into the CZ and suppressing biosynthesis. The fields of protein stability (RM) and instability (PZ) brought about by the hormone responses also appears to define the number of WUS producing cells, and eventually, the concentration of WUS molecules that reach the CZ, forming an indirect, but stable set of feedback loops that share WUS as an anchor.

The CLV3 pathway may represent another feedback loop within this framework, as it is also activated by WUS in the CZ, similar to the postulated activation of hormone biosynthesis genes. Although the intermediate steps are not clear, CLV3 appears to suppress cytokinin-induced proliferation, as seen by the hypersensitive response of *clv3-2* mutant to exogenous cytokinin (Figure 3.1). By doing so, it may potentially function as a third feedback loop, negatively regulating WUS transcription though a mechanism that is slightly more direct than either hormone pathway alone. It would thus be of great interest to learn what proteins regulate *WUS* transcription in the RM, as the *ahk2/3/4* RNA in-situ (Figure 3.4) clearly shows that cytokinin responses are not involved.

Materials and Methods

Constructs

With the exception of pTCSn1:mGFP5-ER (col-0), all constructs were in the L*er* ecotype. Constructs p35S:GR-LhG4::p6xpOP:CKX3, and p6xOP:ΔDDK-ARR1-GR were originally described in [11]. pCLV3:mGFP5-ER is as described [156], pWUS:NLS-eGFP-WUS and pWUS:eGFP-WUS are as described [20]. The pTCSn1:mGFP5-ER is as described [6]. Constructs pWUS:eGFP-NES-WUS, pWUS:GR-LhG4, pCLV3:GR-LhG4 were provided courtesy of Mariano Perales, while *wus-1, clv3-2* and *ahk2/3/4* triple mutants were provided

courtesy of Kaori Miyawaki. All plants were bred to obtain complete homozygotes before imaging.

Growth conditions and treatments

All plants were grown in 24 hours continuous light 22°C from dry-sown seeds. For treatments lasting 6 hours or more, seedling plants were placed horizontally on 1% agar containing 1/4x MS salts, beginning at appropriate intervals before the plants became 7 days old. The plates were placed vertically in growth chamber to avoid hypocotyl curvature. For treatments less than 6 hours, the seedling plants were suspended in 30ml of 1xPBS. All chemical treatments were performed using the following concentration: 10μM cycloheximide, 10μM MG132, 10μM 6-benzylaminopurine, 10μM naphthalene acetic acid, and/or 10μM dexamethasone.

Sectioning

Longitudinal sections of 10-14 seedling SAM's were prepared from seven day old plants for each treatment. The plants were embedded whole in 4% agarose, 1% gelatin dissolved in 1xPBS, pre-heated to 65°C and immediately plunged into 1xPBS pre-chilled to 4°C on ice to solidify. The plants were pre-trimmed to convenient Y-shapes underwater, and hand-cut longitudinal sections were performed with a polished feather-edged razor-blade. The sections were then stained in 100μL of 1xPBS containing 1.25μg FM4-64 for 30 minutes at 4°C for contrast. After staining, the tissue was arranged cut-face down on a large coverslip in a drop of plain 1xPBS, laying a glass slide on top when done. Air gaps were filled with 1xPBS, and the slides were stored dry above ice until imaging.

Imaging

All images were performed using a Leica 510 inverted confocal microscope, with a 40x objective water immersion lens. Z-stack images were obtained from 0.25μM optical slices, taken under 3x zoom, 4x line averaging, and 77.21 μM pinhole (1 AU). Fluorescence was activated with the 488nm laser line set at 20% power, and filtered to 30%. Three channels were recorded: Green (492-554nm), Red 590-640nm), and bright field DIC optics.

Semi-quantification of the WUS longitudinal profiles

Fluorescent confocal images of pWUS:EGFP-WUS plants were analyzed with ImageJ 1.6.0 software, using the LOCI plugin to manipulate Leica image file formats. For gradients, the "plot profile" feature was used to record a 20μM tall and 180μM wide rectangular box centered on the apex of the SAM, which was rotated to the horizontal position. The data was divided into bins based on measured cell diameters, and then averaged across samples on a layer by layer basis. Two non-adjacent optical slices were selected from each meristem, using a minimum of 4 meristems per treatment.

Nuclear/cytoplasmic distribution

Meristems used for nuclear/cytoplasmic measurements were stained with FM4-64 and DAPI to help delimit cell walls and nuclei, respectively. Cell volume was assumed to be cubic-rectangular, and estimated by calculating depth as an average of length and width measurements. Nuclei were assumed to be spherical, and their volumes were calculated directly from their maximum cross-sectional diameter. The relative concentration of fluorophores in each subcellular compartment was then estimated by sampling a representative volume to calculate the average concentration in "fluorphore units/μM^3" units, based on the voxel dimensions in the

optical section. This figure was then multiplied by the volume of each subcellar compartment to estimate the relative amount of fluorophore units present in each. At least 4 cells from each of three tissue layers were sampled in each meristem, and a minimum of 5 meristems were sampled for each treatment, for a total of 180 measurements.

In-situ hybridization

All steps were performed largely as described in [157], with the following modifications: no salt was included in the ethanol dehydration series, and the RNAase digestion step was not performed. The WUS probe was amplified from full length WUS cDNA by PCR, then synthesized with dioxigenin-labeled rUTP. Following RNA hybridization, the probes was imuno-blotted with anti-DIG and developed with Western Blue® alkaline phosphatase.

Works cited:

1. Laufs, P., et al., *Cellular Parameters of the Shoot Apical Meristem in Arabidopsis.* Plant Cell, 1998. **10**(8): p. 1375-1389.

2. Murray, J.A.H., et al., *Systems Analysis of Shoot Apical Meristem Growth and Development: Integrating Hormonal and Mechanical Signaling.* The Plant Cell, 2012. **24**(10): p. 3907-3919.

3. Bishopp, A., et al., *A Mutually Inhibitory Interaction between Auxin and Cytokinin Specifies Vascular Pattern in Roots.* Current Biology, 2011. **21**(11): p. 917-926.

4. De Rybel, B., et al., *Integration of growth and patterning during vascular tissue formation in Arabidopsis.* Science, 2014. **345**(6197).

5. Cheng, Z.J., et al., *Pattern of auxin and cytokinin responses for shoot meristem induction results from the regulation of cytokinin biosynthesis by AUXIN RESPONSE FACTOR3.* Plant Physiology, 2013. **161**(1): p. 240-251.

6. Zürcher, E., et al., *A Robust and Sensitive Synthetic Sensor to Monitor the Transcriptional Output of the Cytokinin Signaling Network in Planta.* Plant Physiology, 2013. **161**(3): p. 1066-1075.

7. Reinhardt, D., et al., *Regulation of phyllotaxis by polar auxin transport.* Nature, 2003. **426**(6964): p. 255-260.

8. Heisler, M.G., et al., *Patterns of Auxin Transport and Gene Expression during Primordium Development Revealed by Live Imaging of the Arabidopsis Inflorescence Meristem.* Current Biology, 2005. **15**(21): p. 1899-1911.

9. Yadav, R.K., et al., *A high-resolution gene expression map of the Arabidopsis shoot meristem stem cell niche.* Development, 2014. **141**(13): p. 2735-2744.

10. Chickarmane, V.S., et al., *Cytokinin signaling as a positional cue for patterning the apical-basal axis of the growing Arabidopsis shoot meristem.* Proceedings of the National Acadamy of Sciences of the United States of America, 2012. **109**(10): p. 4002-4007.

11. Xie, M., *Live Imaging Study on Cytokinin Function and Regulation in Stem-cell Homeostasis*, in *Botany and Plant Sciences*. 2010, University of California: Riverside. p. 143.

12. Kurakawa, T., et al., *Direct control of shoot meristem activity by a cytokinin-activating enzyme.* Nature, 2007. **445**(7128): p. 652-655.

13. Stepanova, A.N., et al., *TAA1-Mediated Auxin Biosynthesis Is Essential for Hormone Crosstalk and Plant Development.* Cell, 2008. **133**(1): p. 177-191.

14. Corbesier, L., et al., *Cytokinin levels in leaves, leaf exudate and shoot apical meristem of Arabidopsis thaliana during floral transition.* Journal of Experimental Botany, 2003. **54**(392): p. 2511-2517.

15. Petersson, S.V., et al., *An Auxin Gradient and Maximum in the Arabidopsis Root Apex Shown by High-Resolution Cell-Specific Analysis of IAA Distribution and Synthesis.* The Plant Cell, 2009. **21**(6): p. 1659-1668.

16. Laux, T., et al., *The WUSCHEL gene is required for shoot and floral meristem integrity in Arabidopsis.* Development, 1996. **122**(1): p. 87-96.

17. Mayer, K.F.X., et al., *Role of WUSCHEL in regulating stem cell fate in the Arabidopsis shoot meristem.* Cell, 1998. **95**(6): p. 805-815.

18. Brand, U., et al., *Dependence of stem cell fate in Arabidopsis on a feedback loop regulated by CLV3 activity.* Science, 2000. **289**(5479): p. 617-619.

19. Brandt, R., et al., *Control of stem cell homeostasis via interlocking microRNA and microProtein feedback loops.* Mechanisms of Development, 2012. **130**(1): p. 25-33.

20. Yadav, R.K., et al., *WUSCHEL protein movement mediates stem cell homeostasis in the Arabidopsis shoot apex.* Genes & Development, 2011. **25**(19): p. 2025-2030.

21. Daum, G., et al., *A mechanistic framework for noncell autonomous stem cell induction in Arabidopsis.* Proceedings of the National Academy of Sciences, 2014.

22. Brand, U., et al., *Regulation of CLV3 expression by two homeobox genes in Arabidopsis.* Plant Physiology, 2002. **129**(2): p. 565-575.

23. Lenhard, M. and T. Laux, *Stem cell homeostasis in the Arabidopsis shoot meristem is regulated by intercellular movement of CLAVATA3 and its sequestration by CLAVATA1.* Development, 2003. **130**(14): p. 3163-3173.

24. Kondo, T., et al., *A Plant Peptide Encoded by CLV3 Identified by in Situ MALDI-TOF MS Analysis.* Science, 2006. **313**(5788): p. 845-848.

25. Ohyama, K., M. Ogawa, and Y. Matsubayashi, *Identification of a biologically active, small, secreted peptide in Arabidopsis by in silico gene screening, followed by LC-MS-based structure analysis.* Plant Journal, 2008. **55**(1): p. 152-160.

26. Clark, S.E., R.W. Williams, and E.M. Meyerowitz, *The CLAVATA1 gene encodes a putative receptor kinase that controls shoot and floral meristem size in arabidopsis.* Cell, 1997. **89**(4): p. 575-585.

27. Fletcher, J.C., et al., *Signaling of cell fate decisions by CLAVATA3 in Arabidopsis shoot meristems.* Science, 1999. **283**(5409): p. 1911-1914.

28. Shinohara, H. and Y. Matsubayashi, *Reevaluation of the CLV3-receptor interaction in the shoot apical meristem: dissection of the CLV3 signaling pathway from a direct ligand-binding point of view.* Plant Journal, 2015.

29. Schoof, H., et al., *The Stem Cell Population of Arabidopsis Shoot Meristems Is Maintained by a Regulatory Loop between the CLAVATA and WUSCHEL Genes.* Cell, 2000. **100**(6): p. 635-644.

30. Leibfried, A., et al., *WUSCHEL controls meristem function by direct regulation of cytokinin-inducible response regulators.* Nature, 2005. **438**(7071): p. 1172-1175.

31. Lindsay, D.L., V.K. Sawhney, and P.C. Bonham-Smith, *Cytokinin-induced changes in CLAVATA1 and WUSCHEL expression temporally coincide with altered floral development in Arabidopsis.* Plant Science, 2006. **170**(6): p. 1111-1117.

32. Gordon, S.P., et al., *Multiple feedback loops through cytokinin signaling control stem cell number within the Arabidopsis shoot meristem.* Proceedings of the National Acadamy of Sciences of the United States of America, 2009. **106**(38): p. 16529-16534.

33. Zhao, Z., et al., *Hormonal control of the shoot stem-cell niche.* Nature, 2010. **465**(7301): p. 1089-1092.

34. Tian, H., et al., *WOX5-IAA17 Feedback Circuit-Mediated Cellular Auxin Response Is Crucial for the Patterning of Root Stem Cell Niches in Arabidopsis.* Molecular Plant, 2014. **7**(2): p. 277-289.

35. Chatfield, S.P., et al., *Incipient stem cell niche conversion in tissue culture: using a systems approach to probe early events in WUSCHEL-dependent conversion of lateral root primordia into shoot meristems.* Plant Journal, 2013. **73**(5): p. 798-813.

36. Che, P., S. Lall, and S.H. Howell, *Developmental steps in acquiring competence for shoot development in Arabidopsis tissue culture.* Planta, 2007. **226**(5): p. 1183-1194.

37. Zheng, W., et al., *AtWuschel promotes formation of the embryogenic callus in Gossypium hirsutum.* PLoS One, 2014. **9**(1): p. e87502.

38. Su, Y.H., et al., *Auxin-induced WUS expression is essential for embryonic stem cell renewal during somatic embryogenesis in Arabidopsis.* Plant Journal, 2009. **59**(3): p. 448-460.

39. Qiao, M., et al., *Proper regeneration from in vitro cultured Arabidopsis thaliana requires the miRNA directed action of an auxin response factor.* Plant Journal, 2012.

40. Nikolaev, S.V., et al., *A model study of the role of proteins CLV1, CLV2, CLV3, and WUS in regulation of the structure of the shoot apical meristem.* Russian Journal of Developmental Biology, 2007. **38**(6): p. 383-388.

41. Sahlin, P., P. Melke, and H. Joensson, *Models of sequestration and receptor cross-talk for explaining multiple mutants in plant stem cell regulation.* BMC Systems Biology, 2011. **5**: p. 2.

42. Yadav, R.K., et al., *Plant stem cell maintenance involves direct transcriptional repression of differentiation program.* Molecular Systems Biology, 2013. **9**: p. 654.

43. Ikeda, M., N. Mitsuda, and M. Ohme-Takagi, *Arabidopsis WUSCHEL Is a Bifunctional Transcription Factor That Acts as a Repressor in Stem Cell Regulation and as an Activator in Floral Patterning.* Plant Cell, 2009. **21**: p. 3493-3505.

44. Lohmann, J.U., et al., *A molecular link between stem cell regulation and floral patterning in Arabidopsis.* Cell, 2001. **105**(6): p. 793-803.

45. Zhou, Y., et al., *Control of plant stem cell function by conserved interacting transcriptional regulators.* Nature, 2014. **517**(1): p. 377-380.

46. Engstrom, E.M., et al., *Arabidopsis Homologs of the Petunia HAIRY MERISTEM Gene Are Required for Maintenance of Shoot and Root Indeterminacy.* Plant Physiology, 2011. **155**(2): p. 735-750.

47. Kieffer, M., et al., *Analysis of the transcription factor WUSCHEL and its functional homologue in Antirrhinum reveals a potential mechanism for their roles in meristem maintenance.* Plant Cell, 2006. **18**(3): p. 560-573.

48. Causier, B., et al., *The TOPLESS Interactome: A Framework for Gene Repression in Arabidopsis.* Plant Physiology, 2012. **158**: p. 423-438.

49. Kagale, S. and K. Rozwadowski, *EAR motif-mediated transcriptional repression in plants: An underlying mechanism for epigenetic regulation of gene expression.* Epigenetics, 2011. **6**(2): p. 141-146.

50. Krogan, N.T., K. Hogan, and J.A. Long, *APETALA2 negatively regulates multiple floral organ identity genes in Arabidopsis by recruiting the co-repressor TOPLESS and the histone deacetylase HDA19.* Development, 2012. **139**(22): p. 4180-4190.

51. Uchida, N., M. Shimada, and M. Tasaka, *ERECTA-Family Receptor Kinases Regulate Stem Cell Homeostasis via Buffering its Cytokinin Responsiveness in the Shoot Apical Meristem.* Plant and Cell Physiology, 2013. **54**(3): p. 343-351.

52. Jun, J., et al., *Comprehensive Analysis of CLE Polypeptide Signaling Gene Expression and Overexpression Activity in Arabidopsis.* Plant Physiology, 2010. **154**(4): p. 1721-1736.

53. Ulmasov, T., G. Hagen, and T.J. Guilfoyle, *ARF1, a Transcription Factor That Binds to Auxin Response Elements.* Science, 1997. **276**(5320): p. 1865-1868.

54. Taniguchi, M., et al., *ARR1 Directly Activates Cytokinin Response Genes that Encode Proteins with Diverse Regulatory Functions.* Plant and Cell Physiology, 2007. **48**(2): p. 263-277.

55. Bailey, T.L., et al., *MEME Suite: tools for motif discovery and searching.* Nucleic Acids Research, 2009. **37**(Web Server issue): p. W202-W208.

56. Kosugi, S. and Y. Ohashi, *PCF1 and PCF2 specifically bind to cis elements in the rice proliferating cell nuclear antigen gene.* The Plant Cell, 1997. **9**(9): p. 1607-1619.

57. Cubas, P., et al., *The TCP domain: a motif found in proteins regulating plant growth and development.* The Plant journal : for cell and molecular biology, 1999. **18**(2): p. 215-222.

58. Luo, D., et al., *Origin of floral asymmetry in Antirrhinum.* Nature, 1996. **383**(6603): p. 794-799.

59. Doebley, J., A. Stec, and L. Hubbard, *The evolution of apical dominance in maize.* Nature, 1997. **386**(6624): p. 485-488.

60. Doebley, J., A. Stec, and C. Gustus, *teosinte branched1 and the origin of maize: evidence for epistasis and the evolution of dominance.* Genetics, 1995. **141**(1): p. 333-46.

61. Cliften, P., et al., *Finding Functional Features in Saccharomyces Genomes by Phylogenetic Footprinting.* Science, 2003. **301**(5629): p. 71-76.

62. Hong, R.L., et al., *Regulatory Elements of the Floral Homeotic Gene AGAMOUS Identified by Phylogenetic Footprinting and Shadowing.* Plant Cell, 2003. **15**(6): p. 1296-1309.

63. Cheng, F., et al., *BRAD, the genetics and genomics database for Brassica plants.* BMC Plant Biology, 2011. **11**: p. 136.

64. Oelkers, K., et al., *Bioinformatic analysis of the CLE signaling peptide family.* BMC Plant Biology, 2008. **8**(1).

65. Group, T.A.P., *An update of the Angiosperm Phylogeny Group classification for the orders and families of flowering plants: APG II.* Botanical Journal of the Linnean Society, 2003. **141**(4): p. 399-436.

66. De Bodt, S., G. Theißen, and Y. Van de Peer, *Promoter Analysis of MADS-Box Genes in Eudicots Through Phylogenetic Footprinting.* Molecular Biology and Evolution, 2006. **23**(6): p. 1293-1303.

67. Bustos, R., et al., *A Central Regulatory System Largely Controls Transcriptional Activation and Repression Responses to Phosphate Starvation in Arabidopsis.* PLoS Genetics, 2010. **6**(9): p. e1001102.

68. Wang, X., et al., *The genome of the mesopolyploid crop species Brassica rapa.* Nat Genet, 2011. **43**(10): p. 1035-1039.

69. Bailey, C.D., et al., *Toward a Global Phylogeny of the Brassicaceae.* Molecular Biology and Evolution, 2006. **23**(11): p. 2142-2160.

70. Lee, J.-Y., et al., *Activation of CRABS CLAW in the Nectaries and Carpels of Arabidopsis.* Plant Cell, 2005. **17**(1): p. 25-36.

71. Inada, D.C., et al., *Conserved Noncoding Sequences in the Grasses.* Genome Research, 2003. **13**(9): p. 2030-2041.

72. Colinas, J., K.D. Birnbaum, and P.N. Benfey, *Using Cauliflower to Find Conserved Non-Coding Regions in Arabidopsis.* Plant Physiology, 2002. **129**(2): p. 451-454.

73. Petersen, T.N., et al., *SignalP 4.0: discriminating signal peptides from transmembrane regions.* Nature Methods, 2011. **8**(10): p. 785-786.

74. Rojo, E., et al., *CLV3 is localized to the extracellular space, where it activates the Arabidopsis CLAVATA stem cell signaling pathway.* Plant Cell, 2002. **14**(5): p. 969-977.

75. Smale, S.T. and J.T. Kadonaga, *THE RNA POLYMERASE II CORE PROMOTER.* Annual Review of Biochemistry, 2003. **72**(1): p. 449-479.

76. Yadav, R.K., M. Tavakkoli, and G.V. Reddy, *WUSCHEL mediates stem cell homeostasis by regulating stem cell number and patterns of cell division and differentiation of stem cell progenitors.* Development, 2010. **137**(21): p. 3581-3589.

77. Noyes, M.B., et al., *Analysis of Homeodomain Specificities Allows the Family-wide Prediction of Preferred Recognition Sites.* Cell, 2008. **133**(7): p. 1277-1289.

78. Müller, R., et al., *Dynamic and Compensatory Responses of Arabidopsis Shoot and Floral Meristems to CLV3 Signaling.* Plant Cell, 2006. **18**(5): p. 1188-1198.

79. Koch, M.A., B. Haubold, and T. Mitchell-Olds, *Molecular systematics of the Brassicaceae: evidence from coding plastidic matK and nuclear Chs sequences.* American Journal of Botany, 2001. **88**(3): p. 534-544.

80. Brady, S.M., et al., *A High-Resolution Root Spatiotemporal Map Reveals Dominant Expression Patterns.* Science, 2007. **318**(5851): p. 801-806.

81. Bowman, J.L., G.N. Drews, and E.M. Meyerowitz, *Expression of the Arabidopsis floral homeotic gene AGAMOUS is restricted to specific cell types late in flower development.* The Plant Cell, 1991. **3**(8): p. 749-58.

82. Kim, D.W., et al., *Functional Conservation of a Root Hair Cell-Specific cis-Element in Angiosperms with Different Root Hair Distribution Patterns.* The Plant Cell, 2006. **18**(11): p. 2958-2970.

83. Tatematsu, K., et al., *Identification of cis-Elements That Regulate Gene Expression during Initiation of Axillary Bud Outgrowth in Arabidopsis.* Plant Physiology, 2005. **138**(2): p. 757-766.

84. Causier, B., et al., *TOPLESS co-repressor interactions and their evolutionary conservation in plants.* Plant Signaling & Behavior, 2012. **7**(3): p. 325-328.

85. Hill, K., H. Wang, and S.E. Perry, *A transcriptional repression motif in the MADS factor AGL15 is involved in recruitment of histone deacetylase complex components.* Plant Journal, 2008. **53**(1): p. 172-185.

86. Winter, D., et al., *An "Electronic Fluorescent Pictograph"? Browser for Exploring and Analyzing Large-Scale Biological Data Sets.* PLoS One, 2007. **2**(8): p. e718.

87. Pařenicová, L., et al., *Molecular and Phylogenetic Analyses of the Complete MADS-Box Transcription Factor Family in Arabidopsis: New Openings to the MADS World.* The Plant Cell, 2003. **15**(7): p. 1538-1551.

88. Kofuji, R., et al., *Evolution and Divergence of the MADS-Box Gene Family Based on Genome-Wide Expression Analyses.* Molecular Biology and Evolution, 2003. **20**(12): p. 1963-1977.

89. Gordon, S.P., et al., *Pattern formation during de novo assembly of the Arabidopsis shoot meristem.* Development, 2007. **134**(19): p. 3539-3548.

90. Besnard, F., et al., *Cytokinin signalling inhibitory fields provide robustness to phyllotaxis.* Nature, 2014. **505**(7483): p. 417-421.

91. Guilfoyle, T.J. and G. Hagen, *Auxin response factors.* Current Opinion in Plant Biology, 2007. **10**(5): p. 453-460.

92. Tiwari, S.B., G. Hagen, and T. Guilfoyle, *The Roles of Auxin Response Factor Domains in Auxin-Responsive Transcription.* The Plant Cell, 2003. **15**(2): p. 533-543.

93. Schuettengruber, B., et al., *Functional Anatomy of Polycomb and Trithorax Chromatin Landscapes in Drosophila Embryos.* PLoS Biology, 2009. **7**(1): p. e1000013.

94. Berger, N., et al., *Transcriptional Regulation of Arabidopsis LEAFY COTYLEDON2 Involves RLE, a cis-Element That Regulates Trimethylation of Histone H3 at Lysine-27.* The Plant Cell, 2011. **23**(11): p. 4065-4078.

95. Deng, W., et al., *Arabidopsis Polycomb Repressive Complex 2 binding sites contain putative GAGA factor binding motifs within coding regions of genes.* BMC Genomics, 2013. **14**: p. 593-593.

96. Song, C.-P. and D. Galbraith, *AtSAP18, An Orthologue of Human SAP18, is Involved in the Regulation of Salt Stress and Mediates Transcriptional Repression in Arabidopsis.* Plant Molecular Biology, 2006. **60**(2): p. 241-257.

97. Nicolas, E., et al., *Distinct roles of HDAC complexes in promoter silencing, antisense suppression and DNA damage protection.* Nat Struct Mol Biol, 2007. **14**(5): p. 372-380.

98. Pavan, K.P., et al., *Functional interaction between PML and SATB1 regulates chromatin-loop architecture and transcription of the MHC class I locus.* Nat Cell Biol, 2007. **9**(1): p. 45-56.

99. Bhargava, A., et al., *Identification of Cytokinin-Responsive Genes Using Microarray Meta-Analysis and RNA-Seq in Arabidopsis.* Plant Physiology, 2013. **162**(1): p. 272-294.

100. Jones-Rhoades, M.W., D.P. Bartel, and B. Bartel, *MicroRNAs AND THEIR REGULATORY ROLES IN PLANTS.* Annual Review of Plant Biology, 2006. **57**(1): p. 19-53.

101. Zhu, Z., et al., *Arabidopsis resistance protein SNC1 activates immune responses through association with a transcriptional corepressor.* Proceedings of the National Academy of Sciences, 2010. **107**(31): p. 13960-13965.

102. Stuurman, J., F. Jäggi, and C. Kuhlemeier, *Shoot meristem maintenance is controlled by a GRAS-gene mediated signal from differentiating cells.* Genes & Development, 2002. **16**(17): p. 2213-2218.

103. Sharma, V.K., J. Ramirez, and J.C. Fletcher, *The Arabidopsis CLV3-like (CLE) genes are expressed in diverse tissues and encode secreted proteins.* Plant Molecular Biology, 2003. **51**(3): p. 415-425.

104. Cock, J.M. and S. McCormick, *A Large Family of Genes That Share Homology with CLAVATA3.* Plant Physiology, 2001. **126**(3): p. 939-942.

105. Hobe, M., et al., *Loss of CLE40, a protein functionally equivalent to the stem cell restricting signal CLV3, enhances root waving in Arabidopsis.* Development Genes and Evolution, 2003. **213**(8): p. 371-381.

106. Ni, J. and S.E. Clark, *Evidence for functional conservation, sufficiency, and proteolytic processing of the CLAVATA3 CLE domain.* Plant Physiology, 2006. **140**(2): p. 726-733.

107. Deveaux, Y., et al., *Genes of the most conserved WOX clade in plants affect root and flower development in Arabidopsis.* BMC Evolutionary Biology, 2008. **8**: p. No pp. given.

108. Nardmann, J., P. Reisewitz, and W. Werr, *Discrete shoot and root stem cell-promoting WUS/WOX5 functions are an evolutionary innovation of angiosperms.* Molecular Biology and Evolution, 2009. **26**(8): p. 1745-1755.

109. Strabala, T.J., et al., *Gain-of-Function Phenotypes of Many CLAVATA3/ESR Genes, Including Four New Family Members, Correlate with Tandem Variations in the Conserved CLAVATA3/ESR Domain.* Plant Physiology, 2006. **140**(4): p. 1331-1344.

110. Cheng, Z.-J., et al., *Cytokinin and auxin regulates WUS induction and inflorescence regeneration in vitro in Arabidopsis.* Plant Cell Reports, 2010. **29**(8): p. 927-933.

111. Laux, T., et al., *The WUSCHEL gene is required for shoot and floral meristem integrity in Arabidopsis.* Development, 1996. **122**(1): p. 87-96.

112. Li, J., et al., *Analysis of transgenic tobacco with overexpression of Arabidopsis WUSCHEL gene.* Acta Botanica Sinica, 2004. **46**(2): p. 224-229.

113. Whitford, R., et al., *Plant CLE peptides from two distinct functional classes synergistically induce division of vascular cells.* Proceedings of the National Academy of Sciences, 2008. **105**(47): p. 18625-18630.

114. Lu, Z., et al., *MONOCULM 3, an Ortholog of WUSCHEL in Rice, Is Required for Tiller Bud Formation.* Journal of Genetics and Genomics, 2015. **42**(2): p. 71-8.

115. Della Rovere, F., et al., *Auxin and cytokinin control formation of the quiescent centre in the adventitious root apex of arabidopsis.* Annals of Botany, 2013. **112**(7): p. 1395-1407.

116. Muraro, D., et al., *The role of auxin and cytokinin signalling in specifying the root architecture of Arabidopsis thaliana.* Journal of Theoretical Biology, 2013. **317**: p. 71-86.

117. Zhang, W., et al., *Cytokinin Induces Cell Division in the Quiescent Center of the Arabidopsis Root Apical Meristem.* Current Biology, 2013. **23**(20): p. 1979-1989.

118. Schaller, E.G., A. Bishopp, and J.J. Kieber, *The Yin-Yang of Hormones: Cytokinin and Auxin Interactions in Plant Development.* Plant Cell, 2015. **27**(1): p. 44-63.

119. Steffens, N.O., et al., *AthaMap: an online resource for in silico transcription factor binding sites in the Arabidopsis thaliana genome.* Nucleic Acids Research, 2004. **32**: p. D368-372.

120. Kearse, M., et al., *Geneious Basic: an integrated and extendable desktop software platform for the organization and analysis of sequence data.* Bioinformatics, 2012. **28**(12): p. 1647-1649.

121. Higo, K., et al., *Plant cis-acting regulatory DNA elements (PLACE) database:1999.* Nucleic Acids Research, 1999. **27**(1): p. 297-300.

122. Liu, T., et al., *Cistrome: an integrative platform for transcriptional regulation studies.* Genome Biology, 2011. **12**: p. R83.

123. Jin, J.P., et al., *PlantTFDB 3.0: a portal for the functional and evolutionary study of plant transcription factors.* Nucleic Acids Research, 2014. **42**(D1): p. D1182-D1187.

124. Mathelier, A., et al., *JASPAR 2014: an extensively expanded and updated open-access database of transcription factor binding profiles.* Nucleic Acids Research, 2013.

125. O'Connor, T.R., C. Dyreson, and J.J. Wyrick, *Athena: a resource for rapid visualization and systematic analysis of Arabidopsis promoter sequences.* Bioinformatics, 2005. **21**(24): p. 4411-4413.

126. Griffiths-Jones, S., et al., *miRBase: microRNA sequences, targets and gene nomenclature.* Nucleic Acids Research, 2006. **34**(suppl 1): p. D140-D144.

127. Edgar, R.C., *MUSCLE: multiple sequence alignment with high accuracy and high throughput.* Nucleic Acids Research, 2004. **32**(5): p. 1792-1797.

128. Clough, S.J. and A.F. Bent, *Floral dip: a simplified method forAgrobacterium-mediated transformation ofArabidopsis thaliana.* Plant Journal, 1998. **16**(6): p. 735-743.

129. Lee, D., et al., *Genome-wide expression profiling of ARABIDOPSIS RESPONSE REGULATOR 7(ARR7) overexpression in cytokinin response.* Molecular Genetics and Genomics, 2007. **277**(2): p. 115-137.

130. Bartrina, I., et al., *Cytokinin regulates the activity of reproductive meristems, flower organ size, ovule formation, and thus seed yield in Arabidopsis thaliana.* Plant Cell, 2011. **23**(1): p. 69-80.

131. Schuster, C., et al., *A Regulatory Framework for Shoot Stem Cell Control Integrating Metabolic, Transcriptional, and Phytohormone Signals.* Developmental Cell, 2014. **28**(4): p. 438-449.

132. Busch, W., et al., *Transcriptional control of a plant stem cell niche.* Developmental Cell, 2010. **18**(5): p. 841-853.

133. Zuo, J., et al., *The WUSCHEL gene promotes vegetative-to-embryonic transition in Arabidopsis.* Plant Journal, 2002. **30**(3): p. 349-359.

134. Elhiti, M.A., et al., *Modulation of embryo-forming capacity in culture through the expression of Brassica genes involved in the regulation of the shoot apical meristem.* Journal of Experimental Botany, 2010. **61**(14): p. 4069-4085.

135. Elhiti, M.A. and C. Stasolla, *Ectopic expression of the Brassica SHOOTMERISTEMLESS attenuates the deleterious effects of the auxin transport inhibitor TIBA on somatic embryo number and morphology.* Plant Science, 2011. **180**(2): p. 383-390.

136. Xiang, D., et al., *POPCORN functions in the auxin pathway to regulate embryonic body plan and meristem organization in Arabidopsis.* Plant Cell, 2011. **23**(12): p. 4348-4367.

137. Sakai, H., et al., *ARR1, a Transcription Factor for Genes Immediately Responsive to Cytokinins.* Science, 2001. **294**(5546): p. 1519-1521.

138. Chakraborty, A., et al., *Adaptive Geometric Tessellation for 3D Reconstruction of Anisotropically Developing Cells in Multilayer Tissues from Sparse Volumetric Microscopy Images.* PLoS One, 2013. **8**(8): p. e67202.

139. Huang, W., et al., *ALTERED MERISTEM PROGRAM1 Suppresses Ectopic Stem Cell Niche Formation in the Shoot Apical Meristem in a Largely Cytokinin-Independent Manner*. Plant Physiology, 2015. **167**(4): p. 1471-1486.

140. Ishida, K., et al., *Three Type-B Response Regulators, ARR1, ARR10 and ARR12, Play Essential but Redundant Roles in Cytokinin Signal Transduction Throughout the Life Cycle of Arabidopsis thaliana.* Plant and Cell Physiology, 2008. **49**(1): p. 47-57.

141. Yadav, R.K., et al., *Gene expression map of the Arabidopsis shoot apical meristem stem cell niche.* Proceedings of the National Academy of Sciences, 2009. **106**(12): p. 4941-4946.

142. Pernisová, M., et al., *Cytokinins modulate auxin-induced organogenesis in plants via regulation of the auxin efflux.* Proceedings of the National Academy of Sciences, 2009. **106**(9): p. 3609-3614.

143. Zhang, W., et al., *Type-A response regulators are required for proper root apical meristem function through post-transcriptional regulation of PIN auxin efflux carriers.* Plant Journal, 2011. **68**(1): p. 1-10.

144. Růžička, K., et al., *Cytokinin regulates root meristem activity via modulation of the polar auxin transport.* Proceedings of the National Academy of Sciences, 2009. **106**(11): p. 4284-4289.

145. Marhavy, P., et al., *Cytokinin Modulates Endocytic Trafficking of PIN1 Auxin Efflux Carrier to Control Plant Organogenesis.* Developmental Cell, 2011. **21**(4): p. 796-804.

146. Cui, H., et al., *An Evolutionarily Conserved Mechanism Delimiting SHR Movement Defines a Single Layer of Endodermis in Plants.* Science, 2007. **316**(5823): p. 421-425.

147. Balkunde, R., D. Bouyer, and M. Hülskamp, *Nuclear trapping by GL3 controls intercellular transport and redistribution of TTG1 protein in Arabidopsis.* Development, 2011. **138**(22): p. 5039-5048.

148. Kang, Y.H., et al., *Nuclear Trapping Controls the Position-Dependent Localization of CAPRICE in the Root Epidermis of Arabidopsis.* Plant Physiology, 2013. **163**(1): p. 193-204.

149. Jovtchev, G., et al., *Nuclear DNA content and nuclear and cell volume are positively correlated in angiosperms.* Cytogenetic and Genome Research, 2006. **114**(1): p. 77-82.

150. Ma, J., et al., *Self-regulated viscous channel in the nuclear pore complex.* Proceedings of the National Acadamy of Sciences of the United States of America, 2012. **109**(19): p. 7326-7331.

151. Naim, B., et al., *Passive and Facilitated Transport in Nuclear Pore Complexes Is Largely Uncoupled.* Journal of Biological Chemistry, 2007. **282**(6): p. 3881-3888.

152. Castellanos, C.C.R., *Nuclear Export Signals (NES's) in Arabidopsis thaliana — Development and experimental validation of a prediction tool*, in *Biology*. 2010, Bielefeld University: Moniquirá, Columbia. p. 160.

153. Chen, B.B. and R.K. Mallampalli, *Masking of a Nuclear Signal Motif by Monoubiquitination Leads to Mislocalization and Degradation of the Regulatory Enzyme Cytidylyltransferase.* Molecular and Cellular Biology, 2009. **29**(11): p. 3062-3075.

154. Hansen, M., H.S. Chae, and J.J. Kieber, *Regulation of ACS protein stability by cytokinin and brassinosteroid.* The Plant Journal, 2009. **57**(4): p. 606-614.

155. Kurepa, J., Y. Li, and J.A. Smalle, *Cytokinin signaling stabilizes the response activator ARR1*. Plant Journal, 2014. **78**(1): p. 157-168.

156. Reddy, G.V. and E.M. Meyerowitz, *Stem-Cell Homeostasis and Growth Dynamics Can Be Uncoupled in the Arabidopsis Shoot Apex.* Science, 2005. **310**(5748): p. 663-667.

157. Jackson, D., *In situ hybridization in plants*, in *Molecular plant pathology: a practical approach.*, S.J. Gurr, D.J. Bowles, and M.J. Mcpherson, Editors. 1992, Oxford University Press: Oxford. p. 163-174.

Appendix 1. 389 differentially expressed genes found in response to fruit load in *A. thaliana* inflorescence meristems.

Array_id	LogFC	Description	GO classification
265817_at	6.87	HIS1-3	DNA.synthesis/chromatin structure.histone
264638_at	5.95	FLOWERING LOCUS T	development.unspecified
265983_at	5.71	ATHB21 DNA binding / transcription factor	RNA.regulation of transcription.HB,Homeobox transcription factor family
258809_at	5.53	anac047; transcription factor	RNA.regulation of transcription.NAC domain transcription factor family
251039_at	5.43	unknown protein	not assigned.unknown
262347_at	5.21	AAA-type ATPase family protein	protein.degradation.AAA type
258091_at	4.88	unknown protein	not assigned.unknown
264433_at	4.86	BGLU45; catalytic/ cation binding / hydrolase, hydrolyzing O-glycosyl compounds	misc.gluco-, galacto- and mannosidases
264100_at	4.70	LUP1; beta-amyrin synthase/ lupeol synthase	secondary metabolism.isoprenoids.terpenoids
259616_at	4.64	C/VIF1; enzyme inhibitor/ pectinesterase/ pectinesterase inhibitor	misc.invertase/pectin methylesterase inhibitor family protein
266327_at	4.62	ATHB-7; transcription activator/ transcription factor	RNA.regulation of transcription.HB,Homeobox transcription factor family
256300_at	4.61	ANAC029; transcription factor	development.unspecified
249467_at	4.52	ATNAC6; protein heterodimerization/ protein homodimerization/ transcription factor	development.unspecified
256757_at	4.48	ABC transporter family protein	transport.ABC transporters and multidrug resistance systems
259879_at	4.40	CML38 | calcium-binding EF hand family protein	signalling.calcium
255626_at	4.37	meprin and TRAF homology domain-containing protein / MATH domain-containing protein	not assigned.no ontology
256442_at	4.36	unknown protein	not assigned.unknown
249979_s_at	4.34	inosine-uridine preferring nucleoside hydrolase family protein	nucleotide metabolism.degradation
267357_at	4.33	HSPRO2	not assigned.unknown
253217_at	4.29	ADF9; actin binding	cell.organisation

Array_id	LogFC	Description	GO classification
266719_at	4.27	CCA1; DNA binding / transcription activator/ transcription factor/ transcription repressor	RNA.regulation of transcription.MYB-related transcription factor family
266322_at	4.17	auxin-responsive family protein	hormone metabolism.auxin.SAUR
251272_at	4.15	ATHB-12; transcription activator/ transcription factor	RNA.regulation of transcription.HB,Homeobox transcription factor family
257280_at	4.15	NCED3; 9-cis-epoxycarotenoid dioxygenase	hormone metabolism.abscisic acid.synthesis-degradation.synthesis.9-cis-epoxycarotenoid dioxygenase
259765_at	4.12	unknown protein	not assigned.unknown
245643_at	4.12	AtMYB116; DNA binding / transcription factor	RNA.regulation of transcription.MYB domain transcription factor family
245385_at	4.12	rapid alkalinization factor (RALF) family protein	not assigned.no ontology
264102_at	4.06	ECT8	not assigned.unknown
267644_s_at	4.01	meprin and TRAF homology domain-containing protein / MATH domain-containing protein	not assigned.no ontology
252232_at	3.99	AtbZIP5; DNA binding / transcription factor	RNA.regulation of transcription.bZIP transcription factor family
247109_at	3.97	ATPSK5; growth factor	development.unspecified
264590_at	3.97	unknown protein	not assigned.unknown
262050_at	3.94	binding	not assigned.unknown
266097_at	3.93	SOUL-1	not assigned.no ontology
252993_at	3.88	monooxygenase, putative (MO2)	misc.oxidases - copper, flavone etc.
262211_at	3.85	ORA47 | ORA47; DNA binding / transcription factor	RNA.regulation of transcription.AP2/EREBP, APETALA2/Ethylene-responsive element binding protein family
258468_at	3.81	unknown protein	not assigned.unknown
250881_at	3.74	unknown protein	not assigned.unknown
247061_at	3.72	unknown protein	not assigned.unknown
246168_at	3.69	DNA binding	RNA.regulation of transcription.B3 transcription factor family
256266_at	3.68	unknown protein	not assigned.unknown
255795_at	3.67	RD20	signalling.calcium
248218_at	3.64	unknown protein	not assigned.unknown
263934_at	3.64	EDA12	not assigned.unknown
261410_at	3.63	MT1C | MT1C; copper ion binding	metal handling.binding, chelation and storage

Array_id	LogFC	Description	GO classification
246922_at	3.62	CIPK25; ATP binding / kinase/ protein kinase/ protein serine/threonine kinase	protein.postranslational modification
265122_at	3.57	FMO GS-OX2; methylthiopropyl glucosinolate S-oxygenase	secondary metabolism.sulfur-containing.glucosinolates.synthesis.aliphatic.flavin-containing monooxygenase
248276_at	3.57	YSL3; oligopeptide transporter	transport.metal
262049_at	3.52	unknown protein	not assigned.unknown
250446_at	3.51	chloroplast nucleoid DNA-binding protein, putative	RNA.regulation of transcription.unclassified
260004_at	3.49	unknown protein	not assigned.unknown
265670_s_at	3.48	unknown protein	not assigned.unknown
248194_at	3.48	unknown protein	not assigned.unknown
262736_at	3.46	GDSL-motif lipase, putative	misc.GDSL-motif lipase
246566_at	3.45	proton-dependent oligopeptide transport (POT) family protein	transport.peptides and oligopeptides
261881_at	3.44	NIP6.1; boron transporter/ glycerol transmembrane transporter/ urea transmembrane transporter/ water channel/	transport.Major Intrinsic Proteins.NIP
251733_at	3.43	CCH; copper chaperone	metal handling.binding, chelation and storage
245677_at	3.43	unknown protein	not assigned.unknown
251360_at	3.42	embryo-abundant protein-related	development.unspecified
262229_at	3.38	hydrolase	lipid metabolism.lipid degradation.lysophospholipases.carboxylesterase
254101_at	3.38	ATAMY1; alpha-amylase	major CHO metabolism.degradation.starch.starch cleavage
263956_at	3.37	BLH1; DNA binding / protein heterodimerization/ protein homodimerization/ transcription factor	RNA.regulation of transcription.HB,Homeobox transcription factor family
249134_at	3.36	unknown protein	not assigned.unknown
256580_s_at	3.36	unknown protein	not assigned.unknown
249800_at	3.36	MTN3	development.unspecified
262137_at	3.35	bZIP family transcription factor	RNA.regulation of transcription.bZIP transcription factor family

Array_id	LogFC	Description	GO classification
248964_at	3.35	CYP707A3; (+)-abscisic acid 8'-hydroxylase/ oxygen binding	misc.cytochrome P450
254090_at	3.34	nodulin MtN3 family protein	development.unspecified
253152_at	3.28	unknown protein	not assigned.unknown
247228_at	3.28	TPPJ	minor CHO metabolism.trehalose.TPP
253619_at	3.28	glycine-rich protein	not assigned.no ontology.glycine rich proteins
253831_at	3.27	unknown protein	not assigned.unknown
257824_at	3.27	auxin-responsive family protein	hormone metabolism.auxin.induced-regulated-responsive-activated
252858_at	3.27	TPPH	minor CHO metabolism.trehalose.TPP
253532_at	3.24	unknown protein	DNA.synthesis/chromatin structure
257532_at	3.23	unknown protein	not assigned.unknown
263475_at	3.21	unknown protein	not assigned.unknown
263680_at	3.21	kelch repeat-containing F-box family protein	protein.degradation.ubiquitin.E3.SCF.FBOX
253358_at	3.17	GAMMA-VPE; cysteine-type endopeptidase	protein.targeting.secretory pathway.vacuole
253048_at	3.16	formamidase, putative / formamide amidohydrolase, putative	misc.misc2
264524_at	3.14	ATBCAT-2; branched-chain-amino-acid transaminase/ catalytic	Co-factor and vitamine metabolism.pantothenate.branched-chain amino acid aminotransferase
256114_at	3.14	unknown protein	not assigned.unknown
246195_at	3.13	UBC17; small conjugating protein ligase/ ubiquitin-protein ligase	protein.degradation.ubiquitin.E2
245840_at	3.12	unknown protein	not assigned.unknown
248918_at	3.11	SAG12; cysteine-type peptidase	protein.degradation.cysteine protease
254667_at	3.10	glycine-rich cell wall protein-related	not assigned.no ontology.glycine rich proteins
247925_at	3.10	TCH4; hydrolase, acting on glycosyl bonds / xyloglucan:xyloglucosyl transferase	cell wall.modification
266320_at	3.10	unknown protein	not assigned.unknown
248374_at	3.08	AGL71; transcription factor	RNA.regulation of transcription.MADS box transcription factor family
260012_at	3.08	unknown protein	not assigned.unknown
259520_at	3.06	unknown protein	not assigned.unknown
263295_at	3.06	AGL44; DNA binding / transcription factor	RNA.regulation of transcription.MADS box transcription factor family
263545_at	3.05	unknown protein	not assigned.no ontology

Array_id	LogFC	Description	GO classification
255694_at	3.04	UNE10; DNA binding / transcription factor	RNA.regulation of transcription.bHLH,Basic Helix-Loop-Helix family
260011_at	3.03	epsin N-terminal homology (ENTH) domain-containing protein / clathrin assembly protein-related	not assigned.no ontology.epsin N-terminal homology (ENTH) domain-containing protein
248470_at	3.02	unknown protein	not assigned.unknown
256569_at	3.02	unknown protein	not assigned.unknown
247718_at	3.02	LTP4; lipid binding	lipid metabolism.lipid transfer proteins etc
249377_at	3.01	unknown protein	not assigned.unknown
255895_at	3.00	12-oxophytodienoate reductase, putative	hormone metabolism.jasmonate.synthesis-degradation.12-Oxo-PDA-reductase
258647_at	2.99	F-box family protein	protein.degradation.ubiquitin.E3.SCF.FBOX
247819_at	2.99	WNK4; kinase/ protein kinase	signalling.MAP kinases
260831_at	2.99	glutaredoxin family protein	redox.glutaredoxins
249454_at	2.99	unknown protein	not assigned.unknown
266462_at	2.98	benzodiazepine receptor-related	hormone metabolism.abscisic acid.induced-regulated-responsive-activated
263950_at	2.98	HVA22J	hormone metabolism.abscisic acid.synthesis-degradation
260414_at	2.97	ATNRT1.2;calcium ion binding / transporter	transport.nitrate
252591_at	2.96	TET3	development.unspecified
256356_s_at	2.96	S-locus protein-related	RNA.regulation of transcription.unclassified
250028_at	2.96	unknown protein	not assigned.unknown
246440_at	2.96	glycine/proline-rich protein	not assigned.no ontology.glycine rich proteins
265404_at	2.93	BGAL13; beta-galactosidase	misc.gluco-, galacto- and mannosidases.beta-galactosidase
247488_at	2.92	unknown protein	not assigned.unknown
248448_at	2.92	AP2 domain-containing transcription factor, putative	hormone metabolism.ethylene.signal transduction
267181_at	2.91	aldo/keto reductase family protein	minor CHO metabolism.others
253373_at	2.91	lysine-ketoglutarate reductase/saccharopine dehydrogenase bifunctional enzyme	amino acid metabolism.degradation.aspartate family.lysine
248146_at	2.91	eukaryotic translation initiation factor SUI1, putative	protein.synthesis.initiation
248969_at	2.90	unknown protein	not assigned.unknown

Array_id	LogFC	Description	GO classification
255129_at	2.90	nodulin MtN21 family protein	development.unspecified
261957_at	2.90	ATMGL; catalytic/ methionine gamma-lyase	amino acid metabolism.degradation.aspartate family.methionine.methionine gamma-lyase
250100_at	2.90	GLN1;4; glutamate-ammonia ligase	N-metabolism.ammonia metabolism.glutamine synthase
253814_at	2.88	unknown protein	not assigned.unknown
257186_at	2.88	unknown protein	not assigned.unknown
247358_at	2.88	FLS2; flavonol synthase	secondary metabolism.flavonoids.flavonols
247052_at	2.88	HB53; DNA binding / transcription factor	RNA.regulation of transcription.HB,Homeobox transcription factor family
246208_at	2.87	ATSFH12; phosphatidylinositol transporter/ transporter	transport.misc
254998_at	2.86	choline kinase, putative	lipid metabolism.Phospholipid synthesis.choline kinase
256818_at	2.84	oxidoreductase, 2OG-Fe(II) oxygenase family protein	secondary metabolism.flavonoids.flavonols
261569_at	2.83	LHY1; DNA binding / transcription factor	RNA.regulation of transcription.MYB-related transcription factor family
259793_at	2.83	AP2 domain-containing transcription factor, putative	RNA.regulation of transcription.AP2/EREBP, APETALA2/Ethylene-responsive element binding protein family
251668_at	2.83	strictosidine synthase family protein	secondary metabolism.N misc.alkaloid-like
259705_at	2.80	anac032; transcription factor	development.unspecified
261576_at	2.80	nodulin MtN21 family protein	development.unspecified
255028_at	2.80	unknown protein	not assigned.unknown
254384_at	2.79	26.5 kDa class P-related heat shock protein (HSP26.5-P)	stress.abiotic.heat
252938_at	2.79	unknown protein	not assigned.unknown
267036_at	2.78	unknown protein	not assigned.unknown
253519_at	2.78	unknown protein	not assigned.unknown
267126_s_at	2.77	ATMES8; hydrolase/ hydrolase, acting on ester bonds	hormone metabolism misc.nitrilases, *nitrile lyases, berberine bridge enzymes, reticuline oxidases, troponine reductases
247212_at	2.76	senescence-associated protein-related	development.unspecified
245777_at	2.76	atnudt21; hydrolase	nucleotide metabolism.salvage.NUDIX hydrolases
261033_at	2.76	JAZ5	not assigned.unknown
254657_s_at	2.75	PUP10; purine transmembrane transporter	transport.nucleotides

Array_id	LogFC	Description	GO classification
261438_at	2.74	MT1A; copper ion binding / metal ion binding	not assigned.disagreeing hits
264514_at	2.74	cinnamyl-alcohol dehydrogenase family / CAD family	misc.alcohol dehydrogenases
254691_at	2.72	unknown protein	not assigned.unknown
246279_at	2.72	ATHB40; DNA binding / transcription factor	RNA.regulation of transcription.HB,Homeobox transcription factor family
254024_at	2.72	pathogenesis-related protein, putative	stress.biotic
252085_s_at	2.71	scpl37; serine-type carboxypeptidase	protein.degradation.serine protease
260435_at	2.71	MYB62; DNA binding / transcription factor	RNA.regulation of transcription.MYB domain transcription factor family
256021_at	2.70	ZW9	not assigned.no ontology
260023_at	2.69	ATGA2OX2; gibberellin 2-beta-dioxygenase	hormone metabolism.gibberelin.synthesis-degradation.GA2 oxidase
263252_at	2.67	STH; protein domain specific binding / transcription factor/ zinc ion binding	RNA.regulation of transcription.C2C2(Zn) CO-like, Constans-like zinc finger family
253915_at	2.67	calcium-binding EF hand family protein	signalling.calcium
261261_at	2.66	EXS family protein / ERD1/XPR1/SYG1 family protein	transport.phosphate
262749_at	2.63	GDSL-motif lipase, putative	misc.GDSL-motif lipase
258168_at	2.62	unknown protein	not assigned.unknown
265494_at	2.62	calmodulin-related protein, putative	signalling.calcium
261431_at	2.62	AtMYB47; DNA binding / transcription factor	RNA.regulation of transcription.MYB domain transcription factor family
262454_at	2.60	BFN1; T/G mismatch-specific endonuclease/ endoribonuclease,	DNA.synthesis/chromatin structure
259293_at	2.59	DNA-binding protein, putative	RNA.regulation of transcription.ABI3/VP1-related B3-domain-containing transcription factor family
255127_at	2.59	nodulin MtN21 family protein	development.unspecified
247282_at	2.59	AtMC3; cysteine-type endopeptidase	protein.degradation
251780_s_at	2.59	binding / catalytic/ oxidoreductase	misc.short chain dehydrogenase/reductase (SDR)

Array_id	LogFC	Description	GO classification
267559_at	2.58	CYP76C2; electron carrier/ heme binding / iron ion binding / monooxygenase/ oxygen binding	misc.cytochrome P450
250408_at	2.58	CIPK5; ATP binding / kinase/ protein kinase/ protein serine/threonine kinase	protein.postranslational modification
257502_at	2.58	unknown protein	not assigned.unknown
259076_at	2.57	TMAC2	not assigned.unknown
259786_at	2.57	GDSL-motif lipase/hydrolase family protein	misc.GDSL-motif lipase
248164_at	2.57	PBP1; calcium ion binding / protein binding	signalling.calcium
267517_at	2.56	RPT2; protein binding	signalling.light
262916_at	2.56	ATGSTU16; glutathione transferase	misc.glutathione S transferases
265170_at	2.56	ATBCA3; carbonate dehydratase/ zinc ion binding	TCA / org. Transformation.carbonic anhydrases
251713_at	2.55	dehydration-responsive protein-related	stress.abiotic.drought/salt
247304_at	2.55	AAP4; acidic amino acid transmembrane transporter	transport.amino acids
264692_at	2.54	DNA-binding family protein	RNA.regulation of transcription.MYB-related transcription factor family
254629_at	2.52	unknown protein	not assigned.unknown
256789_at	2.52	seven in absentia (SINA) family protein	development.unspecified
248172_at	2.52	heat shock protein-related	stress.abiotic.heat
266415_at	2.51	LTP2; lipid binding	lipid metabolism.lipid transfer proteins etc
260661_at	2.51	unknown protein	not assigned.unknown
245088_at	2.48	identical protein binding / serine-type endopeptidase	protein.degradation.subtilases
267380_at	2.48	MAX1; electron carrier/ heme binding / iron ion binding / monooxygenase/ oxygen binding	hormone metabolism.auxin.signal transduction
245628_at	2.47	PAP1; DNA binding / transcription factor	secondary metabolism.flavonoids.anthocyanins
245143_at	2.46	ZPR1; protein binding	not assigned.unknown
260357_at	2.46	AFP1	not assigned.unknown
262607_at	2.46	unknown protein	not assigned.unknown
260841_at	2.45	unknown protein	not assigned.unknown

Array_id	LogFC	Description	GO classification
251706_at	2.45	integral membrane family protein / nodulin MtN21-related	development.unspecified
258184_at	2.45	AHP1; histidine phosphotransfer kinase	signalling.phosphorelay
264204_at	2.45	SUC2, sucrose:hydrogen symporter	transporter.sugars.sucrose
247035_at	2.43	ALC (ALCATRAZ); DNA binding / transcription factor	RNA.regulation of transcription.bHLH,Basic Helix-Loop-Helix family
259464_at	2.43	unknown protein	not assigned.unknown
265823_at	2.41	integral membrane family protein	not assigned.no ontology
265472_at	2.41	zinc finger (C3HC4-type RING finger) family protein	protein.degradation.ubiquitin.E3.RING
260840_at	2.41	unknown protein	not assigned.unknown
249306_at	2.41	zinc finger (C3HC4-type RING finger) family protein	protein.degradation.ubiquitin.E3.RING
256168_at	2.41	(at1g51805): leucine-rich repeat protein kinase, putative	signalling.receptor kinases.misc
252004_at	2.41	ATPAP20; acid phosphatase/ protein serine/threonine phosphatase	misc.acid and other phosphatases
260696_at	2.40	unknown protein	not assigned.unknown
251028_at	2.40	haloacid dehalogenase-like hydrolase family protein	not assigned.no ontology
255448_at	2.34	unknown protein	not assigned.unknown
252881_at	2.34	unknown protein	not assigned.unknown
267509_at	2.34	SOC1; transcription factor	RNA.regulation of transcription.MADS box transcription factor family
247293_at	2.34	unknown protein	not assigned.unknown
262788_at	2.33	unknown protein	not assigned.unknown
266977_at	2.33	esterase/lipase/thioesterase family protein	not assigned.no ontology
266029_at	2.33	scpl38; serine-type carboxypeptidase	protein.degradation.serine protease
263380_at	2.33	basic helix-loop-helix (bHLH) family protein	RNA.regulation of transcription.bHLH,Basic Helix-Loop-Helix family
261711_at	2.32	zinc-binding family protein	RNA.regulation of transcription.unclassified

Array_id	LogFC	Description	GO classification
255957_at	2.32	senescence-associated protein-related	development.unspecified
246396_at	2.32	ATBCA6 carbonic anhydrase family protein / carbonate dehydratase family protein	TCA / org. Transformation.carbonic anhydrases
255255_at	2.31	unknown protein	not assigned.unknown
249583_at	2.31	TCH2; calcium ion binding	signalling.calcium
251770_at	2.30	oxidoreductase, 2OG-Fe(II) oxygenase family protein	secondary metabolism.flavonoids.anthocyanins
261224_at	2.30	SBT5.2; identical protein binding / serine-type endopeptidase	protein.degradation.subtilases
258935_at	2.30	unknown protein	not assigned.unknown
245330_at	2.30	acid phosphatase survival protein SurE, putative	misc.acid and other phosphatases
248505_at	2.29	unknown protein	not assigned.unknown
254562_at	2.28	CYP707A1; (+)-abscisic acid 8'-hydroxylase/ oxygen binding	hormone metabolism.abscisic acid.synthesis-degradation.degradation.8-hydroxylase
253774_at	2.28	anac074; transcription factor	RNA.regulation of transcription.NAC domain transcription factor family
261193_at	2.28	unknown protein	not assigned.unknown
263754_at	2.27	DNAJ heat shock N-terminal domain-containing protein	stress.abiotic.heat
265672_at	2.27	cysteine proteinase inhibitor-related	protein.degradation.cysteine protease
257769_at	2.27	IAA7; transcription factor	RNA.regulation of transcription.Aux/IAA family
252303_at	2.27	unknown protein	not assigned.unknown
256296_at	2.27	EXS family protein / ERD1/XPR1/SYG1 family protein	transport.phosphate
257066_at	2.26	protease inhibitor/seed storage/lipid transfer protein (LTP) family protein	misc.protease inhibitor/seed storage/lipid transfer protein (LTP) family protein
249406_at	2.26	nodulin MtN21 family protein	development.unspecified
263875_at	2.25	SEP2; chlorophyll binding	stress
250858_at	2.25	myb family transcription factor	RNA.regulation of transcription.MYB-related transcription factor family

Array_id	LogFC	Description	GO classification
245349_at	2.25	ATMES16; catalytic/ hydrolase, acting on ester bonds / methyl indole-3-acetate esterase/ methyl jasmonate esterase	misc.nitrilases, *nitrile lyases, berberine bridge enzymes, reticuline oxidases, troponine reductases
245306_at	2.24	ELIP2; chlorophyll binding	signalling.light
258092_at	2.24	unknown protein	not assigned.unknown
246495_at	2.23	50S ribosomal protein-related	protein.synthesis.ribosomal protein.prokaryotic.unknown organellar.50S subunit.unknown
264210_at	2.23	ATMYB3; DNA binding / transcription factor	RNA.regulation of transcription.MYB domain transcription factor family
266545_at	2.23	unknown protein	not assigned.unknown
260264_at	2.22	unknown protein	not assigned.unknown
266015_at	2.21	short-chain dehydrogenase/reductase (SDR) family protein	misc.short chain dehydrogenase/reductase (SDR)
265460_at	2.21	calcium-binding protein, putative	signalling.calcium
247902_at	2.21	AHA3; ATPase/ hydrogen-exporting ATPase, phosphorylative mechanism	transport.p- and v-ATPases.H+-exporting ATPase
258049_at	2.20		not assigned.no ontology
249988_at	2.20	unknown protein	not assigned.unknown
261618_at	2.20	MATE efflux family protein	transport.misc
259789_at	2.20	COR414-TM1 | COR414-TM1	not assigned.no ontology
247800_at	2.19	unknown protein	not assigned.unknown
252133_at	2.19	unknown protein	DNA.unspecified
247768_at	2.19	myb family transcription factor	RNA.regulation of transcription.MYB-related transcription factor family
251739_at	2.18	CAN; nuclease	DNA.unspecified
245671_at	2.18	PUP1; purine nucleoside transmembrane transporter/ purine transmembrane transporter	transport.nucleotides
247751_at	2.18	unknown protein	not assigned.unknown
262667_at	2.18	copper amine oxidase, putative	misc.oxidases - copper, flavone etc.
247646_at	2.17		not assigned.unknown
258880_at	2.16	ATG8H; microtubule binding	protein.degradation.autophagy

Array_id	LogFC	Description	GO classification
246214_at	2.16	HSF4; DNA binding / transcription factor/ transcription repressor	stress.abiotic.heat
253264_at	2.16	OST1; calcium-dependent protein serine/threonine kinase/ kinase/ protein kinase	protein.postranslational modification.kinase
264772_at	2.16	T-complex protein 11	not assigned.no ontology
262940_at	2.16	cation efflux family protein	transport.metal
251665_at	2.16	ARR9, two-component response regulator	Signalling.cytokinin
263296_at	2.15	calmodulin-binding protein-related	signalling.calcium
263947_at	2.15	unknown protein	not assigned.unknown
262531_at	2.15	ATP binding / protein binding / protein kinase/ protein serine/threonine kinase/ protein tyrosine kinase	signalling.receptor kinases.leucine rich repeat XI
258038_at	2.14	glycolipid transfer protein-related	lipid metabolism.lipid transfer proteins etc
255250_at	2.14	AtMYB74; DNA binding / transcription factor	RNA.regulation of transcription.MYB domain transcription factor family
252606_at	2.14	scpl48 | scpl48 (serine carboxypeptidase-like 48); serine-type carboxypeptidase	protein.degradation
247835_at	2.13	unknown protein	not assigned.unknown
261749_at	2.13	ERD14; calcium ion binding	stress.abiotic.unspecified
248230_at	2.13	VQ motif-containing protein	not assigned.no ontology
250031_at	2.11	MYR1, transcription factor	RNA.regulation of transcription.G2-like transcription factor family, GARP
245637_at	2.11	purple acid phosphatase family protein	misc.acid and other phosphatases
257805_at	2.11	ATPLT5	transporter.sugars
251544_at	2.10	GAUT15; polygalacturonate 4-alpha-galacturonosyltransferase/ transferase, transferring glycosyl groups / transferase, transferring hexosyl groups	misc.UDP glucosyl and glucoronyl transferases

Array_id	LogFC	Description	GO classification
261335_at	2.10	nodulin MtN21 family protein	development.unspecified
249211_at	2.09	unknown protein	not assigned.unknown
258724_at	2.08	myb family transcription factor	RNA.regulation of transcription.MYB-related transcription factor family
265357_at	2.07	UBC29; ubiquitin-protein ligase	protein.degradation.ubiquitin.E2
265184_at	2.07	unknown protein	not assigned.unknown
251132_at	2.07	myb family transcription factor	RNA.regulation of transcription.MYB-related transcription factor family
255794_at	2.07	ANAC041; transcription factor	RNA.regulation of transcription.NAC domain transcription factor family
249393_at	2.06	AtRLP54; kinase/ protein binding	stress.biotic.PR-proteins
257925_at	2.06	unknown protein	not assigned.unknown
246429_at	2.06	heavy-metal-associated domain-containing protein / copper chaperone (CCH)-related	metal handling.binding, chelation and storage
264886_at	2.06	TPS04; (E,E)-geranyllinalool synthase	secondary metabolism.isoprenoids.terpenoids
267538_at	2.05	remorin family protein	RNA.regulation of transcription.putative transcription regulator
267238_at	2.01	kelch repeat-containing F-box family protein	protein.degradation.ubiquitin.E3.SCF.FBOX
254809_at	2.00	auxin-responsive family protein	hormone metabolism.auxin.SAUR
254169_at	-2.00		not assigned.unknown
265764_at	-2.01	unknown protein	not assigned.unknown
261815_at	-2.01	bZIP family transcription factor	RNA.regulation of transcription.bZIP transcription factor family
266019_at	-2.02	calmodulin-binding protein	signalling.calcium
253800_at	-2.04	hydroxyproline-rich glycoprotein family protein	cell wall.cell wall proteins.HRGP
257267_at	-2.04	TCP4; transcription factor	RNA.regulation of transcription.TCP transcription factor family
256094_at	-2.05	SAUL1; ubiquitin-protein ligase	stress.biotic
258930_at	-2.06	transcription factor	RNA.regulation of transcription.Trihelix, Triple-Helix transcription factor family
263022_s_at	-2.07	GAMMA-ADAPTIN 1; binding / clathrin binding	cell.vesicle transport
245462_at	-2.07	transcription factor-related	RNA.regulation of transcription.General Transcription

Array_id	LogFC	Description	GO classification
258926_s_at	-2.08	ANAC050	development.unspecified
251083_at	-2.12	unknown protein	not assigned.unknown
261947_at	-2.14	ubiquitin family protein	protein.degradation.ubiquitin
262750_at	-2.16	unknown protein	not assigned.unknown
245227_s_at	-2.20	GTP-binding family protein	signalling.G-proteins
253736_at	-2.20	GDSL-motif lipase/hydrolase family protein	misc.GDSL-motif lipase
260041_at	-2.21	leucine-rich repeat family protein	not assigned.no ontology
264876_at	-2.23	ARID/BRIGHT DNA-binding domain-containing protein	RNA.regulation of transcription.AT-rich interaction domain containing transcription factor family
246959_at	-2.23		not assigned.unknown
262199_at	-2.24	endonuclease	not assigned.unknown
245075_at	-2.24	CYP96A1; electron carrier/ heme binding / iron ion binding / monooxygenase/ oxygen binding	misc.cytochrome P450
250201_at	-2.24	protein binding	cell.organisation
252280_at	-2.25	iqd21; calmodulin binding	signalling.calcium
260618_at	-2.26	TCP3; transcription factor	development.leaf
249209_at	-2.26	metalloendopeptidase/ zinc ion binding	protein.degradation
245719_at	-2.28	DNA topoisomerase II family protein	DNA.synthesis/chromatin structure
245587_at	-2.28	DNA binding / protein dimerization	not assigned.unknown
264630_at	-2.28	FAS1; histone binding	DNA.synthesis/chromatin structure
261611_at	-2.28	protein kinase family protein	signalling.receptor kinases.misc
260957_at	-2.28	ADS1; oxidoreductase	lipid metabolism.FA desaturation.desaturase
250517_at	-2.28	scpl35; serine-type carboxypeptidase	protein.degradation.serine protease
251041_at	-2.30	PRT6; ubiquitin-protein ligase	protein.degradation.ubiquitin
266909_at	-2.30	BRA transcription regulatory protein SNF2, putative	RNA.regulation of transcription.Chromatin Remodeling Factors
263163_at	-2.31	FZL; GTP binding / GTPase/ thiamin-phosphate diphosphorylase	signalling.G-proteins

Array_id	LogFC	Description	GO classification
262516_at	-2.33	ATGSTU26; glutathione transferase	misc.glutathione S transferases
258985_at	-2.33	binding / protein transporter	transport
245897_at	-2.33	KUP7; potassium ion transmembrane transporter	transport.potassium
250140_at	-2.38	DRM2; N-methyltransferase	RNA.regulation of transcription.DNA methyltransferases
254202_at	-2.39	hydrolase, alpha/beta fold family protein	not assigned.no ontology
262474_at	-2.40	FU; protein serine/threonine kinase	not assigned.no ontology.armadillo/beta-catenin repeat family protein
264065_at	-2.40	unknown protein	not assigned.unknown
266254_at	-2.43	NAT12 | xanthine/uracil permease family protein	transport.misc
261054_at	-2.44	tetratricopeptide repeat (TPR)-containing protein	not assigned.no ontology.pentatricopeptide (PPR) repeat-containing protein
258214_at	-2.46	atToc64-III | atToc64-III (*Arabidopsis thaliana* translocon at the outer membrane of chloroplasts 64-III); binding / carbon-nitrogen ligase, with glutamine as amido-N-donor	protein.targeting.chloroplast
260282_at	-2.49	EMB2753; binding	misc.acyl transferases
247629_at	-2.55	ATSIZ1; DNA binding / SUMO ligase	RNA.regulation of transcription.putative transcription regulator
265731_at	-2.56	ATP binding / ATP-dependent helicase/ RNA binding / double-stranded RNA binding / helicase/ nucleic acid binding	DNA.synthesis/chromatin structure
266436_at	-2.56	epsin N-terminal homology (ENTH) domain-containing protein	not assigned.no ontology.epsin N-terminal homology (ENTH) domain-containing protein
248062_at	-2.56	protease inhibitor/seed storage/lipid transfer protein (LTP) family protein	misc.protease inhibitor/seed storage/lipid transfer protein (LTP) family protein
255673_at	-2.58	RLK4; protein kinase/ sugar binding	misc.myrosinases-lectin-jacalin
266651_at	-2.59	protein kinase family protein	protein.postranslational modification
253605_at	-2.61	binding	not assigned.unknown

Array_id	LogFC	Description	GO classification
245434_at	-2.63		not assigned.no ontology.C2 domain-containing protein
252162_at	-2.64	nucleotide binding	not assigned.no ontology
254635_at	-2.65	protein binding / structural constituent of cell wall	cell wall.cell wall proteins.LRR
246961_at	-2.66		not assigned.no ontology
250275_at	-2.67	unknown protein	not assigned.unknown
245482_at	-2.70	unknown protein	not assigned.unknown
252576_s_at	-2.71	ATCLPC, ATHSP93-III, HSP93-III | HSP93-III; ATP binding / ATPase/ DNA binding / nuclease/ nucleoside-triphosphatase/ nucleotide binding / protein binding	protein.degradation.serine protease
250835_at	-2.71	DME; DNA N-glycosylase/ DNA-(apurinic or apyrimidinic site) lyase	RNA.regulation of transcription.Orphan family
258525_at	-2.71	IBR3; acyl-CoA dehydrogenase/ oxidoreductase	lipid metabolism.lipid degradation.beta-oxidation.acyl CoA DH
264081_at	-2.71	nucleic acid binding / nucleotide binding / protein binding / zinc ion binding	RNA.RNA binding
255907_at	-2.72	HDG12; transcription factor	RNA.regulation of transcription.HB,Homeobox transcription factor family
255687_at	-2.72	KEA2, ATKEA2 | KEA2; potassium ion transmembrane transporter/ potassium:hydrogen antiporter	transport.potassium
258217_at	-2.73	NMT1, XPL1, PEAMT | XPL1 (XIPOTL 1); methyltransferase/ phosphoethanolamine N-methyltransferase	lipid metabolism.Phospholipid synthesis

Array_id	LogFC	Description	GO classification
244975_at	-2.74	PSBH | Encodes a 8 kD phosphoprotein that is a component of the photosystem II oxygen evolving core. Its exact molecular function has not been determined but it may play a role in mediating electron transfer between the secondary quinone acceptors, QA and QB, associated with the acceptor side of PSII.	PS.lightreaction.photosystem II.PSII polypeptide subunits
249813_at	-2.74	EMB3009; transferase/ transferase, transferring acyl groups other than amino-acyl groups	not assigned.no ontology
255693_s_at	-2.77	MEE43, EDA20, BRCA2(IV), BRCA2A | protein binding / single-stranded DNA binding	cell.cycle
265580_at	-2.80	ATP binding / cAMP-dependent protein kinase regulator/ catalytic/ protein kinase/ protein serine/threonine phosphatase	protein.postranslational modification
264007_at	-2.80	ATPRP2	cell wall.cell wall proteins.proline rich proteins
265779_at	-2.84	SH3 domain-containing protein	not assigned.no ontology
253209_at	-2.85		not assigned.no ontology.pentatricopeptide (PPR) repeat-containing protein
258562_at	-2.88	unknown protein	not assigned.unknown
266990_at	-2.88	ATH8; transporter	not assigned.no ontology.ABC1 family protein
267144_at	-2.96	ATGPAT6; 1-acylglycerol-3-phosphate O-acyltransferase/ acyltransferase	lipid metabolism.Phospholipid synthesis
252028_at	-2.96	nicastrin-related	transport.misc
263751_at	-2.98	kinesin motor family protein	cell.organisation
252948_at	-3.07	KAK; ubiquitin-protein ligase	protein.degradation.ubiquitin.E3.HECT
260241_at	-3.07	CYP86A7; fatty acid (omega-1)-hydroxylase/ oxygen binding	misc.cytochrome P450

Array_id	LogFC	Description	GO classification
264518_at	-3.14		not assigned.unknown
260461_at	-3.14		not assigned.unknown
263447_s_at	-3.15	ATX2; DNA binding / histone methyltransferase(H3-K4 specific)	RNA.regulation of transcription.SET-domain transcriptional regulator family
251829_at	-3.15	RabGAP/TBC domain-containing protein	signalling.G-proteins
257709_at	-3.16	hydrolase, acting on ester bonds	not assigned.unknown
260670_at	-3.22	NFD5	not assigned.no ontology.pentatricopeptide (PPR) repeat-containing protein
249722_at	-3.27	binding	not assigned.unknown
258387_at	-3.30	unknown protein	not assigned.unknown
259048_at	-3.30	DegP7; catalytic/ protein binding / serine-type endopeptidase/ serine-type peptidase	protein.degradation.serine protease
261988_at	-3.37	RNA binding / nucleic acid binding	not assigned.no ontology
264795_at	-3.41	ZIGA4; ARF GTPase activator/ DNA binding / zinc ion binding	RNA.regulation of transcription.unclassified
253881_at	-3.47	importin beta-2 subunit family protein	protein.targeting.nucleus
260355_at	-3.50	CRC; transcription factor	RNA.regulation of transcription.C2C2(Zn) YABBY family
258125_s_at	-3.50	cyclopropane fatty acid synthase, putative / CPA-FA synthase, putative	lipid metabolism.Phospholipid synthesis.cyclopropane-fatty-acyl-phospholipid synthase
257008_at	-3.51	ESM1; carboxylesterase/ hydrolase, acting on ester bonds	secondary metabolism.sulfur-containing.glucosinolates.degradation.myrosinase
255662_at	-3.54	GPAT8; acyltransferase/ glycerol-3-phosphate O-acyltransferase	lipid metabolism.Phospholipid synthesis
245007_at	-3.54	PSAA | Encodes psaA protein comprising the reaction center for photosystem I along with psaB protein; hydrophobic protein encoded by the chloroplast genome.	PS.lightreaction.photosystem I.PSI polypeptide subunits
257085_at	-3.65	UBP14; ubiquitin-specific protease	protein.degradation.ubiquitin.ubiquitin protease

Array_id	LogFC	Description	GO classification
264147_at	-3.81	CER1; octadecanal decarbonylase	secondary metabolism.wax
246519_at	-4.12	pollen Ole e 1 allergen and extensin family protein	stress.abiotic.unspecified
262479_at	-4.15	SUB, protein binding / receptor signaling protein serine/threonine kinase	signalling.receptor kinases.leucine rich repeat V
252971_at	-4.21	PRP4	cell wall.cell wall proteins.proline rich proteins
260869_at	-4.56	acyl-(acyl-carrier-protein) desaturase, putative / stearoyl-ACP desaturase, putative	lipid metabolism.FA synthesis and FA elongation.ACP desaturase
247508_at	-4.75	ARF2; protein binding / transcription factor	RNA.regulation of transcription.ARF, Auxin Response Factor family

Appendix 2. 117 differentially expressed genes removed from microarray results due to potential bias.

Array_id	LogFC	description	Expression pattern
247512_at	3.90	unknown protein	pollen
251358_at	2.75	shaggy-related protein kinase beta / ASK-beta (ASK2)	pollen
255423_at	3.73	calcium-binding protein, putative	pollen
255479_at	4.62	SAG21	pollen
256966_at	4.47	sks13; copper ion binding / oxidoreductase	pollen
265022_at	3.80	BCP1 | BCP1	pollen
248037_at	2.23	OPT1; oligopeptide transporter	pollen
253181_at	2.48	LHT7; amino acid transmembrane transporter	pollen
263126_at	2.95	SOUL heme-binding family protein	pollen
257121_at	4.17	auxin-responsive protein, putative	pollen
263144_at	3.39	dormancy/auxin associated protein-related	pollen
248926_at	4.74	pollen Ole e 1 allergen and extensin family protein	pollen
246841_at	4.41	germin-like protein, putative	pollen
260888_at	3.61	pollen Ole e 1 allergen and extensin family protein	pollen
258748_at	3.37	GLP8; manganese ion binding / nutrient reservoir	pollen
248404_at	-2.09	TPPA	pollen
258605_at	2.56	EXL6	pollen
246582_at	3.89	proline-rich family protein	pollen
245528_at	4.88	PPDK, phosphate dikinase	pollen
245700_at	4.06	ATACA3, /zinc ion binding	pollen
266115_at	4.13	LCR72; peptidase inhibitor	pollen
245946_at	3.49	glyoxal oxidase-related	pollen
263243_at	2.24	GLX2-5 hydroxyacylglutathione hydrolase/ iron ion binding / zinc ion binding	pollen
248822_at	3.74	peroxidase, putative	pollen
262760_at	4.98	invertase/pectin methylesterase inhibitor family protein	pollen
255515_at	4.88	invertase/pectin methylesterase inhibitor family protein	pollen
266764_at	4.08	invertase/pectin methylesterase inhibitor family protein	pollen
248534_at	3.66	invertase/pectin methylesterase inhibitor family protein	pollen
254123_at	3.28	APPB1 pectinesterase inhibitor	pollen
256955_at	3.01	sks11; copper ion binding / oxidoreductase	pollen
265080_at	2.83	sks12; copper ion binding / oxidoreductase	pollen
261623_at	2.80	ATSEC1A; FAD binding / catalytic/ electron carrier/ oxidoreductase	pollen

Array_id	LogFC	description	Expression pattern
265007_s_at	6.04	RALFL8	pollen
257819_at	4.17	RALFL25	pollen
245658_at	3.86	RALFL4	pollen
257821_at	3.72	RALFL26	pollen
258077_at	4.04		pollen
265133_s_at	3.98		pollen
250174_at	4.13	AGP6	pollen
257986_at	3.94	AGP40	pollen
251590_at	3.63	AGP23	pollen
249375_at	2.65	AGP24	pollen
252710_at	3.03	AtGH9A4; catalytic/ hydrolase, hydrolyzing O-glycosyl compounds	pollen
251228_at	2.91	glycosyl hydrolase family 3 protein	pollen
258639_at	5.57	polygalacturonase 3 (PGA3) / pectinase	pollen
262122_at	4.90	PGA4; polygalacturonase	pollen
248714_at	4.42	polygalacturonase, putative / pectinase, putative	pollen
259269_at	4.16	pectate lyase family protein	pollen
246545_at	3.20	lyase/ pectate lyase	pollen
261528_at	2.90	AT59; pectate lyase	pollen
266750_s_at	5.31	VGDH1; enzyme inhibitor/ pectinesterase	pollen
250631_at	4.93	pectinesterase family protein	pollen
250606_s_at	4.92	ATPPME1; pectinesterase	pollen
251258_at	4.22	VGDH2;pectinesterase	pollen
258889_at	3.47	pectinesterase family protein	pollen
257886_at	3.00	pectinesterase family protein	pollen
261506_at	2.16	ATCK1; choline kinase	pollen
259266_at	5.63	unknown protein	pollen
256584_at	5.15	unknown protein	pollen
249429_at	4.98	unknown protein	pollen
264923_s_at	4.47	TPX2; antioxidant/ oxidoreductase	pollen
258278_at	4.17		pollen
266918_at	4.12	LIM domain-containing protein	pollen
253226_at	4.14	BGAL11	pollen
264480_at	-2.28	EFS; histone methyltransferase (H3-K36 specific) / histone methyltransferase(H3-K4 specific)	pollen
262314_at	2.97	C2 domain-containing protein	pollen
264580_at	6.35	unknown protein	embryo
263881_at	4.55	unknown protein	embryo
248558_at	2.06	xanthine/uracil permease family protein	embryo
248812_at	2.69	palmitoyl protein thioesterase family protein	embryo
247514_at	2.44	PMSR1; oxidoreductase, acting on sulfur group of donors, disulfide as acceptor /	embryo

Array_id	LogFC	description	Expression pattern
		peptide-methionine-(S)-S-oxide reductase	
258923_at	3.53	SCPL7; serine-type carboxypeptidase	embryo
252915_at	2.97	calcium-binding EF hand family protein	embryo
258652_at	2.94	ATRABC2B; ATP binding / GTP binding / transcription factor binding	embryo
262128_at	5.70	late embryogenesis abundant protein, putative / LEA protein, putative	embryo
250648_at	4.68	late embryogenesis abundant group 1 domain-containing protein / LEA group 1 domain-containing protein	embryo
266544_at	4.26	late embryogenesis abundant group 1 domain-containing protein / LEA group 1 domain-containing protein	embryo
256464_at	3.40	late embryogenesis abundant group 1 domain-containing protein / LEA group 1 domain-containing protein	embryo
246299_at	2.44	ATEM1	embryo
264338_at	2.17	KUP6; potassium ion transmembrane transporter	embryo
261023_at	2.36	flavin-containing monooxygenase family protein / FMO family protein	embryo
252234_at	5.41	ATPSK4; growth factor	embryo
258727_at	4.32	universal stress protein (USP) family protein	embryo
255521_at	4.49	SUS3; UDP-glycosyltransferase/ sucrose synthase/ transferase, transferring glycosyl groups	embryo
247095_at	6.19	RAB18	embryo
258347_at	4.09	late embryogenesis abundant domain-containing protein / LEA domain-containing protein	embryo
258181_at	3.42	NTP3	embryo
266532_at	3.68	UDP-glucoronosyl/UDP-glucosyl transferase family protein	embryo
265111_at	4.07	protease inhibitor/seed storage/lipid transfer protein (LTP) family protein	embryo
250287_at	3.64	Rap2.6L; DNA binding / transcription factor	embryo
262803_at	4.37	zinc-binding family protein	embryo
251084_at	3.55	zinc finger (C3HC4-type RING finger) family protein	embryo
258498_at	5.06	ABA-responsive protein-related	embryo
261077_at	3.82	PP2C, putative	embryo
248496_at	-2.94	nodulin MtN3 family protein	embryo
265962_at	2.44	nodulin MtN21 family protein	embryo
264729_at	6.57	heavy-metal-associated domain-containing protein / copper chaperone (CCH)-related	embryo

Array_id	LogFC	description	Expression pattern
250051_at	-2.06	AtMYB56; DNA binding / transcription factor	embryo
250099_at	3.58	myb family transcription factor	embryo
256481_at	-4.45	galactosyltransferase family protein	flower bud
254465_at	-4.84	tapetum-specific protein-related	flower bud
267203_at	-3.33		flower bud
246416_at	-3.90		flower bud
253641_at	-4.34	unknown protein	flower bud
266530_at	-4.07	AMS; DNA binding / transcription factor	flower bud
261096_at	-4.35	ACOS5; 4-coumarate-CoA ligase/ long-chain-fatty-acid-CoA ligase/ medium-chain-fatty-acid-CoA ligase	flower bud
245488_at	-4.69	peroxidase 40	flower bud
250619_at	-4.48	protease inhibitor/seed storage/lipid transfer protein (LTP) family protein	flower bud
259063_at	-5.41	protease inhibitor/seed storage/lipid transfer protein (LTP) family protein	flower bud
252090_at	-5.42	protease inhibitor/seed storage/lipid transfer protein (LTP) family protein	flower bud
253222_at	-4.20	chalcone and stilbene synthase family protein	flower bud
252780_at	-3.96	ATA1; binding / catalytic/ oxidoreductase	flower bud
245622_at	-5.28	MEE48; catalytic/ cation binding / hydrolase, hydrolyzing O-glycosyl compounds	flower bud
260451_at	2.23	ethylene-responsive element-binding protein, putative	flower bud
257491_at	-3.34	basic helix-loop-helix (bHLH) family protein	flower bud
262022_at	2.91	bZIP family transcription factor	flower bud
265263_at	-3.14	DNA-binding family protein	flower bud